Mathematical modeling, simulation and analysis of metabolic oscillations in *Bacillus subtilis* biofilms

Dissertation

To Fulfill the
Requirements for the Degree of „doctor rerum naturalium“
(Dr. rer. nat.)

Submitted to the Council of the Faculty
of Biological Sciences
of the Friedrich Schiller University Jena

By
Ravindra Garde,
MSc Bioinformatics,
born on 13.02.1993 in
India

Date of Defense: 24th Nov 2020

Thesis committee head: Prof. Dr. Peter F. Zipfel (Hans-Knöll Institute, Jena)

Prof. Dr. Marc Thilo Figge (Hans-Knöll Institute, Jena)

Prof. Dr. David G. Heckel (Max-Planck-Institut für chemische Ökologie, Jena)

Prof. Dr Steve Hoffmann (Fritz Lipmann Institute, Jena)

Prof. Dr. Stefan Schuster (Friedrich-Schiller University, Jena)

Prof. Dr. Bashar Ibrahim (Friedrich-Schiller University, Jena)

Prof. Dr. Marko Marhl (University of Maribor, Slovenia)

Prof. Dr. Jan Schirawski (Friedrich-Schiller University, Jena)

"Experimenters are the shock troops of science… An experiment is a question which science poses to Nature, and a measurement is the recording of Nature's answer. But before an experiment can be performed, it must be planned – the question to nature must be formulated before being posed. Before the result of a measurement can be used, it must be interpreted – Nature's answer must be understood properly. These two tasks are those of theorists, who find himself always more and more dependent on the tools of abstract mathematics."

-Scientific Autobiography and Other Papers, Max Planck, 1949

"Our century was destined to make use of the possibilities afforded by the microscope in the study of nature, and it is very pleasing to see how the application of this instrument opens ever more doors and how, in ever larger circles, yields the most interesting results."

-Das Auge und das Mikroskop by Matthias Schleiden, 1848

Abstract

Bacterial biofilms have long been under the microscope for their fascinating organisation which is also thought to be the origin of multicellularity. Metabolic oscillations in biofilms of *Bacillus subtilis* have been reported as periodic halting of growth in the expansion of the colony growing in a microfluidics chamber by Liu *et al* (2015). This thesis is aimed at understanding these oscillations through minimal dynamic model involving three ordinary differential equations (ODEs). The model is first applied in its basic form in order to describe the oscillations. We present a detailed analysis of the model with respect to sensitivity of parameters and Hopf bifurcations. We also present a quasi-steady state approximation (QSSA) for two variables which also helps identify that oscillations are mainly influenced by ammonia. The model successfully describes the periodic halting of the expansion of the *B. subtilis* biofilm.

Next, various modifications of the model are discussed in detail and the results of each modification are viewed in light of the underlying biology. The four modifications investigate the mechanism of oscillations with respect to spatial effects, reversible reactions and more robust reaction kinetics. We learn that spatial effects play no role in the biofilm oscillations and can therefore be ignored. Oscillations in biofilm help in mitigating nutrient limitation. They are a means to ensure adequate supply of nutrients to the interior cells. Oscillations will no longer be observed when nutrients are plenty. The four modifications also show that minimal models are highly versatile tools to study and describe biological phenomena and can be modified as per the experimental observations.

Finally, we apply the minimal model in a broader perspective in order to understand population dynamics in a typical community of a social organism. We consider three interacting subpopulations of a species that have their own distinct phenotypes. None of the subpopulations have an absolute advantage over the other two. This gives rise to cyclic dynamics like the rock paper scissors game which is analysed using evolutionary game theory. We also present an asymmetrical two-player two-strategy game describing the same system, where the phenotype of each subpopulation is considered as a strategy. This investigation tests the ideal strategies for three different levels of antibiotic stress. We observe bet-hedging in the form of production of resistant cells which are a costly choice in the absence of the antibiotic stress.

Although the population dynamics study is described with a broad range of applicability, we also discuss its applications in the *B. subtilis* biofilm. Bacteria are like the minimal models of nature with only the most primitive components required to carry out the life processes and exhibit intricate social behaviour that resembles multicellular organisms.

Zusammenfassung

Bakterielle Biofilme wurden vielfach unter die Lupe genommen hinsichtlich ihrer faszinierenden Organisation, die auch als Ursprung von Mehrzelligkeit angesehen wird. Oszillationen im Metabolismus der Biofilme von *Bacillus subtilis* wurden von Liu et al. (2015) als periodische Wachstumsstopps bei der Expansion von Kolonien in einer Mikrofluidkammer beschrieben. Diese Arbeit zielt darauf ab, diese Oszillationen durch ein minimales dynamisches Modell zu verstehen, das drei gewöhnliche Differentialgleichungen (ODEs) umfasst. Das Modell wird zunächst in seiner Grundform angewendet, um die Oszillationen zu beschreiben. Wir präsentieren eine detaillierte Analyse des Modells hinsichtlich der Sensitivität von Parametern und Hopf-Bifurkationen. Wir präsentieren auch eine Quasi-Steady-State-Approximation (QSSA) für zwei Variablen, mit deren Hilfe auch bestätigt werden kann, dass Oszillationen hauptsächlich durch Ammoniak beeinflusst werden. Das Modell beschreibt erfolgreich das periodische Stoppen der Expansion des *B. subtilis*-Biofilms.

Des Weiteren werden verschiedene Modifikationen des Modells im Detail diskutiert und die Ergebnisse jeder Modifikation werden im Lichte der zugrunde liegenden Biologie betrachtet. Die vier Modifikationen untersuchen das Verhalten von Oszillationen in Bezug auf räumliche Effekte, reversible Reaktionen und robustere Reaktionskinetiken. Wir zeigen, dass räumliche Effekte bei den Biofilmoszillationen keine Rolle spielen und daher vernachlässigt werden können. Oszillationen im Biofilm führen zur Abmilderung der Nährstoffbegrenzung. Sie sind ein Mittel, um eine ausreichende Nährstoffversorgung der inneren Zellen sicherzustellen. Oszillationen werden nicht mehr beobachtet, wenn ausreichend Nährstoffe vorhanden sind. Die vier Modifikationen des Modells zeigen auch, dass Minimalmodelle äußerst vielseitige Werkzeuge zur Untersuchung und Beschreibung biologischer Phänomene sind und gemäß den experimentellen Beobachtungen erweitert werden können.

Zuletzt wenden wir das Minimalmodell in einem breiteren Kontext an, um die Populationsdynamik in einer typischen Gemeinschaft eines sozialen Organismus zu verstehen. Wir betrachten drei interagierende Subpopulationen einer Art, die unterschiedliche Phänotypen haben. Keine der Subpopulationen hat einen gesamtheitlichen Vorteil gegenüber den beiden anderen. Dies führt zu einer zyklischen Dynamik wie beim Spiel Schere-Stein-Papier, das mithilfe der evolutionären Spieltheorie analysiert wurde. Wir präsentieren auch ein asymmetrisches Zwei-Spieler-Zwei-Strategie-Spiel, das dasselbe System beschreibt, wobei der Phänotyp jeder Subpopulation als Strategie betrachtet wird. Diese Untersuchung analysiert die idealen Strategien für drei verschiedene Level von Stress, die durch Antibiotika induziert sind. Wir beobachten eine Absicherung der Population durch die Produktion resistenter Zellen, die in Abwesenheit von Antibiotika eine kostspielige Strategie darstellen.

Obwohl die Studie der Populationsdynamik ein breites Anwendungsgebiet hat, diskutieren wir die Anwendung auf *B. subtilis* und Biofilmen. Bakterien sind wie Minimalmodelle von Natur aus mit den primitivsten Komponenten, die zur Durchführung der Lebensprozesse erforderlich sind, ausgestattet und zeigen ein kompliziertes soziales Verhalten, das mehrzelligen Organismen ähnelt.

Contents

I. Introduction

A. Historical background

In 1676, a draper and cloth merchant from Delft, the Netherlands had learnt the importance of microscopy. He communicated his recent observations of the natural world to the Royal Society, England. Being a cloth merchant, he was always in need of better magnifying glasses to inspect fabric quality which inspired him to learn the art of glass making. This merchant and self-taught scientist was Antonie van Leeuwenhoek and he would go on to establish a new stream of science that investigates this microscopic world – Microbiology. Being a curious man, Leeuwenhoek observed not just fabric under his lens. Of the various things he observed, he reported, along with hand-drawn illustrations, the sighting of rod shaped organisms in his tooth scrapings, which he called 'animalcules'. These organisms were later called bacteria, plural of bacterium which means staff or cane in Greek, since the very first kind of bacteria that were discovered were rod shaped. This was the first instance that we observed and got fascinated about bacterial biofilms.

Since then, we have come a long way in understanding these microscopic, unicellular organisms. Bacteria can be found everywhere: inside and outside our bodies, in the food we eat, the water we drink, the air we breathe(Mancinelli and Shulls 1978), in the depths of the ocean(Aristides Yayanos 2001), inside the international space station(Checinska Sielaff et al. 2019) or even in radioactive waste(Fredrickson et al. 2004). We now know that diseases like cholera, tuberculosis, leprosy, typhoid are caused by bacteria(Ryan 2014; Sotiriou, Stryjewska, and Hill 2016; 'Cholera vaccines: WHO position paper' 2010; Wain et al. 2015). The German physician Robert Koch played a pivotal role in introducing bacteriology to the field of medicine. This provided impetus to the development of therapeutics to treat bacterial infections. The accidental discovery of Penicillin was a turning point in the field of medicine and microbiology. This also gave rise to newer more dreaded crisis of antimicrobial resistance. We then learned that antimicrobial resistance has several mechanisms, one of which is formation of biofilms(Donlan 2000).

Not all bacteria cause disease, for example, lactobacilli are the reason we can enjoy various milk products like yoghurt, buttermilk, and kefir(Altay et al. 2013). Bacteria also help us digest food(Linares, Ross, and Stanton 2016) and produce certain vitamins(LeBlanc et al. 2013) that help in our growth and metabolism. It is therefore important to understand their metabolism in order to control their growth. The goal of this thesis is to understand the metabolic oscillations in the biofilm of *Bacillus subtilis*. Such oscillations have been reported in experiments where the authors report periodic halting in the expansion of a biofilm, growing in a microfluidics chamber(Liu et al. 2015).

B. Biological background

1. *Bacillus subtilis*

A widely studied model organism, Gram-positive, motile, facultatively anaerobic, rod shaped soil bacterium, earlier known as *Vibrio subtilis* was named *Bacillus subtilis* by Ferdinand Cohn(Cohn 1875). The average size of a typical *B. subtilis* cell is about 0.85 ±0.38 μm^3 (Maass et al. 2011). It is normally found in soil and in the gut of humans and ruminants. It helps in promoting plant growth by producing a lipopeptide antimicrobial agent, surfactin, which protects the roots from infection(Bais, Fall, and Vivanco 2004). It can form endospores which enable it to survive harsh conditions such as heat and chemical stresses. Recently, *B. subtilis* endospores were used in 3D printing and found to be viable after the process, resulting in a 'living' material which has invaluable applications in antibiotic industry, as biosensors or as a self-repair material. These printed endospore capsules could remain viable after exposure to ethanol, osmotic stress, changes in pH and even radiation(Gonzalez, Mukhitov, and Voigt 2019).

The concept of living cells enclosed in a matrix and coexisting as a community isn't something new. Bacteria have been known to live together in self-secreted matrix substances and *B. subtilis* is no exception. These communities have an intricate social structure that exhibits traits like altruism, cheating and co-operation. Based on their immediate physical environment, the cells in different regions in these communities exhibit different phenotypes. Secretion of nutrient-digesting enzymes(Drescher et al. 2014), iron-chelating siderophores(Harrison and Buckling 2009), biosurfactants for group motility(Pollak et al. 2016), and structural components for biofilm formation(Boyle et al. 2013; Dragos and Kovacs 2017) are some of the specialized roles that the cells in the community undertake. Mixed phenotype communities have been shown to perform better than communities with a single homogenous phenotype(Dragos et al. 2018). This can be attributed to the fact that in a community where cells take up specialized roles, there is no regulatory burden of switching between the different tasks. It is implied that the shared tasks are complimentary to one another and the benefits are shared among the participating subpopulations. This makes the community utilize nutrients more efficiently, leading to higher yields.

It has been shown in a study that due to frequent experimentation and growth *in vitro*, the bacteria might have become domesticated and thus lost their ability to form an architecturally robust biofilm(McLoon et al. 2011). The study compares the laboratory strain 168 with the wild type strain NCIB3610 in terms of architecture. They identify four gene mutations, namely *sfp*, *epsC*, *swrA*, and *degQ* (see table 1B) as a cause for the inability of the laboratory strain to form robust biofilms.

Additionally, they also identify a large plasmid present in NCIB3610 but not in 168 that contains a gene *rapP*, which also plays a role in the biofilm architectural complexity.

2. Biofilms

Biofilms are an aggregation of one or more types of bacteria or sometimes even fungi(LeBlanc et al. 2013). Biofilms have been hypothesized to have originated as a defense mechanism of primitive prokaryotes from the harsh conditions of the primitive earth environment(Hall-Stoodley, Costerton, and Stoodley 2004). In addition, biofilms have also been thought of as the attempt of single celled prokaryotes to cooperate and coexist as a community, which laid the foundations of multicellularity(Claessen et al. 2014a).

Bacterial biofilms can be found on a solid surface or floating on top of liquid as a pellicle. Dental plaque is the most relatable encounter of an average human with biofilms. They are a major nuisance if they grow on implants or catheters(Nickel and Costerton 1992; Hall-Stoodley and Stoodley 2009). They also clog pipes and drains in industries(Yan et al. 2009). On the other hand, biofilms play a critical role in bioremediation(Singh, Paul, and Jain 2006), are an excellent source of energy in the form of microbial fuel cells(Logan 2009), and are also invaluable in the commercial production of vitamins(Mahdinia, Demirci, and Berenjian 2019). The extracellular polymeric substances that form the matrix of the biofilm are predominantly exopolysaccharides, amyloid fibers and nucleic acids(Branda et al. 2006). *Bacillus subtilis* biofilms, in particular, are comprised of poly-N-acetyl glucosamine as a predominant polysaccharide(Roux et al. 2015) and an amyloid like protein *tasA*(Romero et al. 2010). The fifteen-gene exopolysaccharide operon *epsA-O* and the three-gene operon *tapA-sipW-tasA* mediate the formation of the biofilm. A potent repressor of both these operons, *sinR*, acts on several sites in the promoter regions of these operons, thus exerting direct negative control(Chu et al. 2006). Tables 1*Table 1*A-B summarize the function of each of these genes as they appear in the SubtiWiki database(Zhu and Stülke 2017).

Table 1A: Genes involved in the biofilm matrix production.

Name	Function
epsA	putative transmembrane modulator of EpsB activity
epsB	protein tyrosine kinase, phosphorylation of EpsE
epsC	UDP-N-acetylglucosamine 4,6-dehydratase, biosynthesis of N,N'-diacetylbacillosamine. (inactive in *B. subtilis* 168)

epsD	similar to glucosyltransferase
epsE	glycosyltransferase, inhibitor of motility
epsF	similar to glucosyltransferase
epsG	Transmembrane protein of glucosyltransferase family.
epsH	undecaprenyl (UnDP) priming UDP-N-acetyl-glucosamine transferase
epsI	glycosyltransferase, synthesis of extracellular poly-N-acetylglucosamine
epsJ	UDP-N-acetyl-glucosamine transferase, synthesis of extracellular poly-N-acetylglucosamine
epsK	export of extracellular poly-N-acetylglucosamine
epsL	similar to UDP-galactose phosphate transferase
epsM	UDP-2,4,6-trideoxy-2-acetamido-4-amino glucose acetyltransferase
epsN	UDP-2,6-dideoxy 2-acetamido 4-keto glucose aminotransferase
epsO	similar to pyruvyltransferase
tapA	TasA anchoring/assembly protein. Minor component of TasA fibers.
sipW	bifunctional signal peptidase I. Cleavage of hydrophobic, N-terminal signal or leader sequences from TasA and TapA(Stover and Driks 1999b, 1999a). Only required for formation of biofilms on solid surfaces(Terra et al. 2012).
tasA	28.15 kDa amyloid protein(Romero et al. 2010). Major component of TasA fibers.

Table 1B: Genes that indirectly influence biofilm formation.

Name	Function
sfp	4-phosphopantetheinyl transferase (surfactin synthetase-activating enzyme), inactive pseudogene in strain 168
swrA	Main activator of flagellar biosynthesis, modulator of DegU activity, converts DegU-P from a repressor to an activator of the fla-che operon, enhances sigD transcription, and controls the number of flagellar basal bodies, inactive pseudogene in strain 168.

degU	two-component response regulator, regulation of degradative enzyme expression, genetic competence, biofilm formation, capsule biosynthesis (together with SwrA), non-phosphorylated DegU is required for swarming motility

This matrix not only keeps the individual cells together but also participates in migration, exchange of genetic material and nutrients, and signaling(Dragoš and Kovács 2017). Within the biofilm community, various cells take up specialized roles. This division of labor facilitates better growth rates, thus making the biofilm community greater than the sum of its parts(Dragoš et al. 2018).

3. Why are biofilms so resilient to antibiotics?

Biofilms, although made mostly of water, consist of exopolyssacharides, DNA, and amyloid fibres(Stewart 2002). Amyloids are known to be hydrophobic(Zeng et al. 2015). This might retard the diffusion rate in the biofilm matrix. Solutes of the size of a typical antibiotic compound diffuse at a much slower rate in biofilms, as compared to that in pure water(Stewart 1998). This has also been measured in polysaccharide or glycoprotein gels which show diffusion rates of 36% to 76% of that in pure water(Cheema, Rassing, and Marriott 1986). This alone however, cannot explain why antibiotics are so ineffective against biofilms. In addition to reduced mobility, another hurdle faced by antibiotics is the extracellular inactivation by a resistance factor or sequestration to the biofilm matrix during diffusion. For example, penicillin can be inactivated during diffusion in the biofilm by a beta lactamase positive bacterium(Anderl, Franklin, and Stewart 2000). Positively charged aminoglycosides bind to the negatively charged matrix polymers which also retards the diffusion of these antimicrobial agents(Kumon et al. 1994; Gordon, Hodges, and Marriott 1988). In addition to retarding and immobilizing antibiotics, rapid degradation is also critical to mitigate the insults of the antibiotic substance. In spite of this, in most of the examples in which effective antibiotic penetration has been demonstrated experimentally, the investigators report survival of the test microorganism(Darouiche et al. 1994; Dunne, Mason, and Kaplan 1993; Anderl, Franklin, and Stewart 2000). This indicates the presence of yet another mechanism that helps biofilms tackle the challenges of antibiotics.

Biofilms often have micro gradients of different substances leading to different metabolic states of cells in different locations of the biofilm. Antibiotics like penicillin, only target metabolically active (growing) cells(Tuomanen et al. 1986). This leaves out the cells in stationary phase unharmed. Bacteria from an aerobic region of the biofilm may show higher resilience to aminoglycosides as compared to those in the anaerobic regions since these antibiotics are strongly inhibitory to anaerobes(Tack and Sabath 1985).

Hence it is difficult to expose the bacteria within a biofilm to a minimal inhibitory concentration (MIC) of the antimicrobial agent. MIC is the lowest amount of antimicrobial substance required to inhibit the bacterial cells. This enables bacteria to develop strategies to evade or neutralize the particular antimicrobial substance in case of exposure in future.

An experimental study by Liu *et. al.*(Liu et al. 2015) investigates a biofilm of *B. subtilis* growing in a thin microfluidics chamber (3mm x 3mm x 6µm), where glutamate is the only source of carbon and nitrogen. It was observed that under such limited nutrient availability, the biofilm population shows a periodic halting of growth. This was further shown to revolve around the metabolism of ammonia. The biofilm as shown in figure I is divided into two compartments - the interior and the periphery. Cells in the periphery have an advantage of obtaining glutamate directly from the environment, enabling a higher growth rate compared to the interior cells. On the downside, they also risk losing small molecules like ammonia to the environment readily. Cells in the interior feed on the 'leftover' glutamate that diffuses in from the periphery, resulting in a sluggish rate of growth. Additionally, the ammonia produced by the interior cells is not directly lost to the environment but instead can be used by the surrounding cells of the periphery.

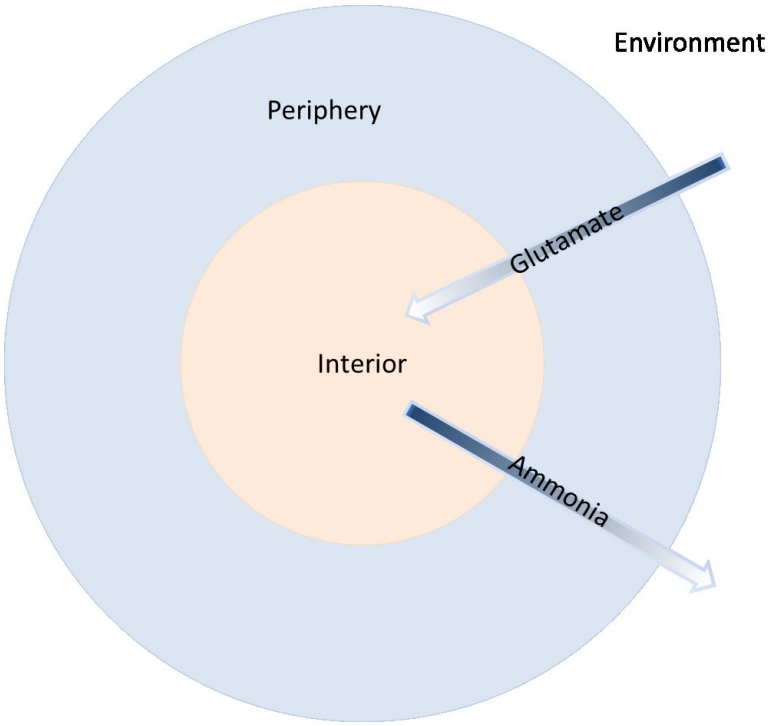

Figure I: Overview of the metabolite gradients in the biofilm. The gradient fades from blue (high concentration) to white (low concentration).

Thus interior cells monopolize the production of ammonia for not just themselves but also for the peripheral cells. In exchange, the periphery shields them from physical and chemical attacks. Ammonia

is a valuable source of nitrogen which is used along with glutamate to produce glutamine. Glutamate is also an ammonia donor for several other amino acids, all of which together form proteins which are considered a proxy for growth. Thus, by controlling the production of ammonia, the interior cells assume a direct control over the growth rate of the peripheral cells. This control enables them to prevent indefinite expansion of the peripheral cells which would make it harder for the interior cells to obtain glutamate. Thus, when peripheral cells grow rapidly, the interior cells begin to starve. This causes ammonia production to plummet, which in turn halts the expansion of the periphery. This restores the supply of glutamate and also the production of ammonia and subsequently, the growth of the periphery. Thus ammonia causes the growth to periodically halt, leading to oscillations. The aim of this study is to model these oscillations using a minimal number of ordinary differential equations (ODEs).

4. Population dynamics of Biofilms

Biofilms are a society of bacteria that is formed when a quorum of cells aggregate(Davey and O'Toole 2000). Bacteria sense this through 'quorum sensing'(Li and Tian 2012), which is a process by which they communicate with each other by releasing and sensing small molecules . These communities show several social dynamics and clustering into micro colonies(Nadell, Drescher, and Foster 2016a). Game theory has been used to study population dynamics of microbial communities(Li et al. 2015). In such an approach, cells are often considered as 'players' and their phenotype is considered as the 'strategies'(Hummert et al. 2014). These strategies are given payoffs and the best strategy is the one that earns the player the highest payoff. The game can be played with the cells of same or different species, so it can model co-operation or competition between two strains(Zomorrodi and Segrè 2017), or the division of labour, altruism and cheating within a population(Schuster et al. 2010); or it could also be used to describe host pathogen interactions(Ewald et al. 2019).

C. Mathematical background

1. Oscillations

Our natural world consists of several phenomena that are periodic in space or time. The rotation of the earth creates cycles of day and night which is the basis for several biological oscillations and also forms the external driving force of circadian rhythms, which is roughly a 24 hour cycle of physiological events in all living beings(Edgar et al. 2012). The movement of the earth around the sun also creates seasons which are periodic on a larger timescale. The movement of the moon around the earth has an effect on the earth's hydrosphere as the gravitational pull of the moon influences the tides in our

oceans. Oscillations can be caused due to either of these mechanisms: positive or negative feedback, time delay, noise and nonlinear nature of regulation (references follow in paragraphs below).

A very common mode of oscillations is through negative feedback(Novak and Tyson 2008). However, it needs to be coupled with other mechanisms in order to obtain self-sustained intrinsically driven oscillations. Gene expression with a negative feedback mechanism is stabilized when the time delay in the feedback loop is minimized(Becskei and Serrano 2000). It intuitively follows that, to obtain oscillations, the delay needs to be introduced. One such example of time delay is gene expression(Monk 2003). The signaling part of the gene expression pathway is fast but once the expression starts, the transcript takes much longer to be fully formed, thus introducing delay. This effect is especially pronounced when it involves a cascade that incorporates multiple intermediate regulation steps(Hooshangi, Thiberge, and Weiss 2005). The downside of delay driven negative feedback oscillators is that they are prone to noise, especially when regulatory components are present in low amounts(Bratsun et al. 2005). Integrated positive and negative feedback can help mitigate the effects of noise and increase tunability of parameters(Pomerening, Sontag, and Ferrell 2003).

Positive feedback along with delay can lead to relaxation oscillations characterized by accumulation of a typical activator up to a certain threshold followed by its self-repression in a switch-like fashion, leading to 'relaxation'(Ferrell, Tsai, and Yang 2011).

Nonlinear regulation can generate oscillations. The Goodwin oscillator, used to model circadian and other genetic oscillations in biology, consists of a single negative feedback and a nonlinear Hill term(Goodwin 1965). It is as follows:

$$\frac{dX}{dt} = k_1 \frac{K_i^n}{K_i^n + Z^n} - k_2 X \qquad \text{(G1)}$$

$$\frac{dY}{dt} = k_3 X - k_4 Y \qquad \text{(G2)}$$

$$\frac{dZ}{dt} = k_5 Y - k_6 Z \qquad \text{(G3)}$$

The regulation is considered non-linear when n>1, however, self-sustained oscillations are obtained only when n>8. Such a high value of non-linearity is deemed unrealistic especially considering simple co-operative dynamics. However, it is shown to be a good one-step approximation of multiple steps provided that they are fast enough. For example, for pathways involving several (de-)phosphorylation steps which are fast enough, the dynamics obtained by the multistep phosphorylation mechanism are in good numerical agreement with the Goodwin model(Gonze and Abou-Jaoude 2013). If *X*, *Y* and *Z* are the concentrations of mRNA of a particular gene, its protein product, and its transcriptional

inhibitor respectively, the high non-linearity (for example, n>8) creates a time delay in the action of the inhibitor which is negligible until it crosses a certain threshold.

Noise is typically detrimental, but sometimes it could be the source of oscillations; for instance, when feedback is simply not sufficient. A study shows that fluctuations in temperature are sufficient to induce oscillations in a non-isothermal chemical system containing a single negative feedback loop, in the absence of any deterministic limit cycle or periodic forcing(Simakov and Pérez-Mercader 2013). Another example of noise driven oscillators is found in bacterial cell size. A typical bacterial cell approximately doubles in size before dividing into two daughter cells. A larger cell will thus divide sooner than a smaller cell. This effect is described by a linear map. A study shows a subset of cell population that exhibits periodicity in cell size that spans across several generations(Tanouchi et al. 2015). The study points out that a noisy linear map helps explain these oscillations i.e. a cell with a larger size divides sooner than a smaller one.

2. Why choose a minimal system?

A well-known principle in philosophy states that if there are two explanations for a phenomenon, the one that uses the least number of assumptions is usually the correct one, or at least the more appropriate one. This is known as Occam's razor, which helps shave off unlikely explanations(Garrett 1991). A typical model contains variables which represent the dynamic components of a phenomenon. Variables can be linked to each other or to time derivatives of variables using parameters. The value of a parameter can either be estimated from experimental data or assumed to have an arbitrary value. This makes it a major source of error. A minimal model implies the least possible number of variables which will contain the least possible number of parameters. One may argue whether minimal models are more accurate than larger models or not. At least they are easy to analyze analytically or numerically due to the low number of parameters. Often they are sufficient to describe the essential features of the phenomenon under study.

A minimal model has been used to describe food absorption in the gut(Worthington 1997). Those authors present three progressively complex models that describe the conversion of two different foods in the gut to the appearance of glucose in the blood plasma. They have shown that the predictions of the minimal model matched the experimental results. This model eliminates the parameters like insulin sensitivity and insulin response, which vary from one person to another. It estimates the parameters such as the percent of the food that appears as plasma glucose, the fractional turnover rate and the transport delay which only vary with the type of food and not with the physiological state of the person eating the food. It is thus much easy to estimate how a particular food will affect the blood sugar which is critical for diabetics.

Another minimal model describes inhibition of tumor growth(Magni* et al. 2008). It is a probabilistic model based on minimal number of assumptions at cellular level. The result is a stochastic cell population model which is used to obtain the growth dynamics of tumor mass. Three cellular phenomena are considered for the model: cell birth, damage inflicted by the drug and the delay between drug action and cell death. The popular tumor growth inhibition model(Simeoni et al. 2004) is a special case of the minimal model presented here and has been widely applied to study the effects of anti-cancer drugs on the inhibition of tumors.

3. Making a minimal model for oscillations

Let us consider a one variable system for describing oscillations. Let μ be the growth rate of our biofilm which oscillates over time. Using nothing but ODEs, the only possible way to obtain oscillations in variable μ, is through an external driving force. This can easily be modeled by a sine function which is periodic in time. The biological driving force is the supply of nutrients, i.e. glutamate which needs to be periodic in time in order to obtain oscillations in our model. This can easily be achieved using a periodic feeding regime which ensures the exact same amounts of glutamate at regular intervals of time. To ensure a sinusoidal pattern of nutrient supply, they can be injected in the microfluidics chamber gradually over a period of time exactly equal to a quarter period of oscillation. However, in the experimental setup of Liu *et. al.*, the nutrients are supplied at a constant rate and the oscillations arise out of a co-operative relationship between the interior and the peripheral cells of the biofilm. In other words, the oscillations are intrinsic. It is possible to obtain intrinsic oscillations in a one variable system using a delay differential equation (DDE). This means, the derivative of our function μ at a particular time denoted as μ_t is given in terms of the values of the function at previous times ($\mu_{t-\tau}$), where τ is the time delay. This implies that the value of μ depends on infinitely many values of τ. This makes our variable infinite dimensional which goes against our condition for minimality.

Let us consider a two variable system, where variable *A* represents the level of ammonia, and variable *G* that of glutamate. Growth rate μ can be expressed in terms of *A* and *G* but is not a part of the model. American mathematician Alfred Lotka independently of the Italian mathematician Vito Volterra proposed a model to describe predator-prey interactions(Lotka 2002). Their system comprised of two variables which can be applied to the biofilm system, as follows:

$$\frac{dA}{dt} = \alpha A - \beta AG \qquad \text{(L-V1)}$$

$$\frac{dG}{dt} = \delta AG - \gamma G \qquad \text{(L-V2)}$$

Although minimal in terms of number of variables, the system involves two bilinear terms in each of the equations, which could be reduced to one or, more ideally, zero bilinear terms to further simplify the model. Other newer two-variable oscillators include the Higgins-Selkov model(Higgins 1967; Sel'kov 1968) which also has two non-linear terms and the Brusselator model(Prigogine and Lefever 1968) which has two terms of the third degree.

Let us look at a three-variable system. Wilhelm and Heinrich had proposed a three-variable oscillator for chemical systems(Wilhelm and Heinrich 1995). They enlisted in decreasing order of importance, four features for minimality for a model aimed at describing oscillations:

1. Lowest number of reactants
2. Lowest number of quadratic terms
3. Minimal number of parameters i.e. minimal number of reactions
4. Minimal number of bimolecular reactions.

In this sense they present their smallest chemical oscillator model with only upto bimolecular reactions (bilinear terms). The model includes five reactions and three species *X*, *Y* and *Z* with variable concentrations. Their model is as follows:

- $\frac{dX}{dT} = k_1AX - k_4Z - k_2XY$ (W-H1)
- $\frac{dY}{dt} = -k_3Y + k_5Z$ (W-H2)
- $\frac{dZ}{dt} = k_4X - k_5Z$ (W-H3)

In the following chapters we will see how this model can be used to described oscillations in *Bacillus subtilis* biofilms

II. Differential equation based minimal model describing metabolic oscillations in *Bacillus subtilis* biofilms

Ravindra Garde, Bashar Ibrahim, Ákos T. Kovács, Stefan Schuster

Published in Royal Society Open Science, volume 7, issue 2, Published on 5th February 2020

Here we describe the periodic halting of growth in the biofilm of *Bacillus subtilis* using three ODEs. This is based on the smallest Chemical oscillator proposed by Wilhelm and Heinrich in 1995. This work highlights the strength of minimal models and also investigates the mechanism of oscillation – a negative feedback loop along with nonlinearity. It further investigates the sensitivity of the model to its parameters. Furthermore, the study indicates that oscillatory growth may not be favorable since the steady state growth rate exceeds it within the first 11 hours.

I performed the simulations, wrote the manuscript and interpreted the results. Prof. Bashar Ibrahim carried out the mathematical analyses and supervised my work. Prof Stefan Schuster suggested the use of the smallest chemical oscillator by Wilhelm and Heinrich, performed the mathematical analysis, refined and structured the manuscript, supervised my work and helped in the interpretation of the results mathematically and biologically. Prof. Ákos T. Kovács helped in the interpretation of the results and edited and structured the manuscript.

ROYAL SOCIETY OPEN SCIENCE

royalsocietypublishing.org/journal/rsos

Research

Cite this article: Garde R, Ibrahim B, Kovács ÁT, Schuster S. 2020 Differential equation-based minimal model describing metabolic oscillations in *Bacillus subtilis* biofilms. *R. Soc. open sci.* **7**: 190810.
http://dx.doi.org/10.1098/rsos.190810

Received: 15 May 2019
Accepted: 15 January 2020

Subject Category:
Mathematics

Subject Areas:
systems biology/computational biology/mathematical modelling

Keywords:
metabolic oscillations, *Bacillus subtilis*, minimal model, biofilm, Hopf bifurcation, glutamate metabolism

Author for correspondence:
Stefan Schuster
e-mail: stefan.schu@uni-jena.de

Electronic supplementary material is available online at https://doi.org/10.6084/m9.figshare.c.4828275.

THE ROYAL SOCIETY PUBLISHING

Differential equation-based minimal model describing metabolic oscillations in *Bacillus subtilis* biofilms

Ravindra Garde[1,2], Bashar Ibrahim[1,4,5], Ákos T. Kovács[3] and Stefan Schuster[1]

[1]Department of Bioinformatics, Matthias Schleiden Institute, Friedrich Schiller University Jena, Ernst-Abbe-Platz 2, 07743 Jena, Germany
[2]Max Planck Institute for Chemical Ecology, Hans-Knöll-Strasse 8, 07745 Jena, Germany
[3]Bacterial Interactions and Evolution Group, DTU Bioengineering, Technical University of Denmark, Søltofts Plads Building 221, 2800 Kgs. Lyngby, Denmark
[4]Centre for Applied Mathematics and Bioinformatics, and [5]Department of Mathematics and Natural Sciences, Gulf University for Science and Technology, Hawally 32093, Kuwait

BI, 0000-0001-7773-0122; ÁTK, 0000-0002-4465-1636; SS, 0000-0003-2828-9355

Biofilms offer an excellent example of ecological interaction among bacteria. Temporal and spatial oscillations in biofilms are an emerging topic. In this paper, we describe the metabolic oscillations in *Bacillus subtilis* biofilms by applying the smallest theoretical chemical reaction system showing Hopf bifurcation proposed by Wilhelm and Heinrich in 1995. The system involves three differential equations and a single bilinear term. We specifically select parameters that are suitable for the biological scenario of biofilm oscillations. We perform computer simulations and a detailed analysis of the system including bifurcation analysis and quasi-steady-state approximation. We also discuss the feedback structure of the system and the correspondence of the simulations to biological observations. Our theoretical work suggests potential scenarios about the oscillatory behaviour of biofilms and also serves as an application of a previously described chemical oscillator to a biological system.

1. Introduction

Development of a complex biofilm provides several benefits to bacteria, including efficient nutrient distribution, defence from chemical attacks or, in the case of a floating pellicle on the surface of liquids, better gaseous exchange [1]. Biofilms are thus complex communities of bacteria and as such, many types of

social dynamics come into play [2,3]. One of these is the division of labour [4,5]. The core of the biofilm growing on a solid surface shows a different metabolic state than the periphery. The periphery can freely access the nutrients from the surrounding environment. The interior, however, faces hindrance in obtaining a stable inflow of nutrients because the peripheral cells use up the nutrients that diffuse towards the interior. An experimental set-up to simulate that situation is provided by a microfluidics chamber [4].

An example of such a nutrient gradient is the production and diffusion of ammonia in the biofilm. Every cell in the biofilm has the ability to produce ammonia [4,6]. However, this small chemical compound is highly diffusive and therefore escapes into the environment as soon as it is produced by the cells in the periphery, thus leading to waste of nitrogen. In the interior, the ammonia produced by the cells diffuses out into the periphery. Thus, the interior cells monopolize ammonia production for the entire biofilm. Ammonia being an essential component of glutamine metabolism could be used to control the growth rate of the periphery by limiting its supply. The interplay between the inner and outer cells is required for glutamine synthesis and therefore the growth of the biofilm [4,6,7].

To understand biofilms more closely and make predictions based on empirical data, several models have been developed [4,7–12]. Liu *et al.* [4] observed oscillations in the biofilm, which they explained by different metabolic roles performed by the different compartments in the biofilm. They also established a model based on six differential equations. They defined two regions: the interior and periphery. Each of the regions has a variable representing glutamate and another representing the concentration of housekeeping proteins like ribosomal proteins. Ammonia and the active form of the enzyme glutamate dehydrogenase are also variables of the model.

Since many biological oscillators have been described by less than six variables [13,14], a simpler model could be established for biofilm oscillations as well. Our ultimate aim was to develop a minimal model to describe the metabolic oscillations happening in a biofilm. Minimal models are the simplest way to describe a certain phenomenon with the least number of parameters [15] and this is in agreement with Occam's razor. For example, minimal models were established for glycolytic oscillations by Higgins [16] and Sel'kov [17] and for calcium oscillations by Somogyi & Stucki [18].

Here, we employ the smallest chemical reaction system showing a Hopf bifurcation [19], which was further analysed [20,21] and used to describe p53 oscillations [22]. At a Hopf bifurcation, damped oscillations turn into undamped oscillations [15,23]. In particular, Wilhelm & Heinrich [19,20] performed a thorough stability analysis of the model. We test to what extent the terms in this model match the processes in a biofilm system. In this analysis, we focus on the Hopf bifurcation, discuss the feedback structure and point out the correspondence of the simulations to biological observations.

In our model, we use three variables only: ammonia, and interior and peripheral glutamate. Besides the quest for minimality, a reason for not considering the concentrations of housekeeping proteins as variables is that they change on a longer time-scale than metabolites. A similarity to the larger Liu model [4] is that, among the various amino acids, we focus on the metabolism of glutamate since glutamate and ammonia are both involved in the production of various amino acids through *trans*-amination, which is then equated to growth.

To study the effect and possible benefit of oscillations, it is of interest to compute the average values of variables, as was done for several oscillators [24–29]. For linear differential equation systems showing oscillations (such as the system describing the harmonic pendulum), the average values equal the values at the marginally stable steady state. For nonlinear differential equation systems, the average values often differ from the values at the unstable steady state surrounded by the oscillations. However, there are some types of nonlinear systems for which equality holds, for example, Lotka–Volterra systems of any dimension [25]. The equality property has also been proved for some models of calcium oscillations [27,30] and the Higgins–Selkov oscillator [27]. Here, we probe the model employed for describing biofilm oscillations for the above-mentioned property.

2. Material and methods

2.1. The model

Based on the scenario described by Liu *et al.* [4], the biofilm was separated into two compartments—the interior and the periphery. Here, we use a minimalist approach and try to model biofilm oscillations with the simplest model possible. Accordingly, we use the smallest chemical reaction system with Hopf

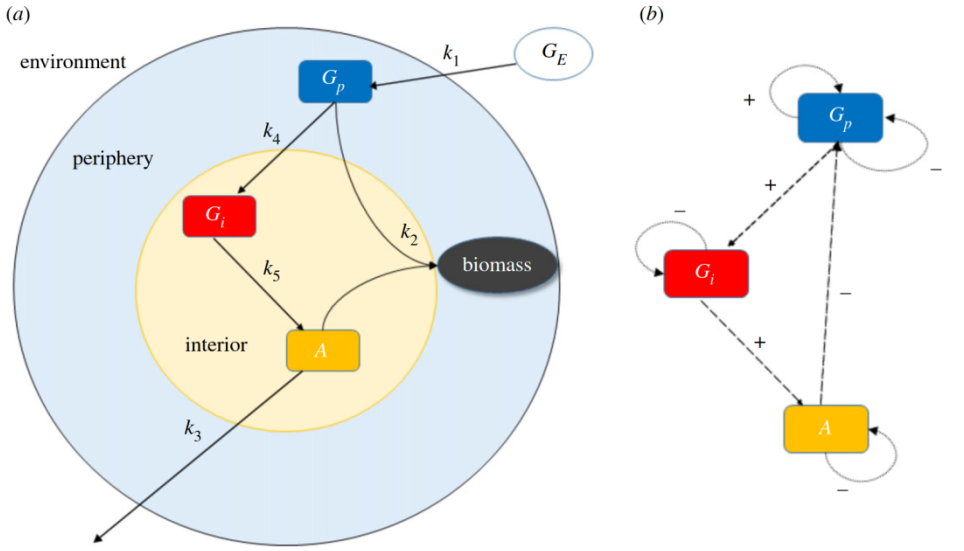

Figure 1. Schematic of the biofilm metabolic oscillation model. (*a*) The five reactions with rate constants k_1 through k_5 between the substances G_i, G_p, A having variable concentrations and G_E considered to be constant. The final result is the production of biomass. (*b*) Feedback structure of the model. G_p is self-amplifying while all three variables are self-degrading. G_p positively influences G_i, which positively influences A which negatively influences G_p, thus, the overall feedback is negative.

bifurcation [19]. The term chemical system mathematically means that only up to bilinear terms are involved. It turns out that this model matches the biological set-up.

The model includes five reactions (figure 1) and three species with variable concentrations. The general variables X, Y and Z from the Wilhelm and Heinrich model can be assigned for the biofilm system to: peripheral glutamate (G_p), ammonia (A) and internal glutamate (G_i), respectively. Based on mass-action kinetics, the reactions have been translated as follows into a system of ordinary differential equations (ODEs):

$$\frac{dG_p}{dt} = k_1 G_E G_p - k_4 G_p - k_2 A G_p, \tag{2.1a}$$

$$\frac{dA}{dt} = -k_3 A + k_5 G_i \tag{2.1b}$$

and

$$\frac{dG_i}{dt} = k_4 G_p - k_5 G_i. \tag{2.1c}$$

Model assumptions and interpretation of terms in the model:

— $k_1 G_E G_p$: The uptake of glutamate from the environment (G_E) by the periphery of the biofilm. G_E is supplied in a large excess, hence considered constant. The uptake of glutamate (G_p) is dependent on itself because glutamate represents the total amino acid and thus protein concentration in the biofilm periphery and can be assumed, in rough approximation, to be proportional to the concentration of various transport proteins embedded in the cell membranes. The greater the concentration of these proteins, the higher is the glutamate uptake rate. Without this self-amplification of glutamate, the system would not oscillate by construction of the minimal model.
— $k_4 G_p$: Diffusion of glutamate from the periphery of the biofilm into its interior. We do not consider self-amplification by G_i in the main text. We analysed the effect of self-amplification of G_i using the term $k_4 G_i G_p$ (electronic supplementary material, figure S4).
— $k_2 A G_p$: Consumption of glutamate and ammonia to produce biomass. As a simplification, we assumed that only the interior cells produce ammonia since that produced by the peripheral cells is rapidly lost to the environment.
— $k_5 G_i$: Consumption of glutamate to produce ammonia.
— $k_3 A$: Diffusion of ammonia into the surroundings. The loss of ammonia due to diffusion is much larger than that taken up by the periphery to produce biomass. Therefore, the term $k_2 A G_p$ does not appear in equation (2.1*b*).

Table 1. List of parameters used in the model. For explanations, see text.

parameter	symbol	value with unit
rate constant of glutamate diffusion from environment to biofilm	k_1	0.3426 (mmol l^{-1} $h)^{-1}$
biomass formation coefficient	k_2	5.3 (mmol l^{-1} $h)^{-1}$
rate constant of ammonia diffusion [32]	k_3	4 h^{-1}
rate constant of glutamate diffusion within biofilm [33,34]	k_4	2 h^{-1}
ammonia production coefficient	k_5	2.3 h^{-1}
glutamate concentration in the environment [4]	G_E	30 mmol l^{-1}
conversion factor for biomass production	b	0.1 ((mmol $l^{-1})^2$ $h)^{-1}$

2.2. Simulation

For computer simulations, we used the software COPASI v. 4.16 and 4.24 [31] and its LSODA deterministic solver. The simulations were double-checked using the Matlab ode15s (MathWorks) function. The figures of the simulations were produced using COPASI, and the three-dimensional (3D) phase plot was generated using the lines3D function of R plot3D library. The biomass plot was generated using the R function ggplot.

Parameter values are given in table 1. They are obtained by rescaling the parameter values from the Wilhelm & Heinrich paper [19] such that the oscillation period observed in the experimental work by Liu *et al.* [4] is matched. The glutamate concentration in the environment was adopted from the Liu *et al.* paper [4]. We have chosen the rate constant of diffusion of ammonia, k_3, to be twice as high as that of glutamate, k_4. This is because the diffusion coefficient for ammonia [32] is about 1.6×10^{-5} cm^2 s^{-1}, while that for glutamate [33,34] is about 8×10^{-6} cm^2 s^{-1}. k_1 and k_2 had to be increased in order to obtain undamped oscillations and to match the same period. Overall, the parameters allow a good comparison to the results by Wilhelm & Heinrich [19], while also being realistic from a physico-chemical point of view.

The predicted doubling time was calculated by averaging the relative increase in biomass at four consecutive time points of the maxima of ammonia concentration.

3. Results

3.1. Steady states

The steady states of the system can be calculated analytically. This gives a trivial steady state (TSS)

$$G_p = A = G_i = 0 \tag{3.1}$$

and a non-trivial steady state (NTSS)

$$G_{p,\mathrm{ss}} = \left(\frac{k_1 G_E - k_4}{k_2 k_4}\right) k_3 \tag{3.2a}$$

$$A_{\mathrm{ss}} = \frac{k_1 G_E - k_4}{k_2} \tag{3.2b}$$

and

$$G_{i,\mathrm{ss}} = \left(\frac{k_1 G_E - k_4}{k_2 k_5}\right) k_3. \tag{3.2c}$$

It is worth noting that the concentrations at the latter state are linear functions of G_E. The TSS and NTSS are stable if $k_1 G_E - k_4$ is negative or positive, respectively [19]. At the threshold, a transcritical bifurcation [35] occurs; that is, the two steady states interchange their stability. At a further threshold, $k_1 G_E = k_3 + k_4 + k_5$, the stable NTSS turns unstable in a Hopf bifurcation [19].

3.2. Time course shows oscillations

We run the time course calculation of the system (2.1*a–c*) for 25 simulation hours with 1000 steps each of size 0.025 h (1.5 min). The period for oscillations is about 126 min (2 h 6 min), which is in agreement with

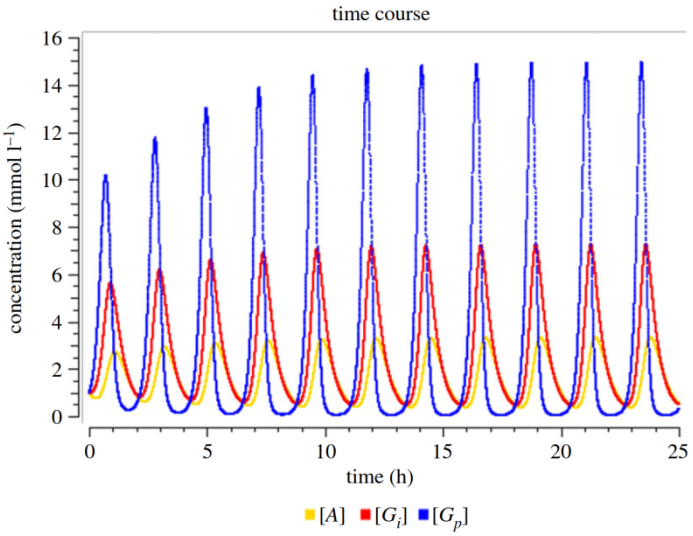

Figure 2. Time course of ammonia (yellow) and interior (red) and peripheral (blue) glutamate as computed by the minimal model. Parameter values: refer to table 1.

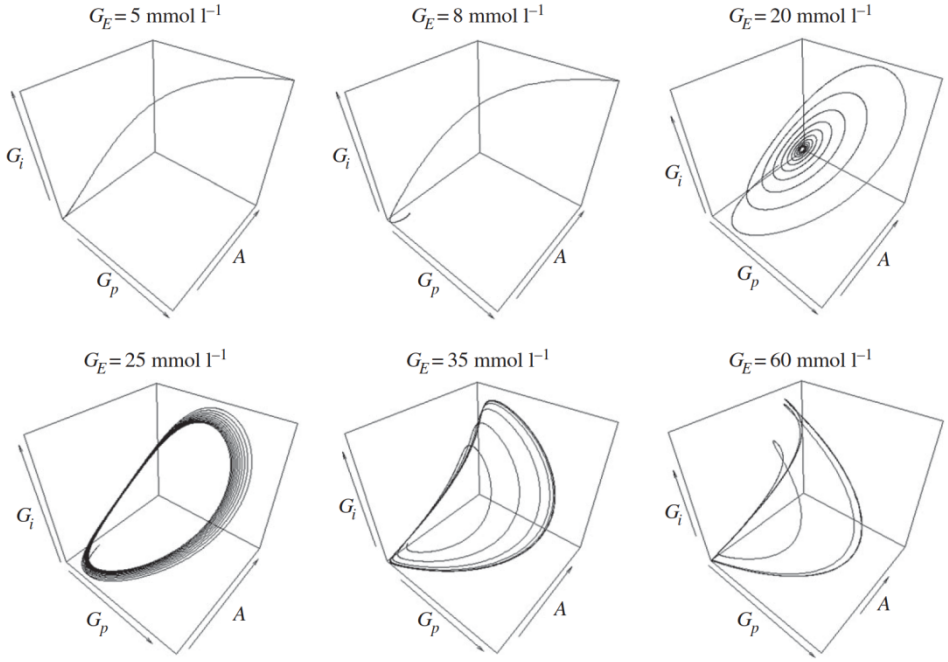

Figure 3. Three-dimensional phase portrait of all the variables at various values of G_E. The trajectory runs anti-clockwise in the perspective shown here. Top three trajectories from left to right depict approaches towards: the TSS, the NTSS in a non-oscillatory way and the NTSS by damped oscillations. The bottom three trajectories depict the convergence towards limit cycles beyond the Hopf bifurcation ($G_E = 24.41$). For parameter values except G_E, see table 1.

the experimental observations [4], because the parameters have been rescaled accordingly (see above). The amplitude of oscillations is observed to be 3.0 mmol l^{-1} for ammonia, 7.1 mmol l^{-1} for interior glutamate and 14.9 mmol l^{-1} for peripheral glutamate (figure 2). It can be seen that the three variables oscillate with phase shifts, i.e. asynchronously.

In order to see the interdependence between the variables of our model, we plot the phase portrait of all three variables for various values of G_E (figure 3). G_E is an appropriate bifurcation parameter because

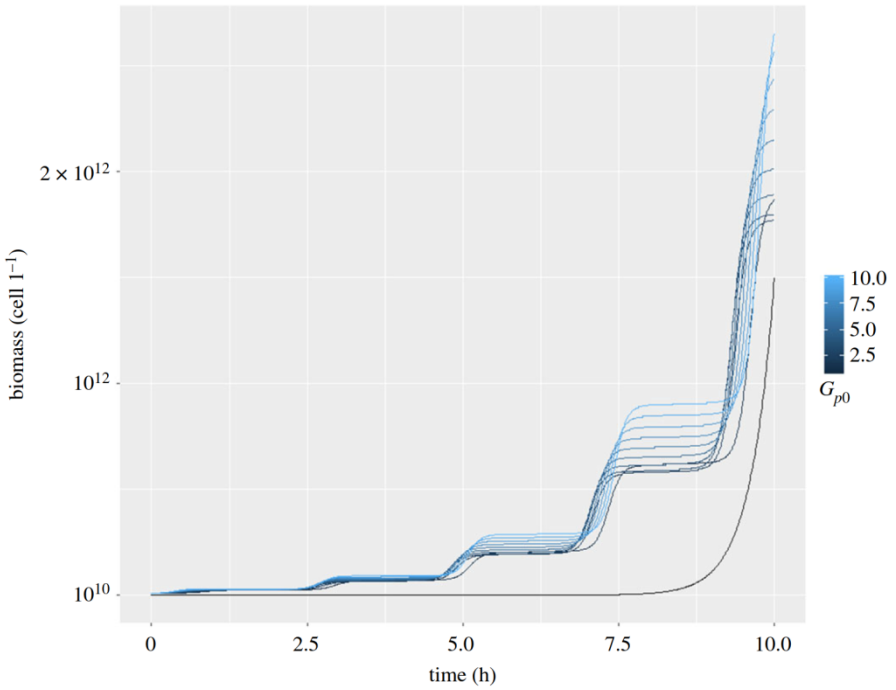

Figure 4. Plot of the time course of growth as calculated from equation (3.4) for various initial values of G_p from 1 to 10 mmol l^{-1} with a step size of 1 mmol l^{-1} (all wavy curves). We took 10^{10} cells l^{-1} as the initial value of B. On average, the curves have a doubling time of about 99 min. The black monotonic curve (initial value: 10 cells l^{-1}) indicates the growth calculated by the steady-state values.

the external glutamate concentration can be changed in experiment. Wilhelm & Heinrich [19] presented a similar figure for the vicinity of the Hopf bifurcation. In our figure 3, also the non-oscillatory relaxation towards the TSS and NTSS for appropriate parameter values is shown. G_E values below 15 mmol l^{-1} eliminate the oscillations (even damped ones).

As per the assumptions of our model, k_2AG_p is a proxy for the input for the synthesis of biomass from ammonia and glutamate and is thus related to the growth of the biofilm. Biomass production can be described by the following differential equation:

$$\frac{\mathrm{d}B}{\mathrm{d}t} = bAG_pB, \tag{3.3}$$

where b is a conversion factor and was tuned to 0.1 ((mmol l^{-1})^2 h)$^{-1}$ so that the doubling time is in agreement with the experimental values [36]. The number of cells can be converted to biomass by taking the volume of a typical *B. subtils* cell of about 0.85 ± 0.38 µm^3 [37] and the average density of 1 g ml^{-1} which results in $8.5 \pm 0.38 \times 10^{-13}$ g cell^{-1}. The numerical solution of equation (3.3) for various initial values of G_p is shown in figure 4. It can be seen that there is periodic retardation in growth.

Figure 4 also displays the growth curve in the hypothetical case where G_p and A subsisted at steady state (black curve).

The initial value of G_p for the growth with constant growth rate (black monotonic curve) was chosen such that biomass is comparable to that for oscillating growth in the first 10 h. If the same initial values as for the growth with varying growth rate were chosen, biomass would grow to higher values right from the beginning. Thus, the numerical calculations suggest that oscillating growth for this system is not in favour of increasing growth rate. As can be seen from electronic supplementary material, figure S5, the steady-state growth rate overtakes the oscillating growth rate at about 10.5 h.

It is an important result that biofilm oscillations can be described by considering a few processes only, which are listed below equation (2.1). They include considerably less processes than the Liu model [4]. However, they do include the diffusion of ammonia to the surroundings, unlike that model. Thus, it is plausible to assume that these are the most relevant processes for the phenomenon of oscillations.

All other processes (such as the diffusion of glutamate from the interior of the biofilm to its periphery and from there to the environment) can be neglected.

3.3. Average concentrations and average growth rate

Motivated by the reasoning in the Introduction, we now compare the average concentrations with the steady-state concentrations. As the model under study is a mixture of a Lotka–Volterra equation, equation (2.1*a*) and two linear equations (2.1*b*,*c*), it can be assumed that the values are equal. To demonstrate this, we divide equation (2.1*a*) by G_p

$$\frac{1}{G_p}\frac{\mathrm{d}G_p}{\mathrm{d}t} = \frac{\mathrm{d}}{\mathrm{d}t}(\ln G_p) = k - k_2 A \quad \text{where} \quad k = k_1 G_E - k_4.$$

We integrate over one oscillation period, T

$$\int_0^T \frac{\mathrm{d}}{\mathrm{d}t}(\ln G_p)\,\mathrm{d}t = 0 = \int_0^T (k - k_2 A)\,\mathrm{d}t$$
$$= kT - k_2 \int_0^T A\,\mathrm{d}t,$$

where the integral is zero because $G_p(T) = G_p(0)$

$$\frac{1}{T}\int_0^T A\,\mathrm{d}t = \langle A\rangle = \frac{k}{k_2} = A_{\mathrm{ss}}.$$

Now, we calculate the integral of $\mathrm{d}A/\mathrm{d}t$:

$$\int_0^T \frac{\mathrm{d}A}{\mathrm{d}t}\,\mathrm{d}t = 0 = \int_0^T (k_5 \mathrm{G_i} - k_3 A)\mathrm{d}t$$
$$= k_5 \int_0^T \mathrm{G_i}\,\mathrm{d}t - k_3 \int_0^T A\,\mathrm{d}t$$
$$k_5\,\langle G_i\rangle = k_3 A_{\mathrm{ss}} = \frac{k\,k_3}{k_2}$$
$$\langle G_i\rangle = \frac{k\,k_3}{k_2 k_5} = G_{i,\mathrm{ss}}.$$

Now, we calculate the integral of $\mathrm{d}G_i/\mathrm{d}t$ and derive, analogously

$$\langle G_p\rangle = G_{p,ss}.$$

Thus, the average concentrations are equal to the steady-state concentrations.

The question arises whether the oscillations have an effect on the average of the bilinear term $k_2 A G_p$. This is not immediately clear, although figure 4 suggests that the average growth rate is slower than that at the metabolic steady state. Note that the growth term bAG_pB is trilinear.

To check whether $\langle A\,G_p\rangle = A_{\mathrm{ss}}.\,G_{p,\mathrm{ss}}$, we integrate $\mathrm{d}G_p/\mathrm{d}t$ over one period, T

$$\int_0^T \frac{\mathrm{d}G_p}{\mathrm{d}t}\,\mathrm{d}t = 0 = \int_0^T kG_p\mathrm{d}t - \int_0^T k_2 A G_p \mathrm{d}t$$
$$= k\langle G_p\rangle T - k_2 A\,G_p T.$$

Since $\langle G_p\rangle = G_{p,\mathrm{ss}}$ and $\langle A\rangle = A_{\mathrm{ss}} = \dfrac{k}{k_2}$, dividing by k_2 and T gives

$$\langle A\,G_p\rangle = A_{\mathrm{ss}}.\,G_{p,\mathrm{ss}}.$$

Thus, the average of the bilinear term, which can be interpreted as the input to biomass, is indeed unaffected by oscillations, although the ammonia and peripheral glutamate levels oscillate asynchronously. For two-dimensional Lotka–Volterra systems, this property was shown earlier [24].

3.4. Bifurcations

Figure 5 shows the two bifurcations: the transcritical bifurcation occurring at $G_E = 5.88$ mmol l^{-1} and the Hopf bifurcation at $G_E = 24.41$ mmol l^{-1}, i.e. the transition from stable steady state to stable limit cycle.

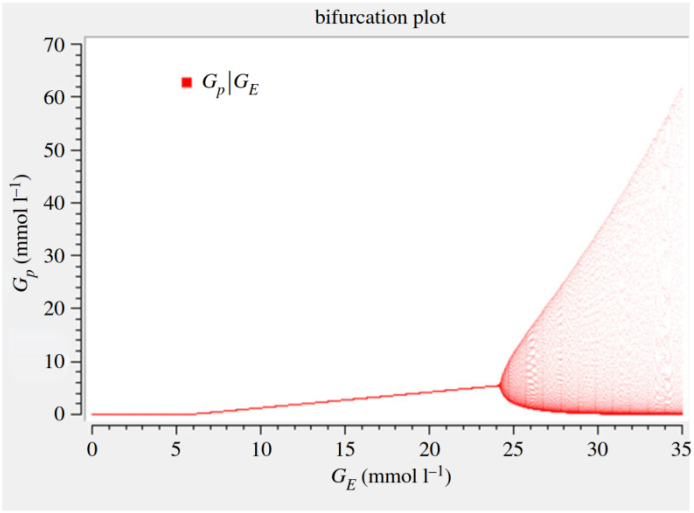

Figure 5. Bifurcation diagram of G_p versus G_E. For parameter values except G_E, see table 1. The transcritical bifurcation occurs at $G_E = 5.88$ mmol l^{-1} and the supercritical Hopf bifurcation at $G_E = 24.41$ mmol l^{-1}. The two arms of the convex hull represent the amplitude of oscillation which widen with increasing value of G_E. It can be seen that the model is sensitive to G_E in terms of oscillation amplitude.

These values can also be calculated from the general formulae for the bifurcations [19]. The steady-state value of G_p is a linear function of the bifurcation parameter G_E, as shown in equation (3.2*a*). It can be seen that the Hopf bifurcation is supercritical; that is, the amplitude grows gradually starting from zero and the limit cycle is stable right from the beginning.

Near the Hopf bifurcation, the obtained time course curve (figure 2) is sinusoidal. For $G_E \gg 24.41$ mmol l^{-1} the oscillations get spike-like and are no longer sinusoidal. It is of interest to speculate about the physiological advantage of spike-like oscillations. This question has been discussed earlier in the context of calcium oscillations [26,38,39]. Whenever the kinetic effect of the oscillating variable (e.g. in activating a protein or in a biochemical conversion) is nonlinear and follows a convex function, the spikes contribute more than proportionately to the effect. Thus, spike-like oscillations can lead to a high average effect even at low average value of the variable. In order that oscillations really enable division of labour in the case of biofilms, it can be expected that they should not be sinusoidal. This deserves further studies. A biological explanation of the bifurcations is given in the Discussion.

We checked the parameter sensitivity in two ways. First, we performed a bifurcation analysis for all parameters (except k_1 since it is equivalent to G_E), see figures 5 and 6 and electronic supplementary material, figures S1–S3. We see a steep increase in the oscillation amplitude with respect to G_E and k_3, a moderately steep increase for k_4, whereas the other parameters show a very gradual increase in the vicinity of the bifurcation. Second, we applied local parameter sensitivity analysis to the steady-state concentrations, which are equal to the average values. This can be done in an analytical way by differentiating the steady-state values given in equation (3.2) consecutively with respect to all parameters. The resulting unscaled sensitivities for the parameter values from table 1 are given in electronic supplementary material, table S1a. Thereafter, we computed the scaled sensitivities by multiplying by the parameter and dividing by the concentration (electronic supplementary material, table S1b). The obtained values for all sensitivities were confirmed by numerical computation using COPASI [40].

The results show that A is not sensitive at all to k_3 and k_5, nor is G_p to k_5. This is counterintuitive because increasing k_5 corresponds to over-expression of glutamate dehydrogenase, which produces ammonia. However, in our model, increasing k_5 leads to a decrease in G_i, so that the term $k_5 G_i$ stays constant. It deserves further study whether a more realistic kinetics leads to non-zero sensitivity for these cases.

Scaled sensitivities are equal to unity if the parameter enters the formula for the steady value in a multiplicative way (that is, as a factor in the numerator) and equal to minus unity if it is a factor in the denominator. Examples are provided by the scaled sensitivities of G_i and G_p with respect to k_3 and of all concentrations with respect to k_2, respectively. The highest scaled sensitivity, 1.24, is found

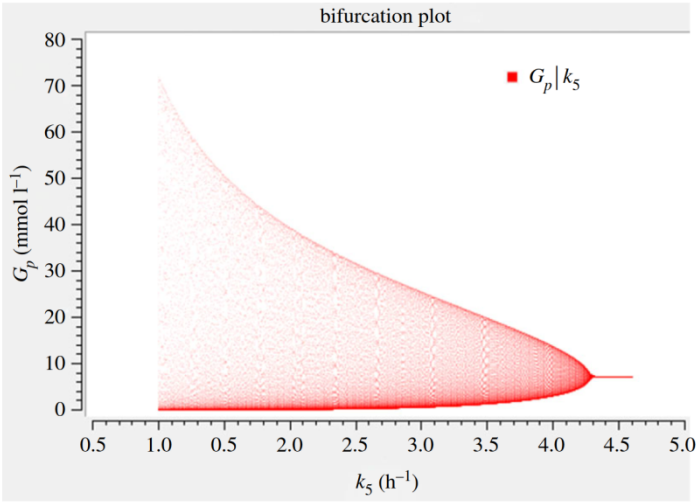

Figure 6. Bifurcation diagram of G_p versus k_5. For parameter values, see table 1, except for k_5, which is varied between 1 and 4.6 h^{-1}. It can be seen that the model is less sensitive to k_5 in terms of oscillation amplitude when compared with G_E.

for all concentrations with respect to k_1. That value means that a 1% increase in a parameter value leads to a 1.24% increase in the concentration.

3.5. Quasi-steady-state approximation

To ascertain the cause of oscillations, which could be a negative feedback with a delay or a positive feedback, we can study a subsystem by eliminating a variable. This can be done by the quasi-steady-state approximation (QSSA) [15]. In our system, we see that G_p exerts a positive feedback on itself which is linear and, thus, quite weak. For example, in the Higgins–Selkov oscillator involving two variables, the feedback is quadratic [16,17]. Moreover, the above system involves a negative feedback: G_p is converted to G_i, G_i is converted to A and A promotes the degradation of G_p (figure 1). In the Goodwin oscillator, which also consists of three variables, a negative feedback is the cause of oscillation [41,42].

Inspired by the observation in figure 5 that the oscillations vanish at high k_5 values, we apply the QSSA for G_i. This corresponds to the special case where glutamate dehydrogenase is overexpressed. In that case, indeed quenching of oscillations was observed in experiment and also predicted by the Liu model [4]. The variable G_i then attains a quasi-steady state

$$\frac{\mathrm{d}G_i}{\mathrm{d}t} = k_4 G_p - k_5 G_i = 0. \tag{3.4}$$

This leads to

$$G_i = \frac{k_4}{k_5} G_p. \tag{3.5}$$

Substituting this into the above model equations (2.1*a–c*) yields a simplified system

$$\frac{\mathrm{d}G_p}{\mathrm{d}t} = (k_1 G_E - k_4) G_p - k_2 G_p A \tag{3.6a}$$

and

$$\frac{\mathrm{d}A}{\mathrm{d}t} = -k_3 A + k_4 G_p. \tag{3.6b}$$

It is of interest to analyse its dynamics. It follows from the general result by Hanusse [43,44] that it cannot give rise to a limit cycle because it involves two variables and only linear and bilinear terms. However, the question still remains whether it gives rise to a stable or unstable steady state, whether damped oscillations are possible, etc.

System (3.6) shows two steady states

$$G_{p1} = A_1 = 0, \tag{3.7a,b}$$

which is the TSS, and

$$G_{p2} = \frac{k_1 G_E - k_4}{k_2 k_4}\, k_3, \quad A_2 = \frac{k_1 G_E - k_4}{k_2}, \tag{3.8a,b}$$

which is the NTSS (see equations (3.2*a*,*b*)). The Jacobian matrix reads

$$\mathbf{M} = \begin{pmatrix} k_1 G_E - k_4 - k_2 A & -k_2 G_p \\ k_4 & -k_3 \end{pmatrix}, \tag{3.9}$$

while for the TSS, it reads

$$\mathbf{M} = \begin{pmatrix} k_1 G_E - k_4 & 0 \\ k_4 & -k_3 \end{pmatrix}. \tag{3.10}$$

For matrices with such a triangular structure, the eigenvalues are given by the diagonal elements. In our case

$$\lambda_1 = k_1 G_E - k_4, \quad \lambda_2 = -k_3. \tag{3.11}$$

In any case, the eigenvalues are real, so that not even damped oscillations are possible. For $k_1 G_E < k_4$, both eigenvalues are negative, so that the TSS is a stable node. For $k_1 G_E > k_4$, one eigenvalue is negative and the other one positive. The steady state then is unstable, it is a saddle point.

For the NTSS (3.8), the Jacobian matrix becomes

$$\mathbf{M} = \begin{pmatrix} 0 & -\dfrac{k_1 G_E - k_4}{k_4} k_3 \\ k_4 & -k_3 \end{pmatrix}. \tag{3.12}$$

The characteristic equation reads

$$\lambda^2 + k_3 \lambda + (k_1 G_E - k_4) k_3 = 0\,. \tag{3.13}$$

This has the solutions

$$\lambda_{1/2} = -\frac{k_3}{2} \pm \sqrt{\frac{k_3^2}{4} - (k_1 G_E - k_4) k_3}. \tag{3.14}$$

Now, we distinguish three cases:

(a) For $k_1 G_E < k_4$, the term under the square root is positive, so that the root is real. Moreover, it is larger than $k_3/2$. Thus, one eigenvalue is negative and the other one positive. The steady state then is unstable, it is a saddle point.
(b) For $0 < k_1 G_E - k_4 < k_3/4$, the root is again real. It is less than $k_5/2$, though. Both eigenvalues are negative; the steady state is a stable node.
(c) For $k_1 G_E - k_4 > k_3/4$, the root is imaginary. Both eigenvalues are complex numbers, with the same negative real part $-k_3/2$. The steady state is a stable focus. This state is, thus, reached by damped oscillations.

From these calculations, the following conclusions can be drawn. At $k_1 G_E = k_4$, the two steady states of the simplified system (3.6) coincide, as in the complete system (2.1). Since the TSS and NTSS interchange their stability at that point, it is a transcritical bifurcation.

There is a second transition point where the qualitative behaviour changes, at $k_1 G_E - k_4 = k_3/4$. This is another point than the Hopf bifurcation in the complete system, which is at $k_1 G_E - k_4 = k_3 + k_5$. At this transition in the simplified system, a stable node turns into a stable focus. Such a transition must also occur in the complete system between the transcritical bifurcation, where an unstable node turns into a stable node, and the Hopf bifurcation, where a stable focus gets unstable. It is difficult to find it exactly in the three-dimensional system. Beyond this transition, the simplified system shows damped oscillations. This implies that the positive feedback of G_p on itself can be considered as a cause of oscillation, yet not as a cause of a limit cycle. The 'inflation' of the oscillation to a limit cycle in the

complete system appears to be brought about by the negative feedback via G_i. The loop via G_i can, moreover, be interpreted as a delay.

In this subsection, we have considered the special case of high k_5. This corresponds to a situation realized in experiments by Liu *et al.* where they overexpress the glutamate dehydrogenase leading to an excessive production of ammonia [4]. In that situation, indeed no oscillations were observed. We have proved analytically that the limit cycle disappears in that case. This generalizes the numerical finding shown in figure 6. Thus, to model limit cycle oscillations in biofilms by equation (2.1), we need the full three-dimensional system with values of k_5 that are not too high.

The QSSA for the rate constant k_3 is given in the electronic supplementary material.

4. Discussion

Here, we have used the smallest chemical system showing a Hopf bifurcation to model metabolic oscillations in *B. subtilis* biofilms. That model had been used earlier to describe p53 oscillations [22]. Here, we have applied the model to describe another biological phenomenon. We have specifically selected the parameter values to describe biofilm dynamics, which makes the model more relevant in the light of the biological observation. In our system, the diffusion of ammonia is critical for biofilm oscillations. All the terms in the model are linear, except k_2AG_p, which is bilinear. The model describes metabolic and diffusion processes as outlined above. As an output, the growth of the biofilm (consisting of incremental and halting phases) was also computed (figure 4).

A major reason of the observed oscillations was demonstrated to be the division of labour between the central and peripheral zones of the biofilm. While the release of usable ammonia is mainly delimited to the former, the production of biomass and, thus, growth, is mainly delimited to the latter.

We have presented bifurcation diagrams, which clearly show supercritical Hopf bifurcations (figure 5 and 6, electronic supplementary material, figures S1–S3). Earlier, Wilhelm & Heinrich [19,20] had analysed that bifurcation and had presented one bifurcation diagram. Here, we have added some mathematical analysis. For example, we show the maxima and minima of oscillations, the knowledge of which gives us a quantitative insight into the biofilm dynamics. Moreover, we performed a QSSA and probed for the equality property of the average values. We analysed the Hopf bifurcation by changing not only the external glutamate G_E but alternatively also all the rate constants except k_1, since changing k_1 has the same effect as changing G_E. Interestingly, a recent model [7] has shown a subcritical bifurcation in describing the behaviour of the stress levels in the biofilm periphery. However, they modelled the stress with a single delay differential equation and did not consider other molecular details, while we do not consider stress. Using a single differential equation meets the quest for minimality. However, a delay differential equation (meaning that the time derivative of a variable depends on that variable at a previous time point) is, from a mathematical point of view, very complex because it requires infinitely many initial values (from zero to the delay period, with a simplifying assumption being that they are all equal). Moreover, stability analysis is then considerably more complicated. Our model is complementary to their model. It is closer to Liu's original model [4] but much simpler because it involves only three rather than six variables, and thus only requires three initial values. We chose the parameters of the model such that they are in agreement with Liu's experimental results, namely the period and the amplitude of oscillations.

In our model, peripheral glutamate exerts a positive feedback on itself. Mathematically, this has the form of a bilinear term involving peripheral and external glutamate concentrations. At very low values of G_E, the feedback is not strong enough to enable a positive steady state. The system then tends to the TSS. In that state, G_p is zero, so that growth is impossible. Biologically, this can be interpreted that the biofilm is too small to be viable. This is in agreement with observations in the recent study from the Suel group [7]. At a certain threshold value of G_E (5.88 mmol l^{-1}), the NTSS turns stable in a transcritical bifurcation. Beyond that value, the feedback is strong enough to enable growth. At high values of G_E, the feedback becomes so strong that an overshoot occurs: more glutamate is taken up than needed, so that the G_p level transiently exceeds the steady-state value. Then, more peripheral glutamate is consumed for release of ammonia or for growth, so that the concentration decreases again. This leads to oscillations.

From a functional point of view, a steady state is quite appropriate [29]. Growth of the biofilm does not require oscillations. However, in this system, oscillations help in mitigating the chemical attack that challenges the biofilm [4]. This may have interesting clinical implications in view of treatment of biofilm-forming bacteria by antibiotics. Furthermore, another study [9] indicates that oscillations in growth

actually help in sharing the nutrients among several biofilms more efficiently. However, not all biofilms show oscillations, indicating that it is not critical for biofilms. Our numerical calculations suggest that the average growth rate is lower when compared with growth at the metabolic steady state.

By contrast, the individual concentration variables (ammonia, peripheral glutamate etc. but not biomass) show the equality property that their average during oscillations equals the value at the unstable state, as usual for Lotka–Volterra systems [25]. Here, we have shown that the bilinear input term k_2AG_p exhibits this equality property as well. This may come as a surprise because the ammonia and peripheral glutamate levels oscillate with a phase shift.

In the paper by Liu *et al.* [4], the oscillations computed by their model have a sinusoidal shape. In our model, such a shape only occurs in the neighbourhood of the Hopf bifurcation. Further beyond it, the shape is more spike-like with the crests being sharper than the troughs.

The question arises whether the model used and analysed here is minimal. On the basis of ODE systems (without delays), at least two variables are needed to generate oscillations [13,14]. However, when only linear and bilinear terms are included, at least three variables are needed, as was proved by Hanusse by an analysis of the Jacobian matrix [43,44]. As shown by Wilhelm & Heinrich [19], such a model requires at least five reactions. Thus, the above model is minimal in terms of the number of variables (criterion with highest priority) and number of reactions, given the type of kinetics. The famous two-variable Brusselator model [45] and the Higgins–Selkov oscillator involve a term of degree three each [16,17]. If the number of reactions is granted the highest priority, the model may look different. Thus, it depends on the criteria what a minimal model is. Note that a delay differential equation [7] is, from the viewpoint of the number of initial values, of infinite dimension. While our model is not necessarily the simplest, it provides a trade-off between simplicity and adequacy to match the observed oscillation in biofilms.

As for any oscillatory system, it is interesting to elucidate the feedback structure. The term $k_1G_EG_p$ represents a positive feedback because peripheral glutamate stimulates its own uptake. This is because glutamate is a proxy for the concentration of various transport proteins embedded in the cell membranes. The higher the concentration of these proteins, the higher is the glutamate uptake rate. Since this positive feedback is the driving force for oscillations, at low values of k_1G_E, we observe a steady state rather than oscillations. In glycolytic and calcium oscillations, the cause of oscillations is also a positive feedback [13,14,17,46], while in a Goodwin oscillator, it is a negative feedback [41,42].

In addition to the positive feedback, there is also a negative feedback loop in the system (figure 1). As seen from the differential equations, peripheral glutamate positively influences internal glutamate, which positively affects ammonia, which then negatively influences peripheral glutamate. Thus, the overall effect is inhibitory. This feedback structure of the Wilhelm–Heinrich model has been highlighted earlier [22].

By applying the QSSA, we have proved analytically that the limit cycle disappears if glutamate is degraded very fast or ammonia diffuses very easily. As mentioned in the Results section, the former case corresponds to a situation realized in experiments by overexpressing the glutamate dehydrogenase [4]. In that situation, no oscillations were observed. By contrast, in the case where oscillations occur, a description by a simple mass-action system requires three variables. Analyses in this direction may be relevant for clinical interventions via inhibition or activation of bacterial enzymes or changing diffusivity in the biofilm.

The model analysed here has several pros and cons. In view of the mathematical analysis, its simplicity is certainly an advantage. In view of an adequate description of the biological and biochemical processes involved, the model may appear oversimplified. For example, describing growth by trilinear term is quite simplistic; usually, it is described by saturation kinetics (e.g. Michaelis–Menten kinetics). In addition, the assumption that glutamate uptake by the periphery is proportional to the glutamate concentration as explained above could be refined in future studies. Moreover, diffusion processes are usually reversible. In the above model, we neglected the backward processes in diffusion, which is justified if concentration differences are high.

Many theoretical and experimental studies have been published on glycolytic oscillations [13,16,17,47,48]. However, these oscillations only occur under very special or even artificial conditions. In living cells, metabolic oscillations are rare, while being quite frequent in signalling systems [13,14,49,50]. The lights of a car are a helpful analogy: the headlights illuminate the street in a permanent way; there is no point in oscillations. By contrast, the side indicators (as signalling device) flash; that is, they emit oscillating light. Interestingly, in the case of biofilms, metabolic oscillations could provide advantages. While the work described here is quite theoretical, we consider it to be an appropriate basis for refined and more sophisticated models of biofilm oscillations.

Data accessibility. No custom code and datasets was used within this study.

Authors' contributions. S.S. conceived the idea of applying the Wilhelm and Heinrich model to the biofilm system. R.G. performed modelling and simulation using COPASI. He and Á.T.K. interpreted the model variables, parameters and results biologically. B.I. verified the results using Matlab and also produced figures and mathematical analyses. S.S. performed QSSA and mathematical proof and mathematical interpretation of the results. R.G. and S.S. wrote the manuscript and B.I. and Á.T.K. edited and structured it. All the authors have read and approved the manuscript.

Competing interests. The authors declare no competing financial interests.

Funding. R.G. was supported by the Max Planck Society through the IMPRS 'Exploration of Ecological Interactions with Molecular and Chemical Techniques'. B.I. was supported by the DFG through the Collaborative Research Center 1127, ChemBioSys Project C07.

Acknowledgements. We acknowledge David Heckel for his valuable inputs in interpreting the biological implications of the results and Frank Hilker for drawing our attention to the paper by Goel *et al*. [24].

References

1. Kovacs AT, Dragos A. 2019 Evolved biofilm: review on the experimental evolution studies of *Bacillus subtilis* pellicles. *J. Mol. Biol.* **431**, 4749–4759. (doi:10.1016/j.jmb.2019.02.005)
2. Kreft JU. 2004 Biofilms promote altruism. *Microbiology* **150**, 2751–2760. (doi:10.1099/mic.0.26829-0)
3. Popat R, Crusz SA, Messina M, Williams P, West SA, Diggle SP. 2012 Quorum-sensing and cheating in bacterial biofilms. *Proc. R. Soc. B* **279**, 4765–4771. (doi:10.1098/rspb.2012.1976)
4. Liu J, Prindle A, Humphries J, Gabalda-Sagarra M, Asally M, Lee DY, Ly S, Garcia-Ojalvo J, Suel GM. 2015 Metabolic co-dependence gives rise to collective oscillations within biofilms. *Nature* **523**, 550–554. (doi:10.1038/nature14660)
5. Dragos A *et al.* 2018 Division of labor during biofilm matrix production. *Curr. Biol.* **28**, 1903–1913.e5. (doi:10.1016/j.cub.2018.04.046)
6. Stannek L, Thiele MJ, Ischebeck T, Gunka K, Hammer E, Volker U, Commichau FM. 2015 Evidence for synergistic control of glutamate biosynthesis by glutamate dehydrogenases and glutamate in *Bacillus subtilis*. *Environ. Microbiol.* **17**, 3379–3390. (doi:10.1111/1462-2920.12813)
7. Martinez-Corral R, Liu J, Suel GM, Garcia-Ojalvo J. 2018 Bistable emergence of oscillations in growing *Bacillus subtilis* biofilms. *Proc. Natl Acad. Sci. USA* **115**, E8333–E8340. (doi:10.1073/pnas.1805004115)
8. Horn H, Lackner S. 2014 Modeling of biofilm systems: a review. *Adv. Biochem. Eng. Biotechnol.* **146**, 53–76. (doi:10.1007/10_2014_275)
9. Liu J, Martinez-Corral R, Prindle A, Lee DD, Larkin J, Gabalda-Sagarra M, Garcia-Ojalvo J, Suel GM. 2017 Coupling between distant biofilms and emergence of nutrient time-sharing. *Science* **356**, 638–642. (doi:10.1126/science.aah4204)
10. Skoneczny S. 2015 Cellular automata-based modelling and simulation of biofilm structure on multi-core computers. *Water Sci. Technol.* **72**, 2071–2081. (doi:10.2166/wst.2015.426)
11. Miller JK *et al.* 2014 Mathematical modelling of *Pseudomonas aeruginosa* biofilm growth and treatment in the cystic fibrosis lung. *Math. Med. Biol.* **31**, 179–204. (doi:10.1093/imammb/dqt003)
12. Rotrattanadumrong R, Endres RG. 2017 Emergence of cooperativity in a model biofilm. *J. Phys. D: Appl. Phys.* **50**, 234006. (doi:10.1088/1361-6463/aa7097)
13. Goldbeter A, Berridge MJ. 1996 Frontmatter. In *Biochemical oscillations and cellular rhythms: the molecular bases of periodic and chaotic behaviour*, pp. i–viii. Cambridge, UK: Cambridge University Press.
14. Schuster S, Marhl M, Hofer T. 2002 Modelling of simple and complex calcium oscillations: from single-cell responses to intercellular signalling. *Eur. J. Biochem.* **269**, 1333–1355. (doi:10.1046/j.0014-2956.2001.02720.x)
15. Heinrich R, Schuster S. 1996 *The regulation of cellular systems*. New York, NY: Chapman and Hall.
16. Higgins J. 1967 The theory of oscillating reactions—kinetics symposium. *Ind. Eng. Chem.* **59**, 18–62. (doi:10.1021/ie50689a006)
17. Sel'kov EE. 1968 Self-oscillations in glycolysis. 1. A simple kinetic model. *Eur. J. Biochem.* **4**, 79–86. (doi:10.1111/j.1432-1033.1968.tb00175.x)
18. Somogyi R, Stucki JW. 1991 Hormone-induced calcium oscillations in liver cells can be explained by a simple one pool model. *J. Biol. Chem.* **266**, 11 068–11 077.
19. Wilhelm T, Heinrich R. 1995 Smallest chemical-reaction system with Hopf-bifurcation. *J. Math. Chem.* **17**, 1–14. (doi:10.1007/Bf01165134)
20. Wilhelm T, Heinrich R. 1996 Mathematical analysis of the smallest chemical reaction system with Hopf bifurcation. *J. Math. Chem.* **19**, 111–130. (doi:10.1007/Bf01165179)
21. Wilhelm T, Schuster S, Heinrich R. 1997 Kinetic and thermodynamic analyses of the reversible version of the smallest chemical reaction system with Hopf bifurcation. *Nonlinear World.* **4**, 295–321.
22. Geva-Zatorsky N *et al.* 2006 Oscillations and variability in the p53 system. *Mol. Syst. Biol.* **2**, 2006 0033. (doi:10.1038/msb4100068)
23. Strogatz SH. 2018 *Nonlinear dynamics and chaos: with applications to physics, biology, chemistry, and engineering*. Boca Raton, FL: CRC Press.
24. Goel NS, Maitra SC, Montroll EW. 1971 On the Volterra and other nonlinear models of interacting populations. *Rev. Mod. Phys.* **43**, 231–276. (doi:10.1103/RevModPhys.43.231)
25. Hofbauer J, Sigmund K. 1998 *Evolutionary games and population dynamics*. Cambridge, UK: Cambridge University Press.
26. Knoke B, Bodenstein C, Marhl M, Perc M, Schuster S. 2010 Jensen's inequality as a tool for explaining the effect of oscillations on the average cytosolic calcium concentration. *Theory Biosci.* **129**, 25–38. (doi:10.1007/s12064-010-0080-1)
27. Knoke B, Marhl M, Perc M, Schuster S. 2008 Equality of average and steady-state levels in some nonlinear models of biological oscillations. *Theory Biosci.* **127**, 1–14. (doi:10.1007/s12064-007-0018-4)
28. Ritter AB, Douglas JM. 1970 Frequency response of nonlinear systems. *Ind. Eng. Chem.* **9**, 21–28.
29. Reimers AM, Reimers AC. 2016 The steady-state assumption in oscillating and growing systems. *J. Theor. Biol.* **406**, 176–186. (doi:10.1016/j.jtbi.2016.06.031)
30. Dupont G. 1993 *Modélisation des oscillations et des ondes de calcium intracellulaire*. Bruxelles, Belgium: Université Libre de Bruxelles.
31. Hoops S *et al.* 2006 COPASI—a COmplex PAthway SImulator. *Bioinformatics* **22**, 3067–3074. (doi:10.1093/bioinformatics/btl485)
32. Cussler EL. 2009 *Diffusion: mass transfer in fluid systems*, 2nd edn. Cambridge, UK: Cambridge University Press.
33. Kullmann DM, Min MY, Asztely F, Rusakov DA. 1999 Extracellular glutamate diffusion determines the occupancy of glutamate receptors at CA1 synapses in the hippocampus. *Phil. Trans. R. Soc. Lond. B* **354**, 395–402. (doi:10.1098/rstb.1999.0392)
34. Ribeiro ACF, Rodrigo MM, Barros MCF, Verissimo LMP, Romero C, Valente AJM, Esteso MA. 2014 Mutual diffusion coefficients of L-glutamic acid and monosodium L-glutamate in aqueous solutions at T = 298.15 K. *J. Chem. Thermodyn.* **74**, 133–137. (doi:10.1016/j.jct.2014.01.017)
35. Strogatz S. 2000 *Nonlinear dynamics and chaos: with applications to physics, biology, chemistry, and engineering*. Cambridge, MA: Perseus Pub.
36. Burdett ID, Kirkwood TB, Whalley JB. 1986 Growth kinetics of individual *Bacillus subtilis* cells and correlation with nucleoid extension. *J. Bacteriol.* **167**, 219–230. (doi:10.1128/jb.167.1.219-230.1986)
37. Maass S *et al.* 2011 Efficient, global-scale quantification of absolute protein amounts by integration of targeted mass spectrometry and two-dimensional gel-based proteomics. *Anal. Chem.* **83**, 2677–2684. (doi:10.1021/ac1031836)
38. Salazar C, Politi AZ, Hofer T. 2008 Decoding of calcium oscillations by phosphorylation cycles:

analytic results. *Biophys. J.* **94**, 1203–1215. (doi:10.1529/biophysj.107.113084)

39. Bodenstein C, Knoke B, Marhl M, Perc M, Schuster S. 2010 Using Jensen's inequality to explain the role of regular calcium oscillations in protein activation. *Phys. Biol.* **7**, 036009. (doi:10.1088/1478-3975/7/3/036009)
40. Kent E, Neumann S, Kummer U, Mendes P. 2013 What can we learn from global sensitivity analysis of biochemical systems? *PLoS ONE* **8**, e79244. (doi:10.1371/journal.pone.0079244)
41. Goodwin BC. 1965 Oscillatory behavior in enzymatic control processes. *Adv. Enzyme Regul.* **3**, 425–438. (doi:10.1016/0065-2571(65)90067-1)
42. Heiland I, Bodenstein C, Hinze T, Weisheit O, Ebenhoeh O, Mittag M, Schuster S. 2012 Modeling temperature entrainment of circadian clocks using the Arrhenius equation and a reconstructed model from *Chlamydomonas reinhardtii*. *J. Biol. Phys.* **38**, 449–464. (doi:10.1007/s10867-012-9264-x)
43. Hanusse P. 1973 Étude des systèmes dissipatifs chimiques à deux et trois espèces intermédiaires. *C. R. Acad. Sci. Paris C* **277**, 263–266.
44. Hanusse P. 1972 De l'Existence d'un Cycle Limite dans l'Evolution des Systèmes Chimiques Ouverts. *C. R. Acad. Sci. Paris, C* **274**, 1245–1247.
45. Prigogine I, Lefever R. 1968 Symmetry breaking instabilities in dissipative systems. II. *J. Chem. Phys.* **48**, 1695–1700. (doi:10.1063/1.1668896)
46. Kummer U, Olsen LF, Dixon CJ, Green AK, Bornberg-Bauer E, Baier G. 2000 Switching from simple to complex oscillations in calcium signaling. *Biophys. J.* **79**, 1188–1195. (doi:10.1016/S0006-3495(00)76373-9)
47. du Preez FB, van Niekerk DD, Kooi B, Rohwer JM, Snoep JL. 2012 From steady-state to synchronized yeast glycolytic oscillations I: model construction. *FEBS J.* **279**, 2810–2822. (doi:10.1111/j.1742-4658.2012.08665.x)
48. du Preez FB, van Niekerk DD, Snoep JL. 2012 From steady-state to synchronized yeast glycolytic oscillations II: model validation. *FEBS J.* **279**, 2823–2836. (doi:10.1111/j.1742-4658.2012.08658.x)
49. Goldbeter A, Dupont G, Berridge MJ. 1990 Minimal model for signal-induced Ca^{2+} oscillations and for their frequency encoding through protein phosphorylation. *Proc. Natl Acad. Sci. USA* **87**, 1461–1465. (doi:10.1073/pnas.87.4.1461)
50. Ewald J, Sieber P, Garde R, Lang SN, Schuster S, Ibrahim B. 2019 Trends in mathematical modeling of host–pathogen interactions. *Cell. Mol. Life Sci.* (doi:10.1007/s00018-019-03382-0)

S. Supplementary Information

1. Applying the quasi-steady-state approximation to ammonia

Just as in the case of the QSSA variable G_i (see main text for details), we apply the same approximation to the variable A.

$$A = \frac{k_5}{k_3}\, G_i \tag{S1}$$

From Eq. (1), we derive a reduced system:

$$\frac{dG_p}{dt} = k_1 G_E G_p - \, k_4 G_p - \frac{k_2 k_5}{k_3}\, G_i G_p \tag{S2}$$

$$\frac{dG_i}{dt} = k_4 G_p \, - \, k_5 G_i \tag{S3}$$

The system shows two steady states:

$$G_{p_1} = G_{i_1} = 0 \tag{S4a,b}$$

$$G_{p_2} = \frac{(k_1 G_E - k_4) k_3}{k_2 k_4}, \; G_{i_2} = \frac{(k_1 G_E - k_4) k_3}{k_2 k_5} \tag{S5a,b}$$

(see Eqs. (3a,c)). The Jacobian matrix reads:

$$\mathbf{M} = \begin{pmatrix} k_1 G_E - k_4 - \frac{k_2 k_5}{k_3} G_i & -\frac{k_2 k_5}{k_3} G_p \\ k_4 & -k_5 \end{pmatrix} \tag{S6}$$

For the trivial steady state (TSS, Eq. (S4)), it leads to:

$$\mathbf{M} = \begin{pmatrix} k_1 G_E - k_4 & 0 \\ k_4 & -k_5 \end{pmatrix} \tag{S7}$$

For matrices with such a triangular structure, the eigenvalues are given by the diagonal elements. In our case:

$$\lambda_1 = k_1 G_E - k_4, \lambda_2 = -k_5 \quad \text{(S8)}$$

In any case, the eigenvalues are real, so that not even damped oscillations are possible. For $k_1 G_E < k_4$, both eigenvalues are negative, so that the trivial steady state is a stable node. For $k_1 G_E > k_4$, one eigenvalue is negative and the other one positive. The steady state then is unstable, it is a saddle point.

For the NTSS (Eq. (S5)), the Jacobian matrix becomes:

$$\mathbf{M} = \begin{pmatrix} 0 & -\frac{k_1 G_E - k_4}{k_4} k_5 \\ k_4 & -k_3 \end{pmatrix} \quad \text{(S9)}$$

The characteristic equation reads:

$$\lambda^2 + k_3 \lambda + (k_1 G_E - k_4) k_5 = 0 \quad \text{(S10)}$$

This has the solutions

$$\lambda_{1/2} = -\frac{k_3}{2} \pm \sqrt{\frac{k_3^2}{4} - (k_1 G_E - k_4) k_5} \quad \text{(S11)}$$

Now, we distinguish three cases:

a) For $k_1 G_E < k_4$, the term under the square root is positive, so that the root is real. Moreover, it is larger than $k_3/2$. Thus, one eigenvalue is negative and the other one positive. The steady state then is unstable, it is a saddle point.

b) For $0 < k_1 G_E - k_4 < \frac{k_3^2}{4k_5}$, the root is again real. It is less than $k_3/2$, though. Both eigenvalues are negative; the steady state is a stable node.

c) For $k_1 G_E - k_4 > \frac{k_3^2}{4k_5}$, the root is imaginary. Both eigenvalues are complex numbers, with the same negative real part $-k_3/2$. The steady state is a stable focus. This state is, thus, reached by damped oscillations.

The transition between stable node and stable focus occurs at $k_1 G_E - k_4 = \frac{k_3^2}{4k_5}$. The results of this approximation are similar to those in the main text section on QSSA. We can conclude that the limit-

cycle oscillations vanish if ammonia diffuses very fast.

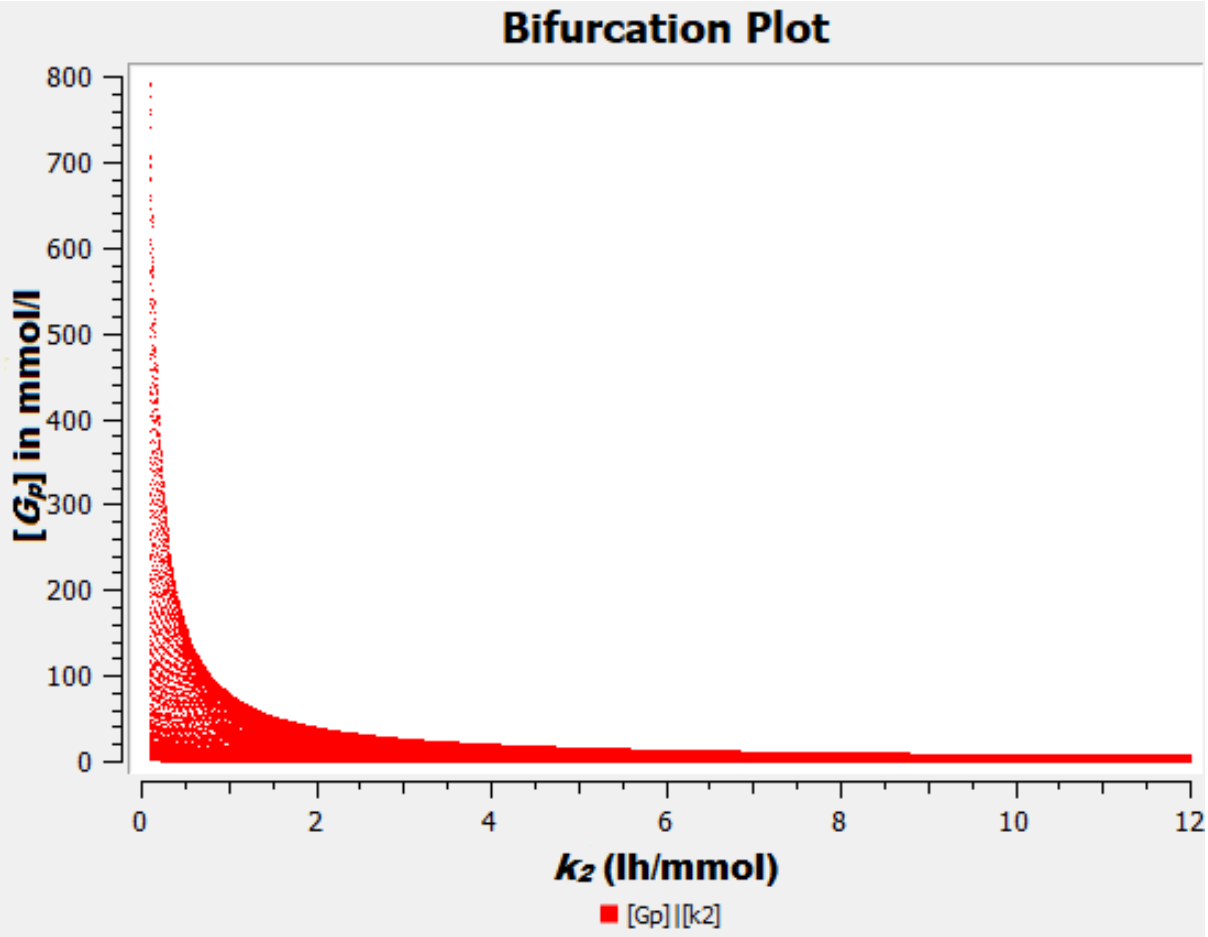

Figure S1: Bifurcation plot of G_p versus k_2. It can be seen that the model is not very sensitive to k_2 in terms of amplitude of oscillations if $k_2 \geq 2\ h^{-1}$.

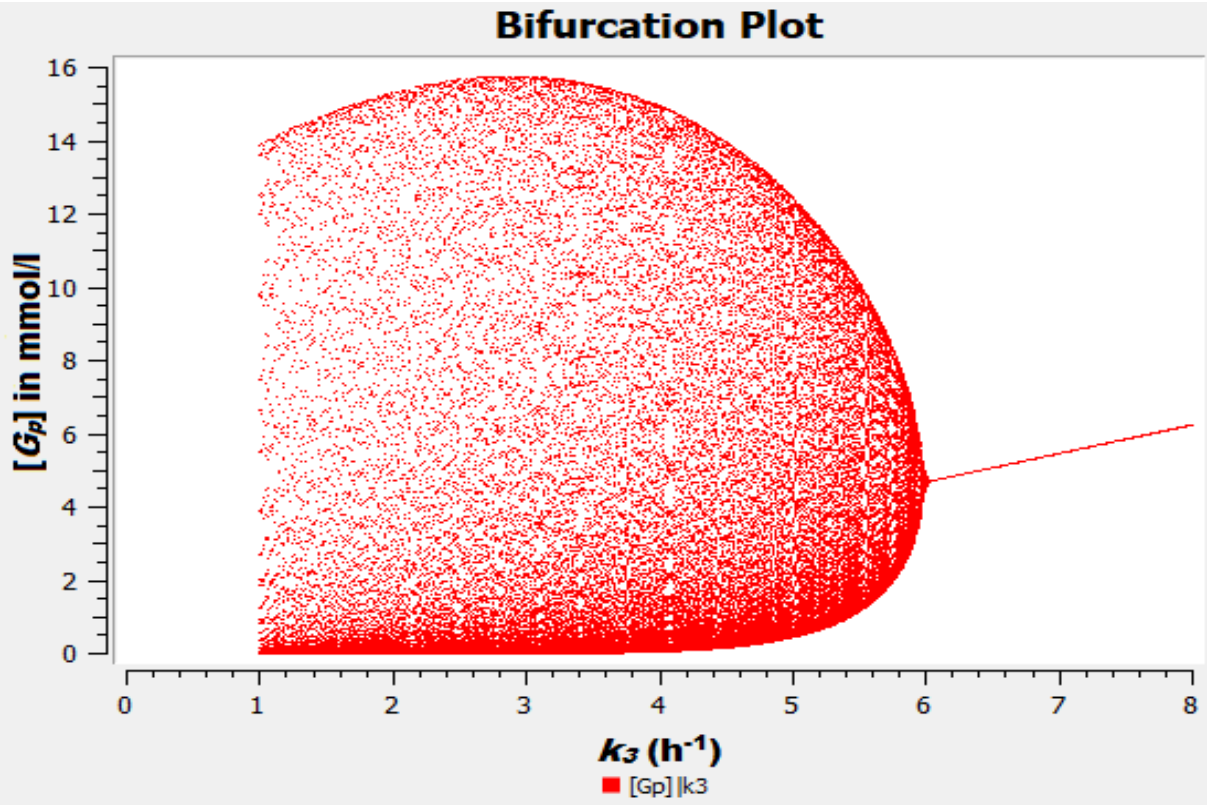

Figure S2: Bifurcation plot of G_p versus k_3. The model is sensitive to k_3 if $k_3 \geq 4$ h^{-1} in terms of amplitude of oscillations.

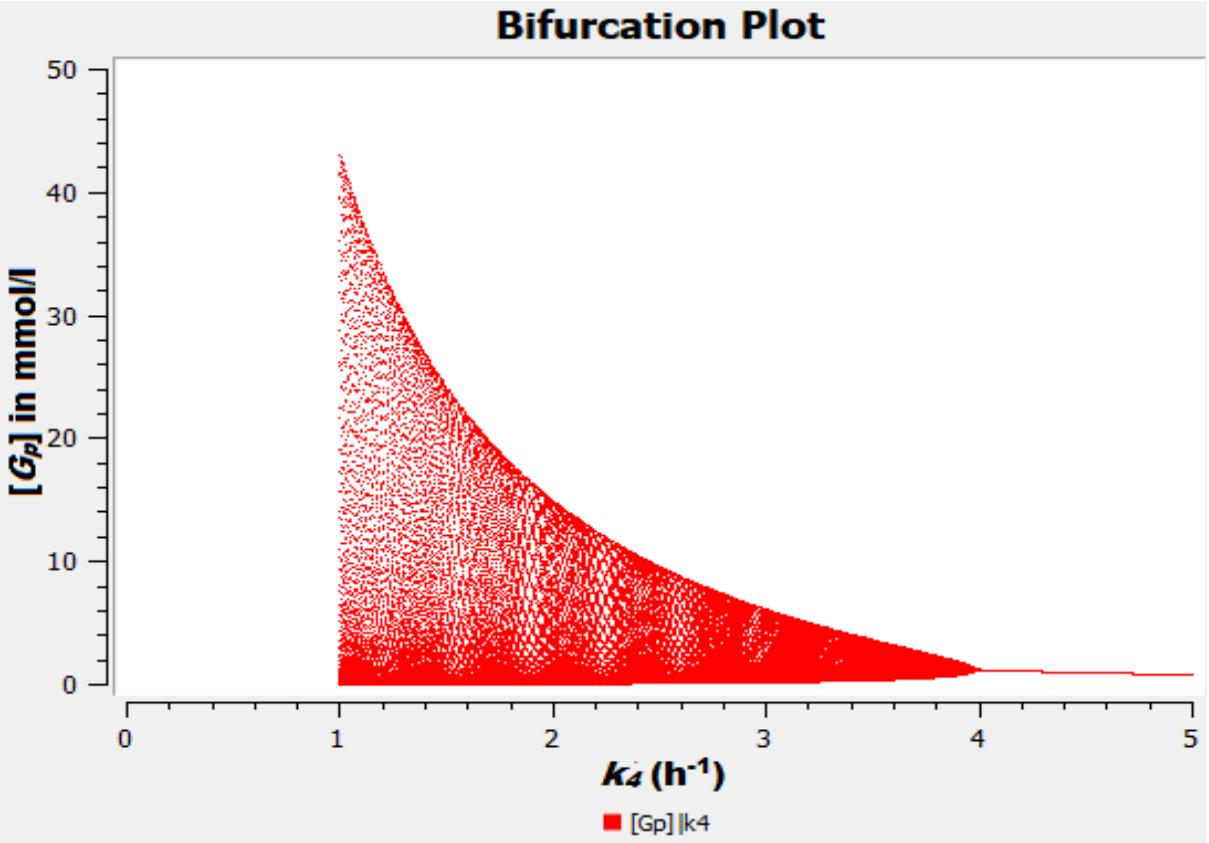

Figure S3: Bifurcation plot of G_p versus k_4. The model is sensitive to k_4 if $k_4 \leq 3$ h^{-1} in terms of amplitude of oscillations.

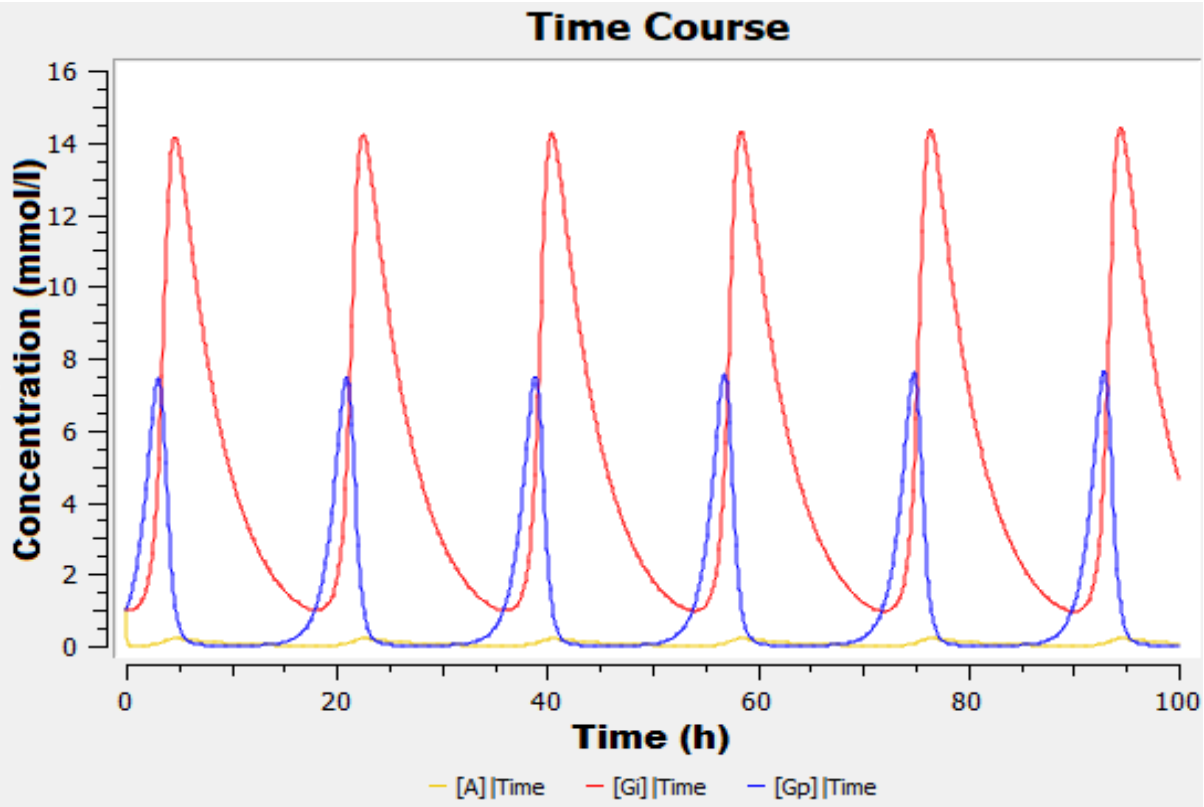

Figure S4: Time course after introducing self-amplification to G_i in addition to G_p. This can be obtained by changing the term k_4G_p to $k_4G_iG_p$ in eq (1). The oscillations become spike-like but no dramatic difference to the results of the minimal model can be seen. In order to obtain realistic oscillations, the parameter values needed to be changed. The parameters from Table 1 were reduced to 10% while k_3 was increased to 15.93 h^{-1}. In the main text, we only use self-amplification for G_p.

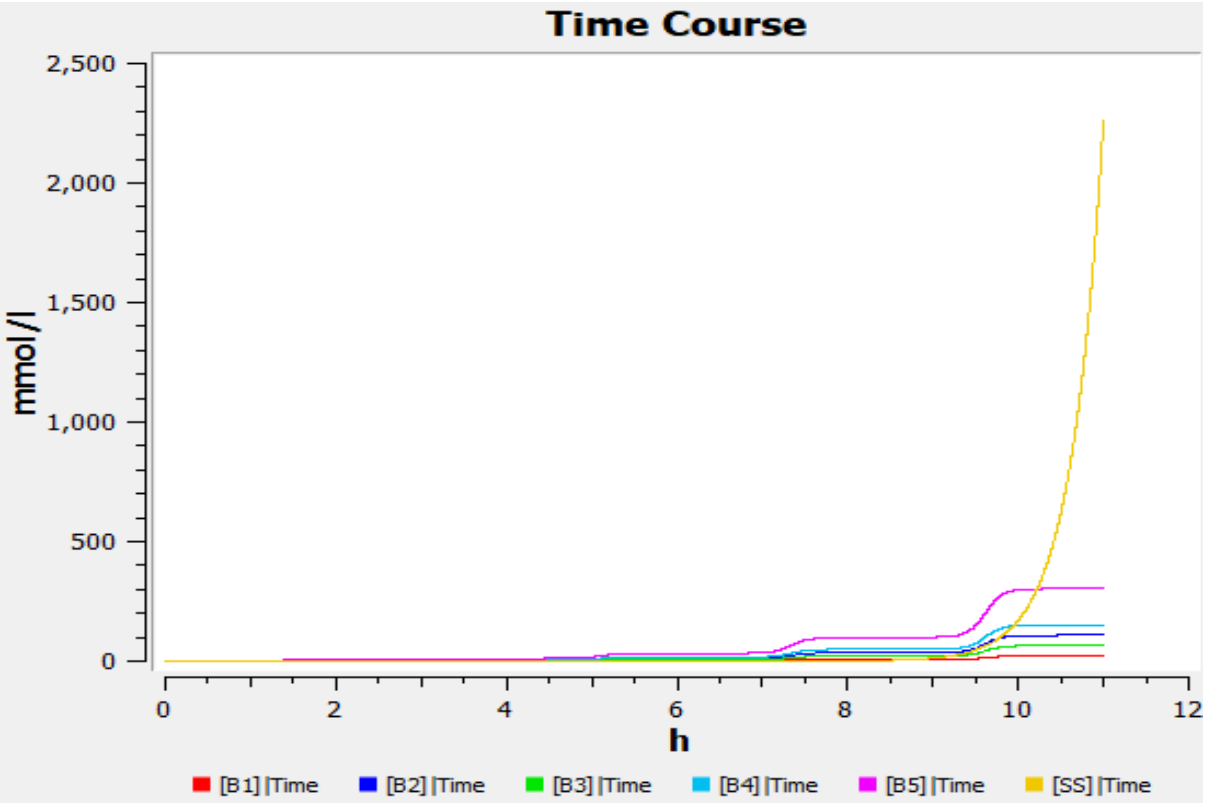

Figure S5: Plot of the time course of growth as calculated from Eq. (4) for various initial values of G_p from 1 mmol/l – 10 mmol/l with a step size of 1 mmol/l (all wavy curves). On average the curves have a doubling time of about 99 minutes. The black monotonic curve (initial value: 10^{-9} mmol/l) indicates the growth calculated by the steady state values. It can be seen that the steady state growth rate overtakes the oscillating growth rate at about 10.5 hours.

Table S1: Sensitivity analysis for all variables at steady state with respect to all parameters. Darker shades denote higher sensitivity. Positive sensitivity is shown in green and negative in red. White means that the variable is not sensitive to that parameter.

a: Values indicate unscaled derivatives at steady state.

	k_1	k_2	k_3	k_4	k_5
$[A]$	5.6604	-0.2944	0	-0.1887	0
$[G_i]$	9.8441	-0.5120	0.6790	-0.3281	-1.1798
$[G_p]$	11.3208	-0.5888	0.7809	-1.9392	0

b: Values indicate scaled derivatives at steady state.

	k_1	k_2	k_3	k_4	k_5
$[A]$	1.2416	-1	0	-0.2416	0
$[G_i]$	1.2416	-1	1	-0.2416	-1
$[G_p]$	1.2416	-1	1	-1.2416	0

III. Extending the minimal model of metabolic oscillations in *Bacillus subtilis* biofilms

Ravindra Garde, Bashar Ibrahim, Stefan Schuster

Published in Scientific Reports, volume 10, issue 1, Published on 27th March 2020

This article studies four different modifications to the model presented in Article 1

1. s6ODE and c6ODE: simple and complex 6 variable model which shows gradients of metabolites can be neglected and that three ODEs are sufficient to model biofilm oscillations.
2. RMM: Reversible and Michaelis-Menten kinetics: realistic diffusion (due to reversibility) and kinetics parameters can be validated experimentally. We also observe a pair of Hopf bifurcations within a single bifurcation analysis. The model predicts that oscillations will be quenched if nutrients are in excess. Conversely, it reconfirms the well observed phenomenon that oscillations only arise in a biofilm under nutrient scarcity.
3. MMK: Michaelis Menten kinetics. We test and find that if MM kinetics is responsible for the bubble.
4. R: Reversible reactions (simple mass action kinetics). We test if reversibility plays a role in obtaining the Hopf bubble. We conclude, it does not unless $k_1 G_E G_p$ is also made reversible (see figure S2). Thus the reaction $k_1 G_E G_p$ either needs to be made reversible or modelled using saturation kinetics in order to have the Hopf bubble.

Another prediction this modification makes is that, at adequately high supply of glutamate, oscillations are no longer necessary. This seems an intuitive prediction but none of the earlier models by Liu *et. al.* and Bocci *et. al.* have made this prediction.

Although our work is theoretical, our results are also consistent with experiments. Our model helps to broaden our understanding about the metabolic oscillations not only mathematically but also biologically.

I performed the simulations, wrote the manuscript and interpreted the results. Prof. Bashar Ibrahim carried out the mathematical analyses and supervised my work. Prof Stefan Schuster suggested the use of three variables for ammonia in the 6ODE models, performed the mathematical analysis, refined and structured the manuscript, supervised my work and helped in the interpretation of the results

mathematically and biologically.

www.nature.com/scientificreports

SCIENTIFIC REPORTS
nature research

OPEN

Extending the minimal model of metabolic oscillations in *Bacillus subtilis* biofilms

Ravindra Garde[1,2,4], Bashar Ibrahim[1,3,4*] & Stefan Schuster[1*]

Biofilms are composed of microorganisms attached to a solid surface or floating on top of a liquid surface. They pose challenges in the field of medicine but can also have useful applications in industry. Regulation of biofilm growth is complex and still largely elusive. Oscillations are thought to be advantageous for biofilms to cope with nutrient starvation and chemical attacks. Recently, a minimal mathematical model has been employed to describe the oscillations in *Bacillus subtilis* biofilms. In this paper, we investigate four different modifications to that minimal model in order to better understand the oscillations in biofilms. Our first modification is towards making a gradient of metabolites from the center of the biofilm to the periphery. We find that it does not improve the model and is therefore, unnecessary. We then use realistic Michaelis-Menten kinetics to replace the highly simple mass-action kinetics for one of the reactions. Further, we use reversible reactions to mimic the diffusion in biofilms. As the final modification, we check the combined effect of using Michaelis-Menten kinetics and reversible reactions on the model behavior. We find that these two modifications alone or in combination improve the description of the biological scenario.

Biofilms, a complex aggregation of cells embedded in a polysaccharide matrix, have been of interest for a long time in history – right when Antoine van Leuwenhoek examined a scraping of his tooth plaqueunder a microscope that he had built[1]. Since then, our understanding of biofilms has greatly broadened. We now know that living as a close aggregation provides several advantages to bacteria, such as the efficient distribution of macronutrients, removal of waste products, defense from chemical stress, and better gaseous exchange in the case of pellicle biofilms on the surface of liquids[2,3]. Biofilms are an elaborate system of coexisting individual cells that exhibit several social dynamics, including the division of labour[4–7].

In experiments using a microfluidics chamber, oscillations were observed in the growth of *Bacillus subtilis*[4] which was supplied with glutamate on one end of the chamber while the waste products of the biofilm were washed off at the other end at a constant rate. The peripheral cells of the biofilm have the advantage of direct access to glutamate. On the downside, they lose small molecules like ammonia which is an important source of nitrogen[8]. Cells in the interior, on the other hand, depend on the leftover glutamate that diffuses inwards in the biofilm, but do not lose gaseous molecules as rapidly as the peripheral cells. Thus cells in different regions of the biofilm will likely exhibit differences in their metabolic behavior[7]. The interior cells produce ammonia, which is required to produce glutamine. Glutamine is a proxy for the protein content and thus for the growth of the biofilm[9]. The peripheral cells depend on the ammonia diffusing from the interior for their growth. Thus, interior cells control the growth of the peripheral cells by monopolizing ammonia supply.

When the peripheral cells grow fast, the interior cells start to starve of glutamate, leading to a decline in the production of ammonia. As a result, the growth rate of the peripheral cells drops until the interior obtains enough glutamate. This oscillating system has not only been studied experimentally but also modeled by Liu *et. al.*[4], using six ordinary differential equations (ODEs) – two for glutamate and the ribosomes (a proxy for cellular machinery) in the two regions of the biofilm each, the enzyme glutamate dehydrogenase and ammonia.

Another approach to modeling this system is using partial differential equations (PDEs), as shown by Bocci *et. al.* in their model that uses four variables instead of six[10]. PDEs are used to simulate the gradient of ammonia

[1]Department of Bioinformatics, Matthias Schleiden Institute, Friedrich Schiller University Jena, Ernst-Abbe-Platz 2, 07743, Jena, Germany. [2]Max Planck Institute for Chemical Ecology Hans-Knöll Str. 8, 07745, Jena, Germany. [3]Centre for Applied Mathematics and Bioinformatics, and Department of Mathematics and Natural Sciences Gulf University for Science and Technology, Hawally, 32093, Kuwait. [4]These authors contributed equally: Ravindra Garde and Bashar Ibrahim. *email: bashar.ibrahim@uni-jena.des; stefan.schu@uni-jena.de

Parameter	Symbol	Value with unit
Glutamate concentration in the environment	G_E	30 mmol/l
Rate constant of glutamate diffusion from the environment to biofilm	k_1	0.34 (mmol/l* h)$^{-1}$
Biomass formation coefficient	k_2	5.3 (mmol/l* h)$^{-1}$
Rate constant of ammonia diffusion[20]	k_3	4 h^{-1}
Rate constant of glutamate diffusion within biofilm[21,22]	k_4	2 h^{-1}
Ammonia production coefficient	k_5	2.3 h^{-1}
Michaelis-Menten constant	K_m	1100 mmol/l
Maximum glutamate uptake rate at saturating concentration	V_{max}	1400 mmol/lh

Table 1. List of all parameters for all the models.

and glutamate, and two more ODEs describe the dynamics of housekeeping proteins and the enzyme glutamate dehydrogenase (GDH). In our approach, we focus solely on the two metabolites: glutamate and ammonia, and thus describe the same process in a minimal model[11]. We did this by employing a previously known minimal oscillator involving three ODEs, proposed by Wilhelm and Heinrich, aimed to describe chemical reactions[12]. The three ODEs in variables X, Y, and Z in the minimal oscillator corresponded, in our adapted model, to glutamate in the periphery (G_p), interior (G_i) and ammonia (A) respectively and were found to adequately describe the biofilm oscillations[11]. The system of equations of the basic model (BM) is as follows:

$$\frac{dG_p}{dt} = k_1 G_E G_p - k_4 G_p - k_2 A G_p \tag{BM1}$$

$$\frac{dA}{dt} = -k_3 A + k_5 G_i \tag{BM2}$$

$$\frac{dG_i}{dt} = k_4 G_p - k_5 G_i \tag{BM3}$$

The parameter names and values are listed in Table 1. Glutamate is the focal amino acid and supplied in the experimental setup. Hence, its external concentration is represented by a constant term (G_E). Its concentration within the cells in the periphery of the biofilm is dynamic and is represented by the variable G_p. It is plausible to assume a positive feedback of G_p on itself ($k_1 G_E G_p$) because as more glutamate is taken up, more proteins are produced, including membrane proteins, which help take up more glutamate. It then diffuses to the interior cells (with rate $k_4 G_p$) and, there, it is represented by G_i. We distinguish the same metabolite using two different variables based on their location in the biofilm since these regions use glutamate for different purposes. Interior cells produce ammonia using glutamate (rate $k_5 G_i$) since that produced by the periphery is lost to the environment and is a waste of nitrogen. Peripheral cells use the ammonia diffusing out from the interior in addition to the glutamate supplied in the microfluidics chamber to produce biomass ($k_2 A G_p$)[11]. However, the loss of ammonia due to diffusion to the environment ($k_3 A$) is much greater than its consumption to produce biomass; hence the term $k_2 A G_p$ is neglected in equation BM2.

This model describes all these processes as irreversible, which is quite unrealistic from a biological point of view. Wilhelm and coworkers[13] did present a reversible version of their oscillator. However, they considered all reactions to be reversible and assumed that the reverse reactions are considerably (10×) slower than the forward reactions, which may not be applicable for all biological scenarios. In particular, the diffusion constant is usually the same for either direction of diffusion.

In this study, we develop four sequels of the basic model to describe the oscillations in the system much more realistically, without compromising too much on minimalism. We first introduce a gradient of metabolites from the center of the biofilm to the periphery using six ODEs (Model 6ODE). Subsequently, we use realistic Michaelis-Menten kinetics instead of mass-action kinetics in addition to including some reversible reactions (Model RMM). Finally, we check the effect of using Michaelis-Menten kinetics (Model MMK) or reversible reactions (Model R) individually in two distinct versions on the model behavior.

Results and Discussion

Towards a continuous diffusion gradient within the biofilm. Having discrete interior and peripheral regions in a biofilm is quite adequate in the minimalist philosophy, but in a realistic scenario, there is no rigid boundary separating the interior from the periphery. Instead, there is a gradient of substances, the concentrations of which vary with the distance from the biofilm center. This is an important feature to test since it has not been considered by the BM[11]. Bocci *et. al.* have already modeled these gradients using PDEs[10].

In our model, we restrict ourselves to ODEs since PDEs are computationally expensive. This can be done by adding several layers (based on ODEs) to the biofilm. As a first step in this regard, we consider one more layer, represented by G_m, at the interface between G_i and G_p (see Fig. 1a,b). Furthermore, the BM only uses one variable (eq. BM2) to describe the dynamics of ammonia with the assumption that diffusion does not play a role in its dynamics because ammonia diffuses fast. We aim to test this assumption by using three separate ODEs for ammonia in the three layers of the model biofilm, namely, A_i, A_m, and A_p. We further subdivide this model into

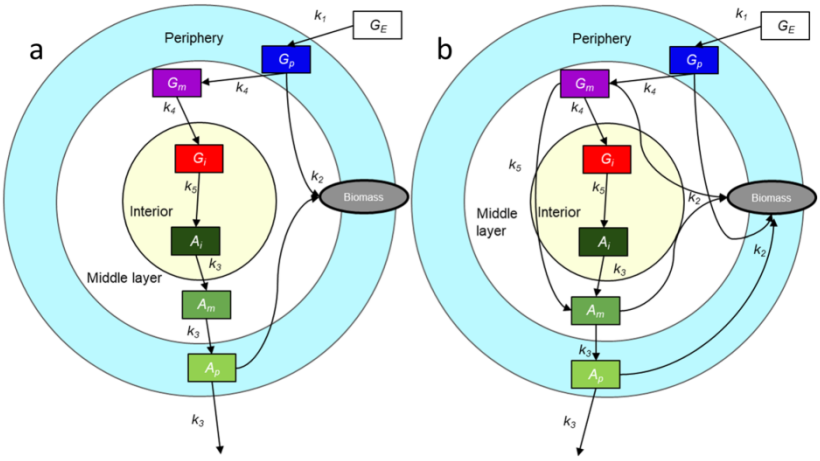

Figure 1. Overview of the six-variable models. (**a**) Simple 6 ODE model (s6ODE): Additional transitional layer between periphery and interior (G_m) connected to G_p and G_i through simple diffusion (k_4G_p and k_4G_m, respectively). Ammonia is represented by three different variables A_i, A_m, and A_p corresponding to each of the three layers also connected through simple diffusion (k_3A_i and k_3A_m). **(b)** Complex 6 ODE model (c6ODE): G_m serves not only as a physical but also a functional transitional layer, since it contributes to ammonia production (k_5G_m) and to biomass production ($k_2A_mG_m$) in addition to being connected through diffusion as in s6ODE. For values of parameters, see Table 1.

two categories based on the function of the middle layer. Since the layer is added between the interior and periphery, it can either act simply as a transitional layer (referred to as s6ODE model, Fig. 1a) or it could have a more complex function (referred to as c6ODE model, Fig. 1b) as a layer that contributes to biomass formation (like the periphery) and also ammonia production (like the interior).

$$\frac{dG_p}{dt} = k_1G_EG_p - k_4G_p - k_2A_pG_p \tag{1a}$$

$$\frac{dA_i}{dt} = -k_3A_i + k_5G_i \tag{1b}$$

$$\frac{dA_m}{dt} = -k_3A_m + k_3A_i \tag{1c}$$

$$\frac{dA_p}{dt} = -k_3A_p + k_3A_m \tag{1d}$$

$$\frac{dG_m}{dt} = k_4G_p - k_4G_m \tag{1e}$$

$$\frac{dG_i}{dt} = k_4G_m - k_5G_i \tag{1f}$$

$$\frac{dG_p}{dt} = k_1G_EG_p - k_4G_p - k_2A_pG_p \tag{2a}$$

$$\frac{dA_i}{dt} = -k_3A_i + k_5G_i \tag{2b}$$

$$\frac{dA_m}{dt} = -k_3A_m + k_3A_i + k_5G_m \tag{2c}$$

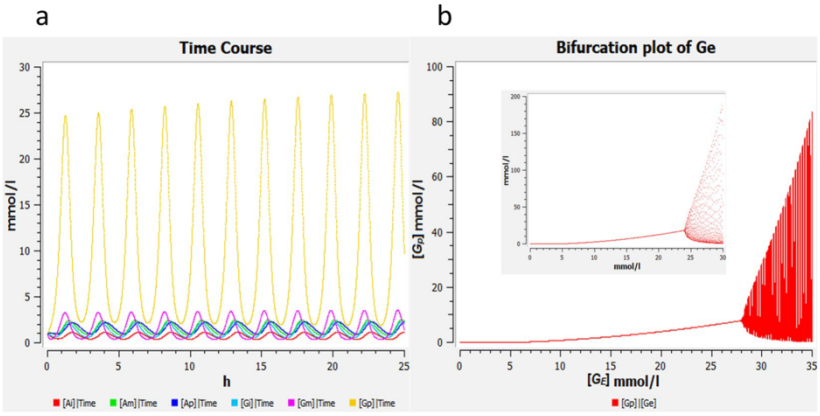

Figure 2. (**a**) Time course of ammonia (red, green and blue) and glutamate (cyan, magenta and yellow) in the interior, middle, and peripheral regions as computed by the c6ODE model. Oscillations are more spike-like than in the BM due to delay in the feedback induced by variable G_m and diffusion of ammonia. For parameters, refer to Table 1. **(b)** Bifurcation diagrams of G_p versus G_E for the c6ODE model and (inset) BM[11]. The supercritical Hopf bifurcation occurs at $G_E = 28$ mmol/l in the c6ODE (for BM bifurcation at $G_E = 24.4$ mmol/l) but qualitatively, the model has not changed. The two arms of the convex hull represent the amplitude of oscillation which widen as the value of G_E increases. The initial values of all variables were 1 mmol/l. Parameter values: refer to Table 1.

$$\frac{dA_p}{dt} = -k_3 A_p + k_3 A_m \tag{2d}$$

$$\frac{dG_m}{dt} = k_4 G_p - k_4 G_m - k_5 G_m - k_2 A_m G_m \tag{2e}$$

$$\frac{dG_i}{dt} = k_4 G_m - k_5 G_i \tag{2f}$$

These two possibilities are modeled and analyzed separately. The results are shown in Fig. 2. For the bifurcation plot of the s6ODE model, see Fig. S1.

Simulating either of these model variants leads to results that do not show qualitative differences from the three-variable version[11], except that the oscillations are more spike-like (Fig. 2a). This is because the middle layer causes a delay in the diffusion of glutamate and ammonia. A comparison of the bifurcation plots (Figs. 2b and S1) and the analogous Fig. 2b(inset) shows that there is no drastic effect on the Hopf bifurcation point nor the amplitude. Thus, we concluded that it is not necessary to go on adding further layers to the s6ODE or c6ODE variant until a smooth gradient is created, and it is adequate to use a three-variable system instead of an n-variable system. This is in support of our assumption that an ODE model instead of a PDE model is sufficient.

Michaelis-Menten kinetics along with reversible reactions. In order to further improve the model by using biologically more realistic kinetics, we employ Michaelis-Menten kinetics to describe the uptake of glutamate from the environment, which is mediated by transport proteins embedded in the membrane of the cell[14]. Additionally, inspired by the reversible version[13] of the BM[12], we also make the following reactions reversible:

$$\begin{aligned} A + G_p &\underset{k_2}{\overset{k_{-2}}{\rightleftharpoons}} A + biomass \\ G_p &\underset{k_4}{\overset{k_{-4}}{\rightleftharpoons}} G_i \\ G_i &\underset{k_5}{\overset{k_{-5}}{\rightleftharpoons}} A \end{aligned} \tag{RMM}$$

The consumption of A and G_p for protein (biomass) is considered reversible. This is biologically meaningful because biomass is subject to a permanent turnover, involving degradation to amino acids and ammonia. In the above reaction equation, we consider A on both sides for technical reasons. This formally implies that

the stoichiometric coefficient of ammonia is zero, which is in line with the approximative assumption that the ammonia balance is almost exclusively affected by diffusion rather than by biomass turnover. Additionally, the diffusion of glutamate between the interior and periphery and the production of ammonia from glutamate is also reversible. The diffusion of ammonia to the surroundings is a rapid irreversible process[8]. Additionally, the uptake of glutamate from the environment is also irreversible since the process is mediated by transporters on the bacterial membrane[14]. Thus, the reversible Michaelis-Menten version of BM[11], called model RMM is governed by the following equations:

$$\frac{dG_p}{dt} = \frac{V_{max}G_EG_p}{k_m + G_p} - k_4G_p - k_2AG_p + k_{-2}A + k_{-4}G_i \quad \text{(RMM1)}$$

$$\frac{dA}{dt} = -k_3A + k_5G_i - k_{-5}A \quad \text{(RMM2)}$$

$$\frac{dG_i}{dt} = k_4G_p - k_5G_i - k_{-4}G_i + k_{-5}A \quad \text{(RMM3)}$$

We then examine the sensitivity of the bifurcation to the parameters of the model. To simplify this, we assume $k_{-2} = k_{-4} = k_{-5} = r$. Note that for bifurcation analyses with respect to all parameters other than r, we use the plausible equality $k_{-2} = k_2$, $k_{-4} = k_4$ and $k_{-5} = k_5$. Bifurcation plots for the parameters G_E, V_{max}, K_m, and r are shown in Fig. 3a–d. We used a wide scan range for each parameter because we do not have experimental values for all parameters. Once the parameters have been measured more accurately, their values can easily be included in the model.

For bifurcation parameter G_E, we once again found the supercritical Hopf bifurcation just like in the BM. Interestingly, when G_E was further increased, we observed another bifurcation which was laterally flipped, supercritical and conjoined to the first bifurcation, so that the diagram resembles a 'bubble' (Fig. 3a). Such a bubble-like pair of Hopf bifurcations was also observed in several models of calcium oscillations[15]. The supercritical bifurcations indicate that there are certain values of G_E where the oscillations vanish with a smoothly decreasing amplitude. This implies that the oscillations will vanish with high availability of glutamate (nutrients), this was also found to be true experimentally[4]. The supercritical nature of the second bifurcation seems more biologically realistic than a switch-like transition (as would occur in a subcritical Hopf bifurcation) since the oscillatory process cannot suddenly halt. A similar effect is also observed when V_{max} is used as a bifurcation parameter instead of G_E (Fig. 3b).

A second Hopf bifurcation also occurs upon variation of the Michaelis-Menten constant, K_m (Fig. 3c). When K_m is very low, the saturation range is reached early, so that the kinetics becomes practically independent of G_p. Therefore, no undamped oscillations can arise in that case. When K_m is very high, the slope of the kinetics is low, so that the feedback is not strong enough to enable undamped oscillations.

As can be seen in Fig. 3d, oscillations occur also if r is in the range of $2\,h^{-1}$, similar to those of the forward reactions (see Table 1), which implies that oscillations can be observed when the rate constants of forward and reverse reactions are approximately equal. In our biological scenario, equal rates of forward and backward reactions are quite suitable.

Michaelis-menten kinetics – fortifying the model to make it biologically plausible. Now we make two modifications to investigate the individual effects of either Michaelis-Menten kinetics or reversibility of reactions on this bubble-like bifurcation and determine which one of them are the cause of such a bifurcation.

We modify equation BM1 describing G_p as follows:

$$\frac{dG_p}{dt} = \frac{V_{max}G_EG_p}{k_m + G_p} - k_4G_p - k_2AG_p \quad \text{(MMK1)}$$

The other equations (MMK2 and MMK3) remain unchanged from the BM (eqs BM2 and BM3)[11].

We found the same bubble-like pair of Hopf bifurcations that was seen for model RMM. This bifurcation could be explained as follows: If G_E gets very high, the glutamate input increases considerably, so that G_p increases up to the saturation range. Then, the kinetics becomes practically independent of G_p, so that the essential properties of the minimal basic model are no longer granted and undamped oscillations can no longer occur (Fig. 4). While usually, the amplitude increases gradually at supercritical Hopf bifurcations, in our system, it increases quite abruptly in one of the bifurcations (Fig. 4a, right part of the bubble). A drawback of this model is the complete lack of reversible reactions which is unrealistic especially in the case of diffusion.

The effect of reversible reactions. In the final modification, we investigate the effect of reversible reactions alone. The model is similar to model RMM except that it uses mass action kinetics instead of Michaelis-Menten. Thus the equation RMM1 from above becomes:

$$\frac{dG_p}{dt} = (k_1G_E - k_4)G_p - k_2AG_p + k_{-2}A + k_{-4}G_i \quad \text{(R1)}$$

And the equations RMM 2,3 are as above:

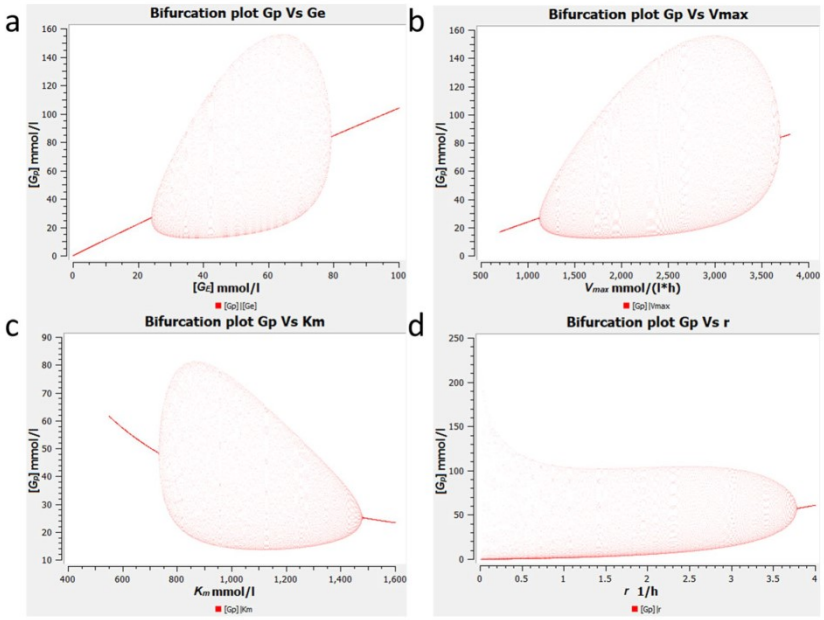

Figure 3. Bifurcation diagrams of G_p versus **(a)** G_E **(b)** V_{max} **(c)** K_m **(d)** r. In (**a–c**), we can observe a peculiar bubble-like pair of Hopf bifurcations. In the case of K_m, the bubble is laterally inverted with respect to that of G_E and V_{max} indicating that increasing K_m implies a steep increase in amplitude at the left bifurcation whereas a gradual decrease at the right bifurcation. For parameter values refer to Table 1.

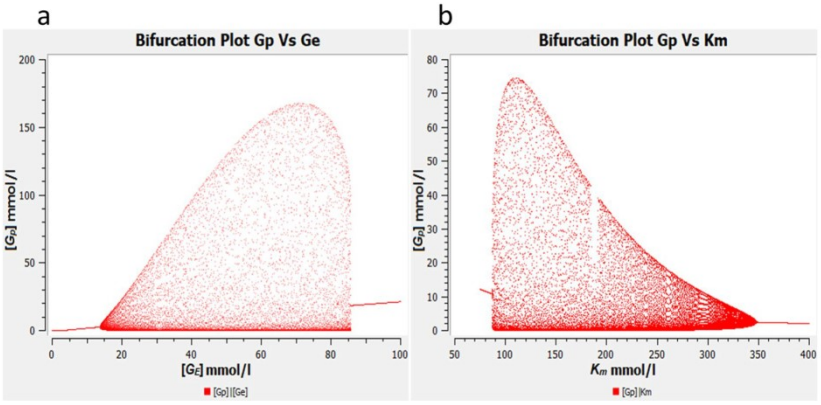

Figure 4. Bifurcation diagram of: **(a)** G_p versus G_E. The same bifurcation bubble as for model RMM is obtained for G_E (and K_m) with the only difference that the oscillations vanish in an abrupt way. Oscillations emerge gradually (supercritical bifurcation occurs at $G_E = 13.6$ mmol/l) and the bubble edges represent the amplitude of the oscillations which initially increases, then starts decreasing and eventually becomes zero (supercritical Hopf bifurcation at $G_E = 85$ mmol/l). Parameters: see Table 1, except: $K_m = 150$ mmol/l, $V_{max} = 100$ mMol-h^{-1}. **b)** The bifurcation diagram is laterally flipped when K_m is used as a bifurcation parameter indicating an inverse relationship between amplitude and K_m.

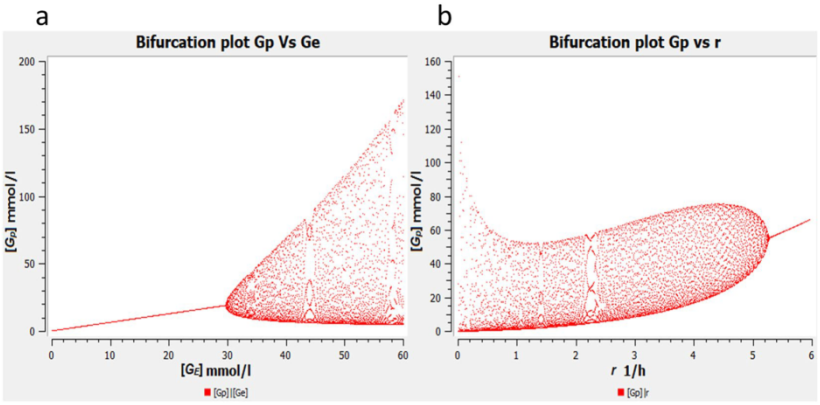

Figure 5. Bifurcation diagram of G_p (**a**) versus G_E. $k_1 = 0.88$ (mmol/l h)$^{-1}$. Hopf bifurcation at $G_E =$ 29.5 mmol/l (**b**) versus r: Oscillations are observed to diminish in amplitude overall as r increases but one can still see oscillations at $r = 5.2\,\mathrm{h}^{-1}$. For further parameter values, see Table 1.

$$\frac{dA}{dt} = -k_3A + k_5G_i - k_{-5}A \tag{R2}$$

$$\frac{dG_i}{dt} = k_4G_p - k_5G_i - k_{-4}G_i + k_{-5}A \tag{R3}$$

Similar to model RMM, r is the rate constant of reverse reactions for the bifurcation analysis with respect to these reactions and $k_{-2} = k_{-4} = k_{-5} = r$. In the bifurcation analysis for the other parameters, we assume $k_{-2} = k_2$, $k_{-4} = k_4$ and $k_{-5} = k_5$.

This is the reversible version of BM[11], called model R. Note that Eqs. R1 and R2 are identical to equations RMM2 and RMM3, respectively.

The system shows no change in the oscillatory behavior in comparison to the BM, in particular, bifurcation analysis with respect to G_E does not show the bubble-like Hopf bifurcation (see Fig. 5a). This indicated that Michaelis-Menten kinetics is the cause for the bubble-like Hopf bifurcation, in line with the explanation for that given above. However, when the reaction for the uptake of glutamate is made reversible, the bubble-like bifurcation can be seen once again (see Fig. S2). This is a new observation and was not anticipated by Wilhelm and Heinrich in their reversible model[13] where they consider all reactions to be reversible with a rate constant of backward reaction 0.1 times that of the forward reaction.

The drawback of model R, however, is that it tends to a steady state when all the backward rate constants are equal to the forward rate constants (data not shown). This can be addressed and oscillations can still be obtained if the value of k_1 is increased from 0.34 (mM* h)$^{-1}$ to 0.88 (mM* h)$^{-1}$ (Fig. 5b).

Quasi-steady-state approximation for the model R. Since ammonia is a small molecule, it diffuses fast. Thus, the question arises whether a quasi-steady-state approximation[16] can be applied. In the following, we analyze the special case where reaction 3 would be very fast. We could then assume that the variable A attains a quasi-steady state:

$$\frac{dA}{dt} = -k_3A + k_5G_i - k_{-5}A \cong 0, \text{ which leads to } A = \frac{k_5}{k_3 + k_{-5}}G_i \tag{5}$$

From Eq. (5), we derive a reduced system:

$$\frac{dG_p}{dt} = (k_1G_E - k_4)G_p - \frac{k_2k_5}{k_3 + k_{-5}}G_iG_p + \left(\frac{k_{-2}k_5}{k_3 + k_{-5}} + k_{-4}\right)G_i \tag{6}$$

$$\frac{dG_i}{dt} = k_4G_p + \left(\frac{k_{-5}k_5}{k_3 + k_{-5}} - k_5 - k_{-4}\right)G_i \tag{7}$$

The system shows two steady states:

$$G_{p_1} = G_{i_1} = 0$$

which is the trivial steady-state (TSS)

$$G_{p_2} = c\frac{(k_1 G_E - k_4)(k_3 + k_{-5})}{k_2 k_5} + \left(\frac{k_{-2}}{k_2} + \frac{(k_3 + k_{-5})k_{-4}}{k_2 k_5}\right) \tag{9a}$$

$$G_{i_2} = \frac{(k_1 G_E - k_4)(k_3 + k_{-5})}{k_2 k_5} + \frac{1}{c}\left(\frac{k_{-2}}{k_2} + \frac{(k_3 + k_{-5})k_{-4}}{k_2 k_5}\right) \tag{9b}$$

which is the non-trivial steady-state (NTSS)
where $c = \frac{k_5 k_3 + k_{-4} k_3 + k_{-4} k_{-5}}{k_4 (k_3 + k_{-5})}$ which is always positive.

The Jacobian matrix for the NTSS reads:

$$\mathbf{M} = \begin{pmatrix} (k_1 G_E - k_4) - \frac{k_2 k_5}{k_3 + k_{-5}} G_i & -\frac{k_2 k_5}{k_3 + k_{-5}} G_p + \frac{k_{-2} k_5}{k_3 + k_{-5}} + k_{-4} \\ k_4 & \frac{k_{-5} k_5}{k_3 + k_{-5}} - k_5 - k_{-4} \end{pmatrix} \tag{10}$$

For the TSS, it reads:

$$\mathbf{M} = \begin{pmatrix} k_1 G_E - k_4 & \frac{k_{-2} k_5}{k_3 + k_{-5}} + k_{-4} \\ k_4 & \frac{k_{-5} k_5}{k_3 + k_{-5}} - k_5 - k_{-4} \end{pmatrix} \tag{11}$$

The eigenvalues are $\lambda_{1,2} = \frac{-b \pm \sqrt{b^2 - 4ac}}{2}$, where

$$\begin{aligned} a &= 1 \\ b &= -a_{11} - a_{22} = -\left[k_1 G_E - k_4 + \frac{k_{-5} k_5}{k_3 + k_{-5}} - k_5 - k_{-4}\right] \\ c &= a_{11} a_{22} - a_{12} a_{21} = (k_1 G_E - k_4)\left(\frac{k_{-5} k_5}{k_3 + k_{-5}} - k_5 - k_{-4}\right) - k_4\left(\frac{k_{-2} k_5}{k_3 + k_{-5}} + k_{-4}\right) \end{aligned} \tag{12}$$

and for the NTSS (see supplement)

For the TSS: the eigenvalues are real if and only if $b^2 > 4ac$ which can be achieved with $k_1 G_E < k_4$. If the root value is smaller than the b value, then both eigenvalues are negative, so that the trivial steady state is a stable node. Otherwise, one eigenvalue is negative and the other one positive. The steady-state then is unstable, it is a saddle point. Furthermore, the case where $b^2 < 4ac$ leads to complex eigenvalues and thus the steady-state is a stable focus (damped oscillations).

This implies that undamped oscillations cannot occur when ammonia diffuses so fast that it can be eliminated as a variable by the quasi-steady-state approximation. This also follows from general results by Hanusse[17,18] saying a system involving two variables and only linear and bilinear terms cannot give rise to limit-cycle oscillations. As oscillations were observed in *B. subtilis* biofilms, we do not consider extremely high diffusion coefficients of ammonia in this study.

Materials and methods

Simulation. For computer simulations, we used the software COPASI versions 4.16 and 4.24[19] and its LSODA deterministic solver. The simulations were double-checked using the Matlab ode15s (MathWorks) function. The figures of the simulations were produced using COPASI.

Except for k_2, k_3, and k_4, the rate constants were adopted from the publication of Wilhelm and Heinrich[12] and were rescaled such that the period of oscillations matched the one in the experimental work by Liu *et al.*[4]. The rate constant of diffusion of ammonia, k_3, is tuned to be twice as high as that of glutamate, k_4. This is because the diffusion coefficient for ammonia[20] is about 1.6E-05 $cm^2\ s^{-1}$ while that for glutamate[21,22] is about 8E-06 $cm^2 s^{-1}$. The values of K_m and V_{max} are arbitrary because we just want to analyse the qualitative effect of enzyme kinetics, without a specific enzyme in mind.

Conclusion

Here, we have analysed various model variants to describe biofilm oscillations. We used ODE systems, as is often done in mathematical biology[16,23]. Bocci *et. al.*[10] used PDEs to describe biofilm oscillations, which is a computationally expensive approach. Our results above show that ODEs yield satisfactory results as well. ODE systems must involve at least two variables to describe limit-cycle oscillations[15,16,24]. When only linear and bilinear kinetics is

used, at least three variables are needed[17,18]. Note that two-dimensional oscillator models such as the Brusselator[25] and the Somogyi-Stucki model[26] involve higher non-linearities. Therefore, our basic model is three-dimensional.

We have tested different modifications of the basic model[11] and discussed salient features and disadvantages for each. All the models analysed here involve a positive feedback, notably of peripheral glutamate on its own uptake. In many biological systems, a positive feedback is the cause of oscillations[15,16,27].

Adding additional layers makes the model more spatial. It may be possible to have more experimental inputs to the model. For example, the diffusion rates of ammonia and glutamate could be obtained from experiments to obtain more realistic amplitudes and wavelengths of oscillation. However, this does not qualitatively change the model. The bifurcation obtained is a supercritical Hopf bifurcation just like in the previous study[11]. We conclude that the modification of adding a middle region (models s6ODE and c6ODE) does not improve the model in any way. It highlights that ODEs describing just two layers are sufficient to model this biological phenomenon and that similar observations can also be obtained, if spatial effects are ignored.

The next modification, RMM, investigates the effect of Michaelis-Menten kinetics and reversibility. It has reversible reactions and the system shows undamped oscillations when the equilibrium constants of the reversible reactions are unity, which is realistic. It also uses Michaelis-Menten kinetics which is more robust to describe the process of nutrient uptake. Thus this modification is well suited to describe the periodic halting of growth of the *Bacillus subtilis* biofilm and has a greater scope to include experimental parameters like K_m and V_{max}. We also obtain a peculiar bubble-like pair of Hopf bifurcations for this system. Such bifurcations were also obtained on models for cellular calcium oscillations[15]. The range beyond the second Hopf bifurcation is then called "overstimulation", meaning that at high agonist levels, no oscillations occur[26,27].

The RMM model predicts that if the nutrient supply gets high enough, oscillations will no longer continue (see Fig. 3a). In other words, metabolic oscillations are a mechanism to mitigate the nutrient limitation and therefore, can only be observed when nutrients are scarce. This observation, although quite intuitive, was not reported in the models of biofilm oscillations shown earlier[4,10,11,28]. This prediction could be validated in experiments, and knowing this threshold could help us control and modulate biofilm growth.

A similar bifurcation was also observed when V_{max} was used as a bifurcation parameter instead of G_E. A second Hopf bifurcation also occurs upon variation of the Michaelis-Menten constant, K_m (Fig. 3c). When K_m is very low, the system reaches the saturation range early, so that the kinetics becomes practically independent of G_p. Thus, the sole bilinear term is lost and the remainder linear system cannot show a limit cycle[16]. When K_m is very high, the slope of the kinetics is low, so that the feedback is not strong enough to enable undamped oscillations. The model also retains its minimality with respect to the number of variables and the number of bilinear terms used which makes it quite easy to analyze.

In order to investigate whether the cause of such bifurcation is the inclusion of reversibility or Michaelis-Menten kinetics, we analysed the two modifications separately in the further models. We also discussed the inspiration behind these individual modifications in the respective paragraphs.

The third extension, MMK, is achieved by using Michaelis-Menten kinetics for the uptake reaction. Uptake of glutamate has been shown to be mediated by a proton/glutamate symport protein in *B. subtilis*[14]. Here we neglect the diffusion of glutamate from the environment to the biofilm periphery but focus mainly on the uptake of glutamate by the cells in the periphery. We found that at one of the Hopf bifurcations, the amplitude increases very steeply. This could be considered physiologically advantageous because a pronounced division of labour is already reached close to the bifurcation. Analogously, in calcium oscillations, this phenomenon is beneficial for signal recognition[29]. For the system studied here, this modification led to a revelation that oscillations vanish after a high enough value of the bifurcation parameter. In terms of G_E, it suggests that beyond a threshold value, the oscillations will no longer persist. This seems quite a likely case since oscillations arise in order to allow the interior of the biofilm obtain a steady input of glutamate. When glutamate is supplied in large excess, the interior will always have a steady supply of it and thus the oscillations will no longer be necessary. From a mathematical point of view, we observe that the saturation kinetics viz. Michaelis-Menten kinetics are crucial for obtaining such a bubble-like Hopf bifurcation. The major contribution of this model is that it identifies the cause of the bubble-like Hopf bifurcations.

The model R has already been inspired by a model established earlier[13]. We adopted and improved it by applying reversibility to only those reactions which are really reversible. For instance, the loss of ammonia is a highly irreversible reaction since ammonia is a small molecule that diffuses very rapidly once it is generated. From a physical point of view, all diffusion processes are reversible. However, when the concentration differences are large, the reverse process can be neglected. This was also done in models of calcium oscillations with respect to the calcium concentrations in the cytosol (low) and endoplasmic reticulum and external space (high)[26,27]. As the difference in glutamate concentrations between the peripheral and interior regions is less pronounced, we here extended the BM so that glutamate diffusion is reversible.

In model R, we found the same bubble-like bifurcation that was seen for the Michaelis-Menten model only when the reaction for the uptake of glutamate (given by the term $k_1 G_E G_p$) is made reversible (see Fig. S2). This was not anticipated by Wilhelm and coworkers[13], who also proposed a fully reversible version of their model, and is thus an interesting new observation. Biologically it implies that when there are reversible reactions involved, there will be a stabilizing effect in the system that will prevent the amplitude to increase indefinitely with the bifurcation parameter. However, the uptake of glutamate is an active process and, therefore, can be modeled to be irreversible. In that case, only a single Hopf bifurcation is observed (Fig. 5a). The drawback is that the system tends to a steady-state (i.e. oscillations vanish) when all the backward rate constants are equal to the forward rate constants, which means that the equilibrium constants of the reversible reactions are unity. This can be resolved by increasing k_1 indicating that a higher glutamate uptake rate is required for oscillations to persist at greater reversibility. Thus, this modification helps to correct the glutamate uptake rate k_1. It also helps identify the reaction that causes the bubble-like Hopf bifurcation.

This work highlights the importance of simple ODE based models to describe the observations of Liu *et al.*[4]. Each modification presented here reveals a new piece of the puzzle which, when put together, will help us see the broader picture that is biofilm oscillations. The extended models presented here are still simpler and easier to handle than the Liu model (which involves 6 ODEs) and describe the experimental observations equally well. The aim of both the Liu model and ours is to describe biofilm oscillations qualitatively or at best semi-quantitatively. It is difficult to say whether the extended models describe the observations better than the basic model because no comprehensive parameter scan had been performed in experiment. As the extended models involve more parameters, it is likely that they can be fitted better to data obtained in the future.

The transition between oscillatory and stationary regimes can be gradual as in the case of model RMM or abrupt as in the case of model MMK which makes the BM flexible to describe two contrasting scenarios. An additional experimental investigation will provide more clarity about the exact nature of oscillations in the biofilm of *Bacillus subtilis*.

Ethical approval and informed consent. Ethics approval was not required for this study and not applicable

Data availability

No data are associated with this article.

Received: 5 November 2019; Accepted: 13 March 2020;
Published online: 27 March 2020

References

1. Pommerville, J. C. *Fundamentals of Microbiology*. (Burlingston, MA, Jones & Bartlett Learning, 2013).
2. Davies, D. Understanding biofilm resistance to antibacterial agents. *Nat. Rev. Drug. Discov.* **2**, 114–122, https://doi.org/10.1038/nrd1008 (2003).
3. Donlan, R. M. & Costerton, J. W. Biofilms: survival mechanisms of clinically relevant microorganisms. *Clin. Microbiol. Rev.* **15**, 167–193, https://doi.org/10.1128/cmr.15.2.167-193.2002 (2002).
4. Liu, J. *et al*. Metabolic co-dependence gives rise to collective oscillations within biofilms. *Nature* **523**, 550–554, https://doi.org/10.1038/nature14660 (2015).
5. Dragos, A. *et al*. Division of labor during biofilm matrix production. *Curr. Biol.* **28**, 1903–1913 e1905, https://doi.org/10.1016/j.cub.2018.04.046 (2018).
6. Vlamakis, H., Aguilar, C., Losick, R. & Kolter, R. Control of cell fate by the formation of an architecturally complex bacterial community. *Genes. Dev.* **22**, 945–953, https://doi.org/10.1101/gad.1645008 (2008).
7. Flemming, H. C. *et al*. Biofilms: an emergent form of bacterial life. *Nat. Rev. Microbiol.* **14**, 563–575, https://doi.org/10.1038/nrmicro.2016.94 (2016).
8. Castorph, H. & Kleiner, D. Some properties of a *Klebsiella pneumoniae* ammonium transport negative mutant (Amt-). *Arch. Microbiol.* **139**, 245–247, https://doi.org/10.1007/bf00402008 (1984).
9. Gunka, K. & Commichau, F. M. Control of glutamate homeostasis in *Bacillus subtilis*: a complex interplay between ammonium assimilation, glutamate biosynthesis and degradation. *Mol. Microbiol.* **85**, 213–224, https://doi.org/10.1111/j.1365-2958.2012.08105.x (2012).
10. Bocci, F., Suzuki, Y., Lu, M. & Onuchic, J. N. Role of metabolic spatiotemporal dynamics in regulating biofilm colony expansion. *Proc. Natl Acad. Sci. USA* **115**, 4288–4293, https://doi.org/10.1073/pnas.1706920115 (2018).
11. Garde, R., Ibrahim, B., Kovács, Á. T. & Schuster, S. Differential equation-based minimal model describing metabolic oscillations in *Bacillus subtilis* biofilms. *Royal Society Open Science* **7** https://doi.org/10.1098/rsos.190810 (2020).
12. Wilhelm, T. & Heinrich, R. Smallest chemical reaction system with Hopf bifurcation. *J. Math. Chem.* **17**, 1–14, https://doi.org/10.1007/bf01165134 (1995).
13. Wilhelm, T., Schuster, S. & Heinrich, R. Kinetic and thermodynamic analyses of the reversible version of the smallest chemical reaction system with Hopf bifurcation. *Nonlinear World*, 295–321 (1997).
14. Tolner, B., Ubbink-Kok, T., Poolman, B. & Konings, W. N. Characterization of the proton/glutamate symport protein of *Bacillus subtilis* and its functional expression in Escherichia coli. *J. Bacteriol.* **177**, 2863–2869, https://doi.org/10.1128/jb.177.10.2863-2869.1995 (1995).
15. Schuster, S., Marhl, M. & Höfer, T. Modelling of simple and complex calcium oscillations. From single-cell responses to intercellular signalling. *Eur. J. Biochem.* **269**, 1333–1355, https://doi.org/10.1046/j.0014-2956.2001.02720.x (2002).
16. Heinrich, R. & Schuster, S. *The Regulation of Cellular Systems*. (Chapman & Hall, New York, 1996).
17. Hanusse, P. De l'existence d'un cycle limite dans l'evolution des systèmes chimiques cuverts. *C. R. Acad. Sci. Paris, C274 (1972)*, 1245–1247 (1972).
18. Hanusse, P. Étude des systèmes dissipatifs chimiques à deux et trois espèces intermédiaires. *C. R. Acad. Sci. Paris C 277*, 263–266 (1973).
19. Hoops, S. *et al*. COPASI–a COmplex PAthway SImulator. *Bioinformatics* **22**, 3067–3074, https://doi.org/10.1093/bioinformatics/btl485 (2006).
20. Cussler, E. L. *Diffusion*. 2 edn, (Cambridge University Press, 2009).
21. Kullmann, D. M., Min, M. Y., Asztely, F. & Rusakov, D. A. Extracellular glutamate diffusion determines the occupancy of glutamate receptors at CA1 synapses in the hippocampus. *Philos. Trans. R. Soc. Lond. B Biol. Sci.* **354**, 395–402, https://doi.org/10.1098/rstb.1999.0392 (1999).
22. Ribeiro, A. C. F. *et al*. Mutual diffusion coefficients of L-glutamic acid and monosodium L-glutamate in aqueous solutions at T=298.15K. *J. Chem. Thermodyn.* **74**, 133–137, https://doi.org/10.1016/j.jct.2014.01.017 (2014).
23. Klipp, E., Herwig, R., Kowald, A., Wierling, C. & Lehrach, H. *Systems Biology in Practice* (Wiley-VCH, Weinheim, 2005).
24. Ewald, J., Sieber, P., Garde, R., Lang, S. N., Schuster, S. & Ibrahim, B. Trends in mathematical modeling of host–pathogen interactions. *Cell. Mol. Life Sci.* **77**, 467–480, https://doi.org/10.1007/s00018-019-03382-0 (2020).
25. Prigogine, I. From being to becoming: Time and complexity in the physical sciences (New York, 1980).
26. Somogyi, R. & Stucki, J. W. Hormone-induced calcium oscillations in liver cells can be explained by a simple one pool model. *J. Biol. Chem.* **266**, 11068–11077 (1991).
27. Goldbeter, A., Dupont, G. & Berridge, M. J. Minimal model for signal-induced Ca2+ oscillations and for their frequency encoding through protein phosphorylation. *Proc. Natl Acad. Sci. USA* **87**, 1461–1465, https://doi.org/10.1073/pnas.87.4.1461 (1990).
28. Martinez-Corral, R., Liu, J., Suel, G. M. & Garcia-Ojalvo, J. Bistable emergence of oscillations in growing *Bacillus subtilis* biofilms. *Proc. Natl Acad. Sci. USA* **115**, E8333–E8340, https://doi.org/10.1073/pnas.1805004115 (2018).

29. Schuster, S. & Marhl, M. Bifurcation analysis of calcium oscillations: Time-scale separation, canards, and frequency lowering. *J. Biol. Syst.* **9**, 291–314, https://doi.org/10.1142/S021833900100044x (2001).

Acknowledgements
We acknowledge the financial support from the Max Planck Society and German Research Foundation. RPG was supported by the Max Planck Society through the IMPRS "Exploration of Ecological Interactions with Molecular and Chemical Techniques". BI was supported by the DFG through the Collaborative Research Center 1127, Chembiosys Project C07.

Author contributions
Ravindra Garde, Bashar Ibrahim and Stefan Schuster conceived the idea of making the various modifications to the minimal model. Ravindra Garde performed modeling and simulation using COPASI and interpreted the results biologically. Bashar Ibrahim verified the results using Matlab and performed all mathematical analyses like QSSA. Ravindra Garde wrote the manuscript and Stefan Schuster and Bashar Ibrahim edited and structured it. All the authors have thoroughly read and consented to the publishing of the manuscript.

Competing interests
The authors declare no competing interests.

Additional information
Supplementary information is available for this paper at https://doi.org/10.1038/s41598-020-62526-6.

Correspondence and requests for materials should be addressed to B.I. or S.S.

Reprints and permissions information is available at www.nature.com/reprints.

Publisher's note Springer Nature remains neutral with regard to jurisdictional claims in published maps and institutional affiliations.

S. Supplementary Information

1. Quasi-steady-state approximation non trivial steady state

The Jacobian matrix for the NTSS reads:

$$\mathbf{M} = \begin{pmatrix} (k_1 G_E - k_4) - \frac{k_2 k_5}{k_3 + k_{-5}} G_i & -\frac{k_2 k_5}{k_3 + k_{-5}} G_p + \frac{k_{-2} k_5}{k_3 + k_{-5}} + k_{-4} \\ k_4 & \frac{k_{-5} k_5}{k_3 + k_{-5}} - k_5 - k_{-4} \end{pmatrix}$$

The eigenvalues are $\lambda_{1,2} = \frac{-b \pm \sqrt{b^2 - 4ac}}{2}$, where

for the NTSS:

$$a = 1$$

$$b = -a_{11} - a_{22} = -[k_1 G_E - k_4 - GG_i + \frac{k_{-5} k_5}{k_3 + k_{-5}} - k_5 - k_{-4}]$$

$$c = a_{11} a_{22} - a_{12} a_{21} = (k_1 G_E - k_4 - GG_i)(\frac{k_{-5} k_5}{k_3 + k_{-5}} - k_5 - k_{-4}) - k_4(\frac{k_{-2} k_5}{k_3 + k_{-5}} + k_{-4})$$

and $GG_i = \frac{k_2 k_5}{k_3 + k_{-5}} G_{iSS}$ (always positive , and $k_3 + k_{-5} \neq 0$)

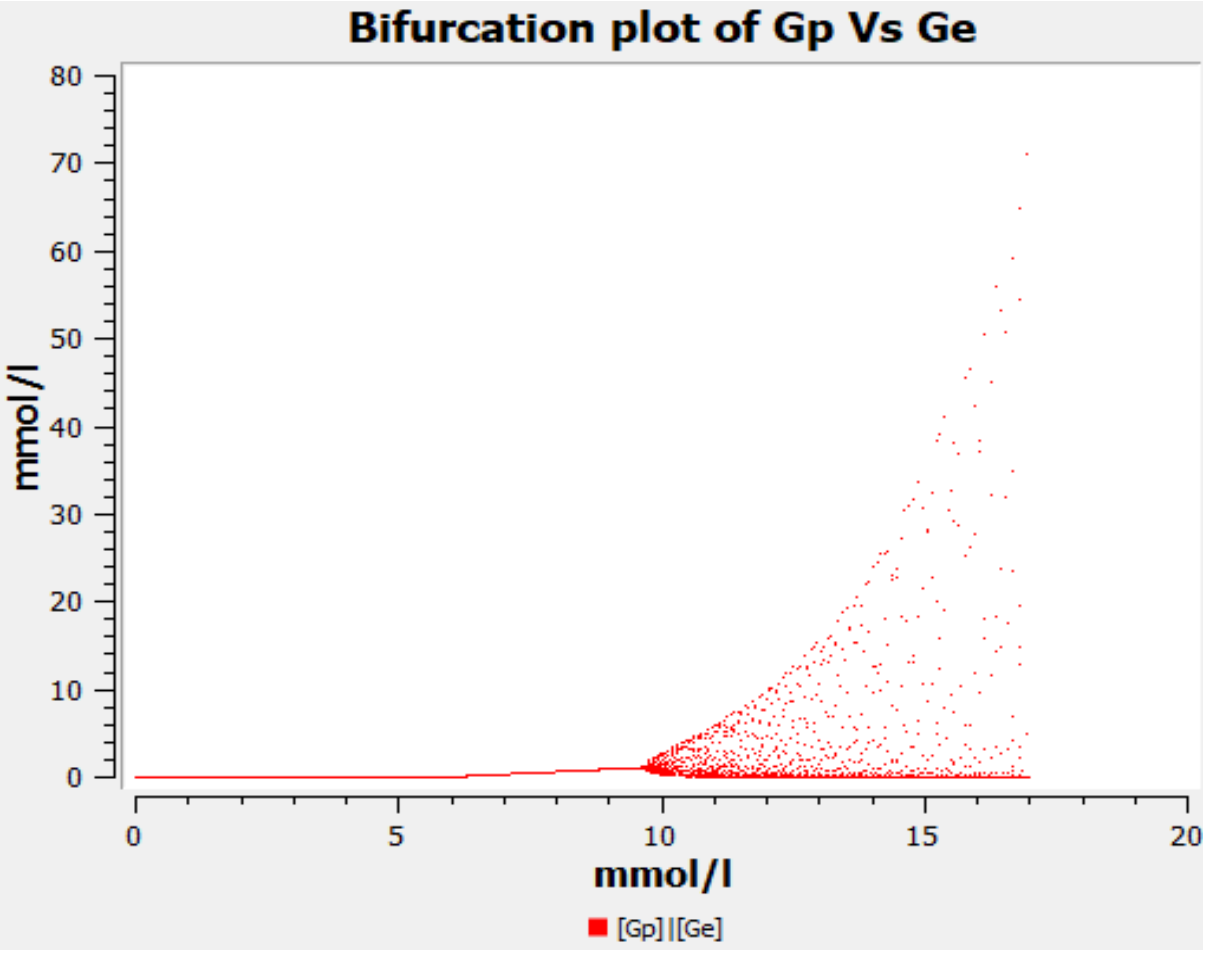

Figure S1: Bifurcation plot of G_p versus G_E (model s6ODE): The Hopf bifurcation occurs at about G_E = 9.6 mmol/l, as opposed to 24.4 mmol/l for model BM or c6ODE.

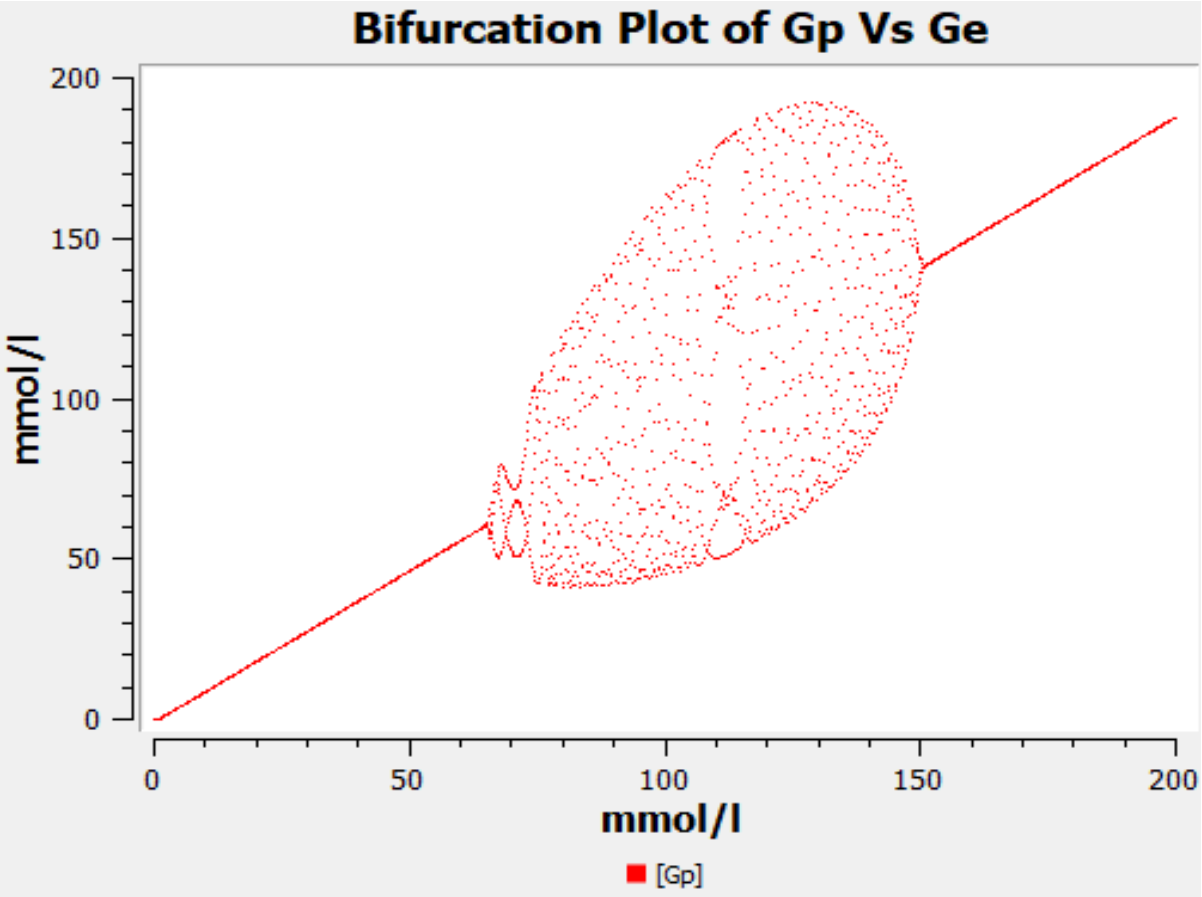

Figure S2: Bifurcation plot of G_p versus G_E (model R): Parameters: k_1 = 0.74 (mM* h)$^{-1}$, k_{-1} = 0.074 (mM* h)$^{-1}$, $k_2 = k_{-2} = k_5 = k_{-5} = k_2$ = 2.3 h^{-1}, $k_3 = k_{-3}$ = 4 h^{-1}, $k_2 = k_2$ = 3 h^{-1}. Only for this set of parameters, and when k_{-1} is non zero, the bubble-like Hopf bifurcation can be observed, indicating that reversibility of reaction 1 is crucial for this kind of a bifurcation.

IV. Modelling population dynamics in a unicellular social organism community using a minimal model and evolutionary game theory

Ravindra Garde, Jan Ewald, Ákos T. Kovács, Stefan Schuster

Published in: Royal Society Open Biology volume 10, issue 11. Published on: 4th November 2020

Here we apply the minimal model to describe the population dynamics of three different phenotypes: the resistant cells, the motile cells and the producer cells. The three subpopulations represent a typical unicellular social organism community. We test the behaviour of the community under three different levels of antibiotic stress. We also present a game theoretical interpretation of the observed behaviour. The work helps understand the strategies that a population makes in order to maximise its chances of survival.

I thought of the application of the model to describe the population dynamics and describe the model behaviour using evolutionary game theory and wrote the manuscript. Prof. Kovács suggested making a generalized model that can be applied to not just bacteria but all communities of unicellular social organisms. Prof. Schuster and Dr. Ewald provided valuable inputs and shaped the manuscript.

Abstract

Most unicellular organisms live in communities, express different phenotypes, and interact with each other. Certain microbes are known to form highly resistant spores and elaborate structures called fruiting bodies for the dispersal of these spores. Another survival mechanism includes secretion of a sticky substance which provides protection from the external perturbations and also enhances nutrient exchange. Other microbes exhibit resistance to antibiotics. Many efforts have been made to study the population dynamics of such complex communities of cells, co-existing as a well-coordinated unit. Minimal models based on ordinary differential equations (ODEs) are powerful tools that can help us understand complex phenomena. They represent an appropriate compromise between complexity and tractability; they allow a profound and comprehensive analysis, which is still easy to understand. Evolutionary game theory is another powerful tool that can help us understand the costs and benefits of the decision that a particular cell of a unicellular social organism takes when faced with the challenges of the biotic and abiotic environment. This work is a binocular view of the population dynamics of a community of such an organism through the objectives of ODE-based minimal modelling and evolutionary game theory. We test the behaviour of the community of a unicellular social organism at three levels of antibiotic stress and observe that even in the absence of the antibiotic; spikes in the fraction of resistant cells can be observed indicating the importance of bet hedging. At moderate level of antibiotic stress, we witness cyclic dynamics reminiscent of the renowned rock-paper-scissors game while at a very high level, the resistant type strategy is the most favourable.

A. Introduction

Many unicellular organisms have been shown to exhibit social interactions. For instance, biofilms such as those of *Bacillus subtilis*(Dragos et al. 2018), *Escherichia coli*(Amanatidou et al. 2019), *Pseudomonas aeruginosa* and many other bacteria show distinct social dynamics including cooperation(Nadell, Drescher, and Foster 2016b; Diggle et al. 2007), competition(Coyte et al. 2017; Griffin, West, and Buckling 2004), division of labour(van Gestel, Vlamakis, and Kolter 2015), altruism(Kreft 2004), cheating(Amanatidou et al. 2019; Jiricny et al. 2010), and even cannibalism(González-Pastor 2011). Such communities do not only represent an aggregation of cells but have long been observed as possible first steps towards the evolution of multicellularity(Claessen et al. 2014b). Different subpopulations within the biofilm are subjected to different microenvironments(Xavier and Foster 2007). Such microenvironments are a consequence of gradients of different substances like nutrients and waste products in the biofilm(de Beer et al. 1994). This often implies that different subpopulations exhibit distinct phenotypes. For example, a subpopulation of metabolically active cells in a *P. aeruginosa* biofilm develops resistance to colistin whereas the metabolically inactive cells can survive ciprofloxacin and tetracycline. In order to destroy the biofilm, a treatment of colistin in combination with either ciprofloxacin or tetracycline is required(Pamp et al. 2008). Similarly, *B. subtilis* biofilm shows phenotypic differences in the cells located in the interior from those located in the periphery(Liu et al. 2015). This system has been studied in detail by Liu *et. al.*(Liu et al. 2015) and has been modelled using minimal models(Garde et al. 2020; Garde, Ibrahim, and Schuster 2020). In this study, we aim to apply a similar minimal modelling approach in the context of population dynamics in a typical community of unicellular social organisms.

Fruiting bodies are observed in eukaryotes like *Dictyostelium discoideum*(Smith, Queller, and Strassmann 2014; Hillmann et al. 2018) and other dictyostelids. The amoebae *Acanthamoeba pyriformis* and *Luapelamoeba arachisporum* form minute sporocarpic fruiting bodies *(Tice et al. 2016)*. Moreover, prokaryotes including *Myxococcus xanthus* and *B. subtilis* among others have been proposed to form similar fruiting bodies(Branda et al. 2001; Hartzell). Motile cells attach to one another and form aerial structures that are the hub for sporulation. These cells lose their motility in order to form the sporulating fruiting body. Our study explores what makes a particular cell take such a decision, to change its phenotype. To do this, we employ a minimal model consisting of three ordinary differential equations (ODEs) as originally proposed by Wilhelm and Heinrich to describe oscillatory chemical reactions(Wilhelm and Heinrich 1995). This model has also been used to describe the periodic halting in the expansion of a *B. subtilis* biofilm. Furthermore, it has been used to study oscillations in the p53 system of higher eukaryotes(Geva-Zatorsky et al. 2006).

Here, we focus on creating a generalized model that can be applied to a wide range of organisms that coexist in a community, in addition to relating the observations to *B. subtilis*. In that regard, the biofilm can be considered a public good, and the spores can be considered a highly resistant and persistent phenotype. We consider three subpopulations in the biofilm that exhibit three different phenotypes (see Figure 1):

- The resistant cells, which are the most resilient to nutrient scarcity and chemical attack,
- The producer cells, which can produce the public goods which help facilitate growth, but are also more susceptible to antibiotics and other chemical and environmental challenges,
- The motile cells which have the ability to move away from antibiotics and towards nutrients (chemotaxis). It also serves as a connecting cell type between the resistant type with the producer type sub-population.

Each of these types is represented by an ODE. We were interested in the proportion of the resistant cells with respect to the producers, therefore, the population distribution for three different cases were studied, each corresponding to a different range of antibiotic stress: when there is no antibiotic, moderate level of antibiotic and very high level of antibiotic.

We then describe the observations in each of the three cases using evolutionary game theory. We do this by considering a two-strategy game and a three-strategy game. Our study suggests that as the antibiotic stress increases, the system tends to stabilise towards a higher proportion of resistant cells. This state is reached through oscillations in the proportion of producers to resistant cells.

B. Methods

1. The ODE model

We consider three subpopulations of an organism, as outlined above. The resistant subpopulation, denoted by *R*, which can survive antibiotics and environmental stresses (see Figure 1). This subpopulation can transit into a motile cell subpopulation denoted by *M*, which is a representative of free-floating cells with chemotaxis. It can also be regarded as an intermediate stage between the resistant phenotype changing into the producer phenotype, denoted by *P*. Subpopulation *P* pays the costs associated with the production of public goods.

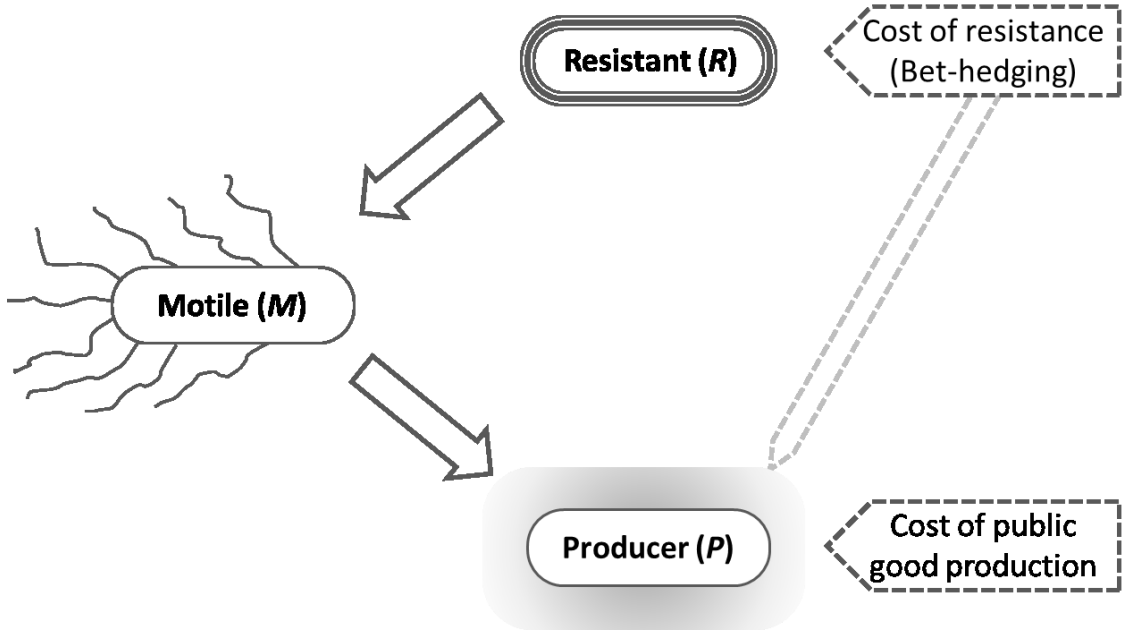

Figure 1: Scheme of the population dynamics of the three subpopulations of the model. *M* cells arise from *R* cells and can differentiate into *P* cells. The *P* cells incur costs of public goods production (indicated dashed pentagon) while the *R* cells are mainly responsible for bet hedging (indicated with dashed pentagon). *P* cells also affect the degree of bet hedging, for example, by contributing to fruiting body establishment.

Thus the dynamics of these subpopulations can be described using three variables based on the model suggested by Wilhelm and Heinrich(Wilhelm and Heinrich 1995), as follows:

- $\frac{dR}{dt} = k_1 NR - k_4 R - k_2 RP$ (1a)
- $\frac{dP}{dt} = -k_3 P + k_5 M$ (1b)
- $\frac{dM}{dt} = k_4 R - k_5 M$ (1c)

2. Assumptions of the model

- The subpopulations are generated in the order *R* —> *M* —> *P*.
- *R* cells show an arrested state of cell growth but show a self-amplifying proliferation because it serves the reproduction of the population. Such behaviour of *R* cells was also shown in *Dictyostelium*(Smith, Queller, and Strassmann 2014; Hillmann et al. 2018). They can be thought of as a reserve of cells that have highly reduced functions and only exhibit resistance phenotypes. In a community such as a biofilm which show efficient nutrient sharing(Liu et al. 2017), *R* cells which have a highly restricted metabolism, and therefore very limited nutrient requirements, obtain a steady supply of nutrients quite easily. This is given by the constant *N*.

- The term k_2RP represents that both subpopulations *R* and *P* are the essential components of the 'sessile' community. Without subpopulation *R*, the community will not be able to survive the biotic and abiotic stress and without subpopulation *P*, the public goods, the very basis for a communal lifestyle, would not be produced. For example, in a fruiting body, the spores (analogous to resistant cells in our model) and the biofilm (analogous to public goods in our model) matrix are both required in order to form a fruiting body. The term also represents the degree of bet-hedging or 'resistance' the community invests in. It follows that a community that produces more public goods, also invests more in bet-hedging.
- The cost of public goods production is given by the constant k_3, whereas k_2 is the cost of resistance. When there is no antibiotic stress, resistance is costlier than producing public goods. When the antibiotic stress is high, producing public goods is costlier than resistance.
- *N* is arbitrarily chosen to be 3 while all the other constants are equal to unity per time unit.

3. Simulation

The simulations were performed using COPASI version 4.27 and its deterministic solver LSODA(Hoops et al. 2006) . All the model parameters have been adapted from the paper by Wilhelm and Heinrich(Wilhelm and Heinrich 1995). We use hour as the time unit, so that the rate constants have the values 1 h^{-1}. We run the time course calculation of the system (2.1a–c) for 25 simulation hours with 1000 steps each of size 0.025 h (1.5 min). Moreover, we use methods from evolutionary game theory. The game theoretical modeling will be explained in the Results section.

C. Results

1. Results of the ODE model

Based on the different antibiotic stresses, we can observe three different behaviours from the subpopulations. Figure 2 shows the ratio of *R* to that of the sum of *R* and *P* over time for three different levels of antibiotic stress. At zero stress, it is observed that the public good production is the dominant strategy (Figure 2a). However, we observe periodic spikes in the proportion of *R* cells. These spikes can be attributed to bet-hedging cycles where the community invests in making *R* cells in spite of high costs and zero stress. At moderate costs, we observe that the ratio of *R* cells oscillates with a shorter period. This implies that there is a constant switching in the dominant subpopulations owing to similar costs of production for either subpopulation (Figure 2b). As the public goods get costlier, the *R* subpopulation emerges to be the dominant strategy. This state is reached through damped oscillations (Figure 2c). For very high costs, the steady state is reached by a monotonic relaxation with practically no oscillation (Figure 2d). In mathematical terms, this corresponds to a stable node. It is

unlikely that this case is of biological relevance because public goods are only produced if costs are not too high.

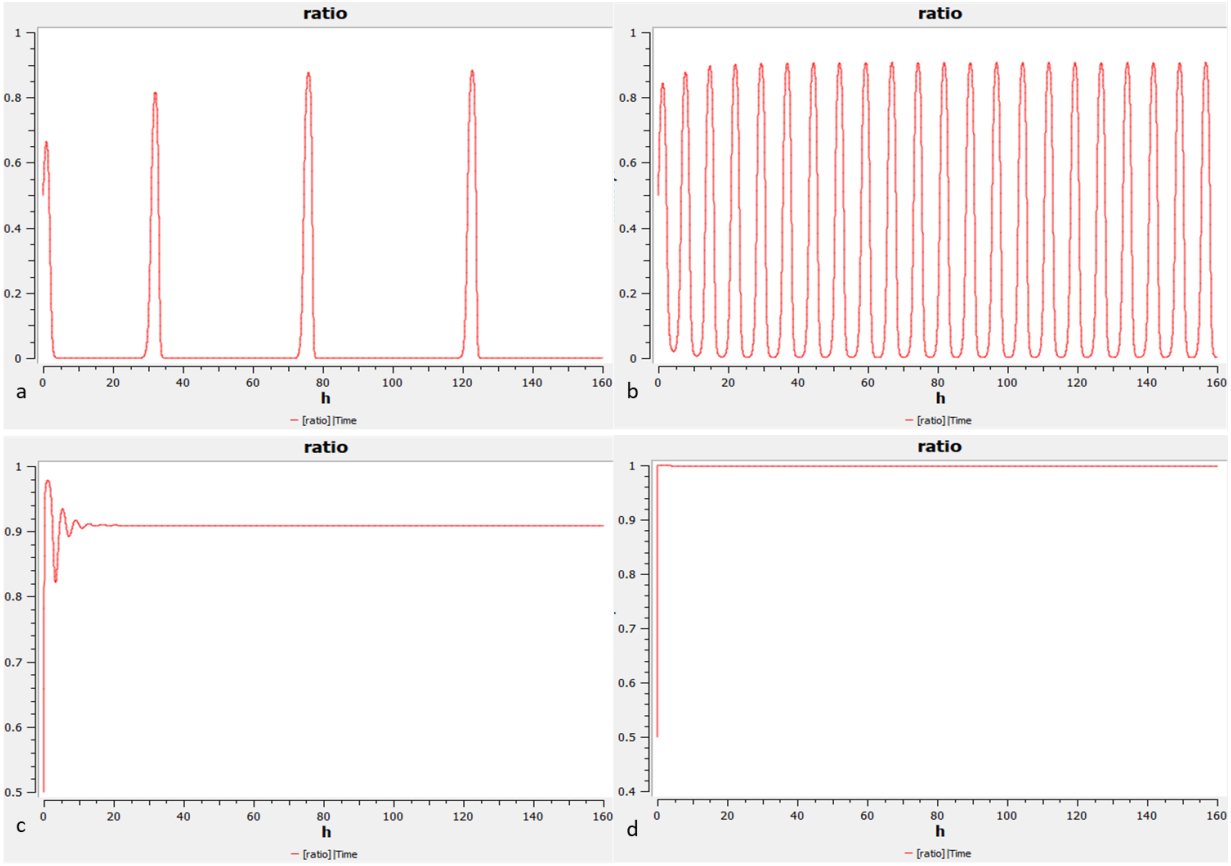

a

Figure 2: Ratio of *R* to that of the sum of *R* and *P* versus time. **a**: when $k_3 < k_2$ (specifically $k_2 = 1$, $k_3 = 0.1$ in the simulation shown); **b**: when k_2 approximately equals k_3 (here $k_2 = k_3 = 1$); **c**: when $2k_2 < k_3$ (here $k_2 = 1$, $k_3 = 10$); **d**: when $k_2 << k_3$ (here $k_2 = 1$, $k_3 = 1000$). The system transitions from spike-like oscillations to sinusoidal ones, then to damped oscillations, leading to a steady state and finally to a nearly monotonic relaxation to a steady state.

The bifurcations separating the different dynamic regimes can be determined in the same way as shown in our earlier paper(Garde et al. 2020). The effect of changing k_3 for this model is shown in

Figure 3. This type of transition is called Hopf bifurcation.

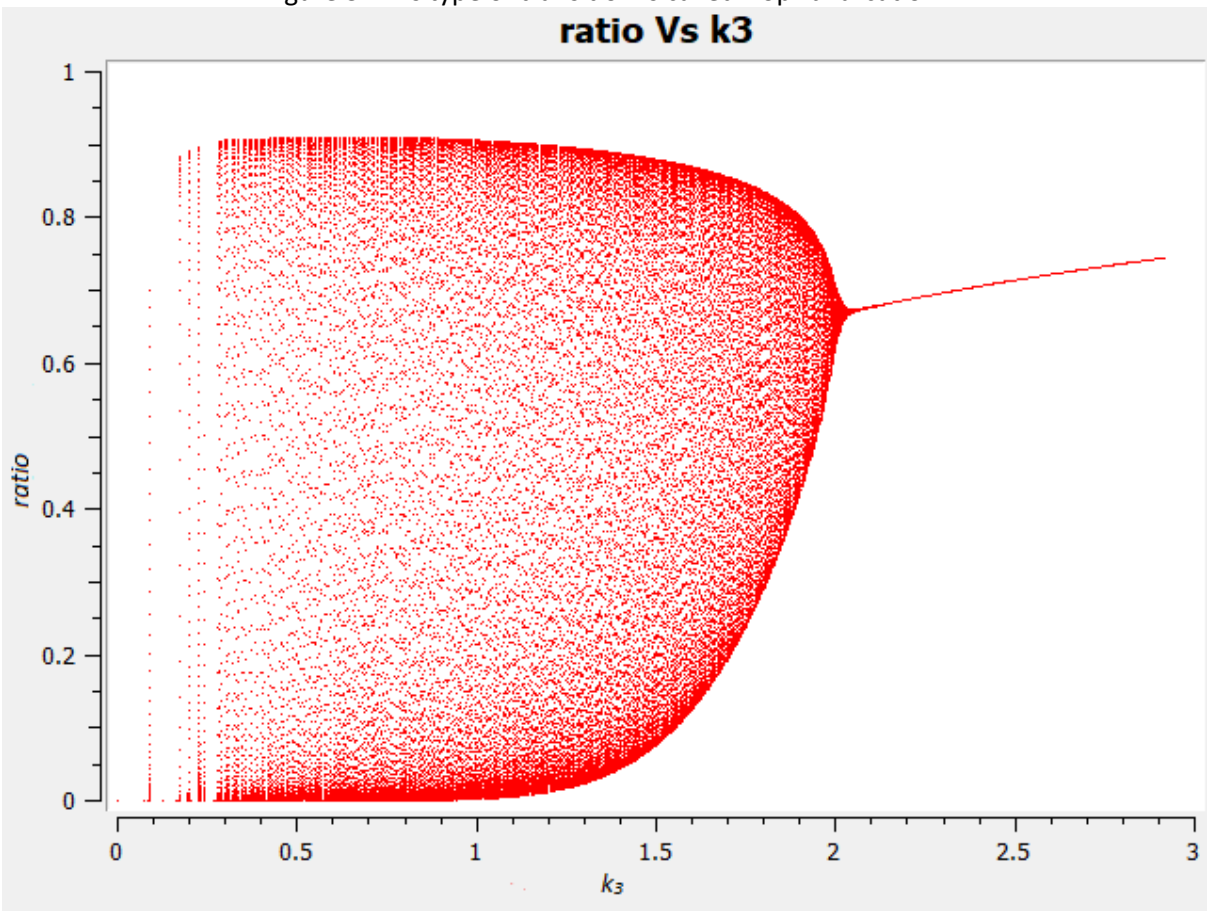

Figure 3: Bifurcation diagram of $R/(R+P)$ against k_3. The ratio oscillates, for example, at $k_3 = k_2$ (=1), but as k_3 increases, the amplitude of oscillation reduces until a steady state is reached at $k_3 = 2$. The two arms of the convex hull represent the maxima and minima of oscillation (amplitude).

2. Describing the results using evolutionary game theory

a) Three-strategy two-player game

The observations of this model can be described using evolutionary game theory. For this, we consider a three-strategy game, where the subpopulations are considered as the three strategies. In order to assign payoffs correctly, we must consider the advantages and disadvantages of each of the subpopulation. Subpopulation *R* has the lowest metabolic activity and hence it can withstand extreme conditions such as nutrient limitation and chemical attacks. Subpopulation *P* on the other hand is the most susceptible to chemical stress such as antibiotics due to high metabolic activity. It has been shown that some antimicrobials such as beta-lactam antibiotics target metabolically active cells(Tuomanen et al. 1986). Subpopulation *M* is not as active metabolically as subpopulation *P* hence it is less susceptible to antimicrobials in comparison. But it is motile and is therefore capable of chemotaxis, i.e. *M* cells can move away from antibiotics and closer to nutrients. Thus no

subpopulation has a clear advantage over the other two and the game is comparable to the well-known rock-paper-scissors (RPS) game (Figure 4).

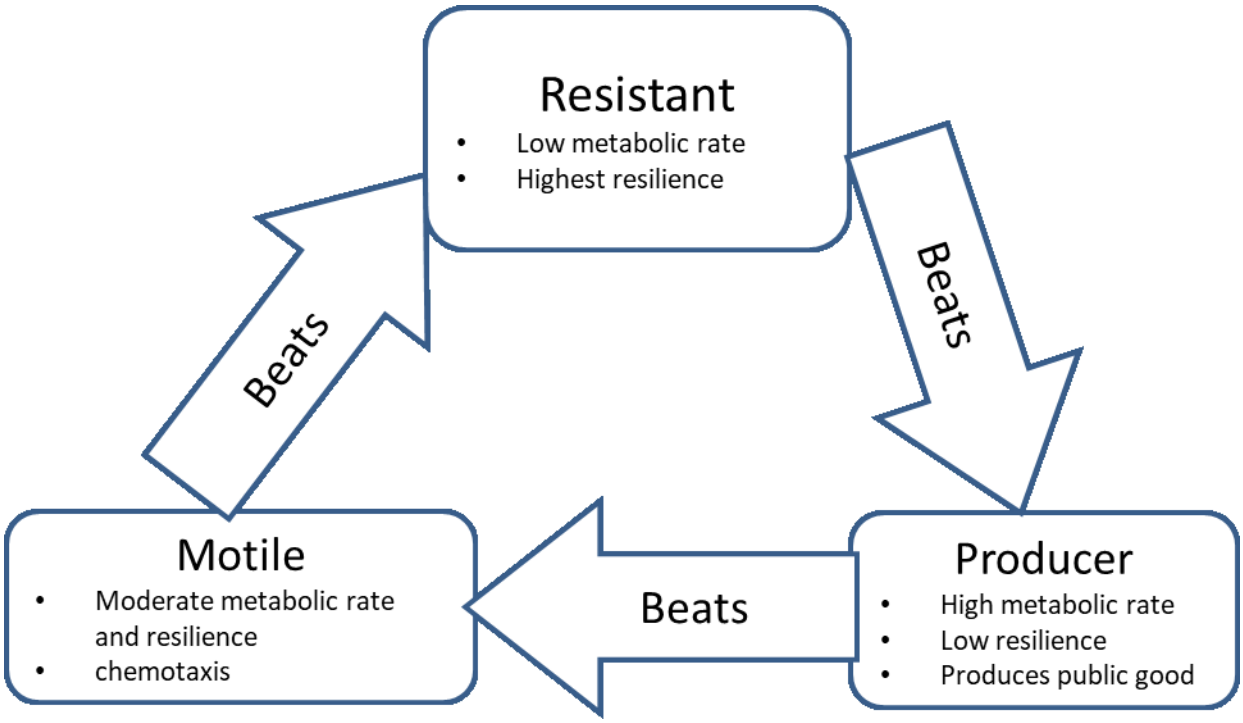

Figure 4: The dynamics of biofilm subpopulations as a three-strategy game. No single strategy is better than both the remaining strategies.

The three subpopulations are considered as the three strategies and we can compare the pay-offs in the all against all fashion in a payoff matrix (Table 1). Based on the interaction given in Figure 4, we award the 'winner' 1 point while the loser loses 1. Draws / ties, such as the ones resulting from playing the same strategies are given no points. Thus, it is a zero-sum game.

Table 1: Pay-offs for the three-strategy, two-player game.

Player 1 \ Player 2	*R*	*M*	*P*
R	0 \ 0	-1 \ 1	1 \ -1
M	1 \ -1	0 \ 0	-1 \ 1
P	-1 \ 1	1 \ -1	0 \ 0

As seen from table 1, for every strategy of player 1, player 2 can change to a better strategy and vice-versa indicating that there is no Nash equilibrium in pure strategies. A similar scenario has also been described for the RPS game, either by pay-off matrices(Gintis 2000) or by an ODE approach(Neumann and Schuster 2007; Czárán, Hoekstra, and Pagie 2002; May and Leonard 1975). The description by

ODEs predicts, depending on parameter values, either undamped oscillations by which one type outcompetes the other two, coexistence of the three types in an oscillatory way or stationary coexistence(Neumann and Schuster 2007).

All the results obtained in evolutionary game theory for the RPS game can be applied to the above system. In particular, there is no pure Nash equilibrium. The only mixed Nash equilibrium is that all the three strategies are played with a probability of 1/3. Other fractions can easily be simulated by taking other payoff values. One way to do this is to simply cycle through the strategies successively. This implies a cyclic dominance of different subpopulations. This explains the life cycle of the community.

b) Two-strategy two-player game

Another method to model this is by considering a two strategy game. For this we exclude the *M* cell population and only consider *R* cells and *P* cells as strategies. We then consider the interaction of a typical single cell with a group of mature cells in the community. The single nascent cell could either be of type *R* or *P*. In evolutionary game theory, this is often called an invading rare mutant (where "invading" does not necessarily mean invasion from the outside, it could also mean occurrence by mutation). Similarly, the group of mature cells within the community can be of type *R* or *P*. The payoffs for this two-strategy game are given in Table 2, white columns.

The best outcome for a nascent resistant cell is against the mature producer – it gets access to the public goods without any costs. Hence, it gets a payoff of 2. The mature producer cells, on the other hand, have a payoff of zero, since they have to share their nutrients with the new 'freeloader' cell.

A nascent resistant cell is not as resilient as compared to the matured resistant cells in the community and is thus outcompeted. For the mature resistant cells, the newcomer is an added taskforce of resistant cells and thus a much desired outcome. The nascent resistant cell gets a payoff of 0 while the matured resistant cells get a payoff of 2.

The nascent *P* cell is exploited by the mature *R* cells for its public goods. Thus it gets a payoff of 0.5 while the resistant cells get a payoff of 1.5. On the other hand, a nascent *P* is added task force for public goods production; hence the mature *P* cells benefit from this and have a payoff of 2. The nascent *P* cell also gets a payoff of 1.

This describes the game when the antibiotic stress is moderate, i.e., when $k_3 = k_2$. For the remaining two cases, one can simply add one point to the payoff of all *P* type strategies in order to obtain the blue column, which describes the dynamics of the same game in the absence of the antibiotic stress,

i.e., when $k_3 < k_2$. Similarly, deducting one point from the payoff of all *P* strategies helps us obtain the dynamics of the game when the antibiotic stress is high, i.e., $k_3 > k_2$, shown in the red column.

Table 2: Pay-offs of the two-strategy two-player player game. The three cases based on the level of antibiotic stress reflected by the cost of resistance in relation to public goods production are given in blue (no stress, i.e. $k_3 < k_2$), white (moderate stress, i.e. $k_3 = k_2$) and red (high stress, i.e. $k_3 > k_2$) columns respectively.

Player 1 \ Player 2	***P* (mature)**			***R* (mature)**		
	$k_3 < k_2$	$k_3 = k_2$	$k_3 > k_2$	$k_3 < k_2$	$k_3 = k_2$	$k_3 > k_2$
***P* (nascent)**	2\3	1\2	0\1	1.5\1.5	0.5\1.5	-0.5\1.5
***R* (nascent)**	2\1	2\0	2\-1	0\2	0\2	0\2

It can be seen from the payoff matrix that there is no pure Nash equilibrium when $k_3 = k_2$ (white columns) and there is no evolutionarily stable strategy because for any change in the strategy of mature cells, the nascent cells can respond with a corresponding change in their strategy as well and one can expect a cyclic nature of the strategies leading to oscillations in the ratio of resistant cells. On the other hand, one can expect public goods production to be a dominant strategy when $k_3 < k_2$ (blue columns), however, since there is no difference in the payoffs of a nascent resistant cell as compared to a nascent producer when playing against matured producers, an occasional switch to the resistant type may be made by the nascent cell. Furthermore, when $k_3 > k_2$ (red columns) one can expect an unequivocal domination by resistance cells. This observation is well reflected in the three ODE model mentioned above (Case c in Fig. 2).

D. Discussion

This study focuses on the population dynamics in a community of a unicellular social organism. Several efforts have been made with respect to *B. subtilis* biofilms in the same direction before(Collins, Jacobsen, and Maxwell 2003; Zimmer et al. 1998; Pantastico-Caldas et al. 1992; Logsdon and Aldridge 2018; Kampf et al. 2018) . This study employs an ODE based minimal model in order to describe the population dynamics in a community of a unicellular social organism. The mathematical model has been proposed by Wilhelm and Heinrich to describe chemical reactions(Wilhelm and Heinrich 1995)

and more recently, it has been also used to describe periodic halting in the expansion of a biofilm of *B. subtilis*(Garde et al. 2020; Garde, Ibrahim, and Schuster 2020).

The model consists of three variables, each representing a subpopulation in the community. Figure 1 describes the relationship of the model variables with each other. As per the assumption, both *R* and *P* type cells are crucial components of the sessile community. The term k_2RP represents the degree of bet-hedging, where k_2 is the cost of resistance. It also follows that the higher the investment into public goods, the higher is the degree of bet hedging. The interplay between the three subpopulations is illustrated in Figure 1.

Based on this relationship, one can visualise a game similar to the RPS game. Table 1 describes the payoffs of this three-strategy game. Such a game with oscillatory dynamics was also described for bacteriocin production in bacteria using a Lotka-Volterra model(Neumann and Schuster 2007). There is a body of literature about modelling the RPS game by ODEs (Neumann and Schuster 2007; May and Leonard 1975; Czárán, Hoekstra, and Pagie 2002) and even PDEs(Reichenbach, Mobilia, and Frey 2007). Our model is an even simpler description of the game and thus a minimal model for the RPS game. What is more interesting is that our model can be applied to not just bacteria but any communal organism with similarly interacting subpopulations. A further similarity of our approach to that of Neumann and Schuster(Neumann and Schuster 2007) is that the Hopf bifurcation is obtained for the bacteriocin parameter, similar to the antibiotic stress as discussed here.

In the model presented above, players can change strategies, while in the previous approach by Neumann and Schuster(Neumann and Schuster 2007) the fraction of strategies changes by different growth rates and competition between the strategies. It is interesting that both cases can be described by the concepts of evolutionary game theory.

In order to gain further insight into the population dynamics, we study the two strategies of resistance and biofilm production further. It can be seen from Figure 2a, which depicts the time course of the ratio of resistant cells to that of the sum of resistant cells and producers, in the absence of the antibiotic stress ($k_3 < k_2$), we observe that biofilm production is the dominant strategy. Furthermore, one can also observe periodic 'resistance spikes' suggesting that the population undergoes bet hedging cycles in order to have a reserve of cells that can survive adverse conditions. This warrants experimental validation in order to conclusively state that such bet-hedging cycles occur, although there have been reports on the sporulation cycles(Hutchison, Miller, and Angert 2014) and bet hedging(Veening, Smits, and Kuipers 2008; Veening et al. 2008) in bacteria. The study indicates that bacteria undergo sporulation even in the absence of nutrient stress as a bet-hedging strategy.

Furthermore, the period of these cycles is also not depicted accurately in this model since the rate constants are chosen arbitrarily because the goal here is to describe the underlying mechanism qualitatively and non-specifically.

This observation can be described using a two-strategy two-player game. In Table 2, the blue columns represent this particular case where the antibiotic stress is absent and hence resistance is a costly investment, i.e. $k_3 < k_2$. Comparing the payoffs, one can expect that the Nash equilibrium would be to produce the public goods. However, since the payoffs for the nascent cell playing either strategy against the matured producer cells are the same, it is also not surprising to see an occasional rise in the resistant type subpopulation.

Figure 2b describes the case when the antibiotic stress is moderate, and hence investing resources in resistance is favourable and, in this case, $k_3 = k_2$, meaning that producing public goods costs as much as resistance. One can observe a cycling of strategies between the resistant and the producer types. This is further explained by the two-strategy game. The white columns in Table 2 depict this case and one can see that there is no pure Nash equilibrium. This means that for every strategy chosen by player one, player two can improve its payoff by switching its own strategy. We can expect that the producer strategy is a suboptimal strategy where both players have relatively high payoffs. We may also hypothesize that when the community is sufficiently large, this cyclic switching of strategies might switch to a stable steady state where the ratio remains constant. This has been observed in the modified version of this ODE system by Garde *et*. *al*(Garde, Ibrahim, and Schuster 2020).

Finally, Figure 2c describes the case when the antibiotic stress is the highest and investing in public goods instead of resistance is costlier, as such, $k_3 > k_2$. As expected the resistant cells emerge as the dominant subpopulation. This can be thought of as extreme resource limitation where the public goods become extremely costly to produce. In such a scenario, it is ideal for the community to produce resistant cells in order to ensure that it can survive this starvation phase until the nutrients are available once again. This scenario is also described in Table 2 in the red column. One can conclude that in this case, resistance is undoubtedly the dominant strategy. Cyclic behaviour is possible in symmetric three-strategy game, while two-strategy game needs to be asymmetric to yield cycles.

This model can be modified in order to describe a particular bacterial biofilm. In such a scenario, the resistant cells can be thought of as spores and the public goods can be thought of as the biofilm matrix. In this study however, we only aim to put forth a generalized mechanism of the (non-cognitive) decision-making happening in the population of a unicellular communal organism (e.g. by entering the next developmental stage caused by an epigenetic switch). The ODE based system also serves as a

minimal model for the three strategy RPS game with cyclic dominance of strategies. Further, the two-strategy game suggests, that as the antibiotic stress increases, the optimal strategy shifts from producing public goods towards producing resistance. Moreover, it also suggests that even in the absence of the antibiotic stress, the community invests in resistance as a bet-hedging strategy.

E. References

Amanatidou, Elli, Andrew C. Matthews, Ute Kuhlicke, Thomas R. Neu, James P. McEvoy, and Ben Raymond. 2019. 'Biofilms facilitate cheating and social exploitation of β-lactam resistance in Escherichia coli', npj Biofilms and Microbiomes, 5: 36.

Branda, S. S., J. E. Gonzalez-Pastor, S. Ben-Yehuda, R. Losick, and R. Kolter. 2001. 'Fruiting body formation by *Bacillus subtilis*', Proc Natl Acad Sci U S A, 98: 11621-6.

Claessen, Dennis, Daniel E. Rozen, Oscar P. Kuipers, Lotte Søgaard-Andersen, and Gilles P. van Wezel. 2014. 'Bacterial solutions to multicellularity: a tale of biofilms, filaments and fruiting bodies', Nature Reviews Microbiology, 12: 115-24.

Collins, Douglas P., Barry J. Jacobsen, and Bruce Maxwell. 2003. 'Spatial and temporal population dynamics of a phyllosphere colonizing *Bacillus subtilis* biological control agent of sugar beet cercospora leaf spot', Biological Control, 26: 224-32.

Coyte, Katharine Z., Hervé Tabuteau, Eamonn A. Gaffney, Kevin R. Foster, and William M. Durham. 2017. 'Microbial competition in porous environments can select against rapid biofilm growth', Proceedings of the National Academy of Sciences, 114: E161.

Czárán, Tamás L., Rolf F. Hoekstra, and Ludo Pagie. 2002. 'Chemical warfare between microbes promotes biodiversity', Proceedings of the National Academy of Sciences, 99: 786-90.

de Beer, Dirk, Paul Stoodley, Frank Roe, and Zbigniew Lewandowski. 1994. 'Effects of biofilm structures on oxygen distribution and mass transport', Biotechnology and Bioengineering, 43: 1131-38.

Diggle, S. P., A. S. Griffin, G. S. Campbell, and S. A. West. 2007. 'Cooperation and conflict in quorum-sensing bacterial populations', Nature, 450: 411-4.

Dragos, A., H. Kiesewalter, M. Martin, C. Y. Hsu, R. Hartmann, T. Wechsler, C. Eriksen, S. Brix, K. Drescher, N. Stanley-Wall, R. Kummerli, and A. T. Kovacs. 2018. 'Division of Labor during Biofilm Matrix Production', Curr Biol, 28: 1903-13 e5.

Garde, R., B. Ibrahim, and S. Schuster. 2020. 'Extending the minimal model of metabolic oscillations in *Bacillus subtilis* biofilms', Sci Rep, 10: 5579.

Garde, Ravindra, Bashar Ibrahim, Ákos T. Kovács, and Stefan Schuster. 2020. 'Differential equation-based minimal model describing metabolic oscillations in *Bacillus subtilis* biofilms', Royal Society Open Science, 7.

Geva-Zatorsky, N., N. Rosenfeld, S. Itzkovitz, R. Milo, A. Sigal, E. Dekel, T. Yarnitzky, Y. Liron, P. Polak, G. Lahav, and U. Alon. 2006. 'Oscillations and variability in the p53 system', Mol Syst Biol, 2: 2006 0033.

Gintis, Herbert. 2000. Game theory evolving: A problem-centered introduction to modeling strategic behavior (Princeton university press: New Jersey).

González-Pastor, José Eduardo. 2011. 'Cannibalism: a social behavior in sporulating *Bacillus subtilis*', FEMS microbiology reviews, 35: 415-24.

Griffin, A. S., S. A. West, and A. Buckling. 2004. 'Cooperation and competition in pathogenic bacteria', Nature, 430: 1024-7.

Hartzell, T. 'Myxobacteria.' in, eLS.

Hillmann, F., G. Forbes, S. Novohradska, I. Ferling, K. Riege, M. Groth, M. Westermann, M. Marz, T. Spaller, T. Winckler, P. Schaap, and G. Glockner. 2018. 'Multiple Roots of Fruiting Body Formation in Amoebozoa', Genome Biol Evol, 10: 591-606.

Hoops, S., S. Sahle, R. Gauges, C. Lee, J. Pahle, N. Simus, M. Singhal, L. Xu, P. Mendes, and U. Kummer. 2006. 'COPASI--a COmplex PAthway SImulator', Bioinformatics, 22: 3067-74.

Hutchison, E. A., D. A. Miller, and E. R. Angert. 2014. 'Sporulation in Bacteria: Beyond the Standard Model', Microbiol Spectr, 2.

Jiricny, N., S. P. Diggle, S. A. West, B. A. Evans, G. Ballantyne, A. Ross-Gillespie, and A. S. Griffin. 2010. 'Fitness correlates with the extent of cheating in a bacterium', J Evol Biol, 23: 738-47.

Kampf, J., J. Gerwig, K. Kruse, R. Cleverley, M. Dormeyer, A. Grunberger, D. Kohlheyer, F. M. Commichau, R. J. Lewis, and J. Stulke. 2018. 'Selective Pressure for Biofilm Formation in *Bacillus subtilis*: Differential Effect of Mutations in the Master Regulator SinR on Bistability', mBio, 9.

Kreft, J. U. 2004. 'Biofilms promote altruism', Microbiology, 150: 2751-60.

Liu, J., R. Martinez-Corral, A. Prindle, D. D. Lee, J. Larkin, M. Gabalda-Sagarra, J. Garcia-Ojalvo, and G. M. Suel. 2017. 'Coupling between distant biofilms and emergence of nutrient time-sharing', Science, 356: 638-42.

Liu, J., A. Prindle, J. Humphries, M. Gabalda-Sagarra, M. Asally, D. Y. Lee, S. Ly, J. Garcia-Ojalvo, and G. M. Suel. 2015. 'Metabolic co-dependence gives rise to collective oscillations within biofilms', Nature, 523: 550-4.

Logsdon, M. M., and B. B. Aldridge. 2018. 'Stable Regulation of Cell Cycle Events in Mycobacteria: Insights From Inherently Heterogeneous Bacterial Populations', Front Microbiol, 9: 514.

May, Robert, and Warren Leonard. 1975. 'Nonlinear Aspects of Competition Between Three Species', SIAM J. Appl. Math., 29: 243.

Nadell, Carey D., Knut Drescher, and Kevin R. Foster. 2016. 'Spatial structure, cooperation and competition in biofilms', Nature Reviews Microbiology, 14: 589-600.

Neumann, Gunter, and Stefan Schuster. 2007. 'Continuous model for the rock–scissors–paper game between bacteriocin producing bacteria', Journal of Mathematical Biology, 54: 815-46.

Pamp, Sünje Johanna, Morten Gjermansen, Helle Krogh Johansen, and Tim Tolker-Nielsen. 2008. 'Tolerance to the antimicrobial peptide colistin in Pseudomonas aeruginosa biofilms is linked to metabolically active cells, and depends on the pmr and mexAB-oprM genes', Molecular Microbiology, 68: 223-40.

Pantastico-Caldas, Marissa, Kathleen E. Duncan, Conrad A. Istock, and Julia A. Bell. 1992. 'Population Dynamics of Bacteriophage and *Bacillus Subtilis* in Soil', Ecology, 73: 1888-902.

Reichenbach, Tobias, Mauro Mobilia, and Erwin Frey. 2007. 'Mobility promotes and jeopardizes biodiversity in rock–paper–scissors games', Nature, 448: 1046-49.

Smith, Jeff, David C. Queller, and Joan E. Strassmann. 2014. 'Fruiting bodies of the social amoeba Dictyostelium discoideum increase spore transport by Drosophila', BMC Evolutionary Biology, 14: 105.

Tice, Alexander K., Lora L. Shadwick, Anna Maria Fiore-Donno, Stefan Geisen, Seungho Kang, Gabriel A. Schuler, Frederick W. Spiegel, Katherine A. Wilkinson, Michael Bonkowski, Kenneth Dumack, Daniel J. G. Lahr, Eckhard Voelcker, Steffen Clauß, Junling Zhang, and Matthew W. Brown. 2016. 'Expansion of the molecular and morphological diversity of Acanthamoebidae (Centramoebida, Amoebozoa) and identification of a novel life cycle type within the group', Biology direct, 11: 69-69.

Tuomanen, E., R. Cozens, W. Tosch, O. Zak, and A. Tomasz. 1986. 'The rate of killing of Escherichia coli by beta-lactam antibiotics is strictly proportional to the rate of bacterial growth', J Gen Microbiol, 132: 1297-304.

van Gestel, J., H. Vlamakis, and R. Kolter. 2015. 'Division of Labor in Biofilms: the Ecology of Cell Differentiation', Microbiol Spectr, 3: Mb-0002-2014.

Veening, J. W., W. K. Smits, and O. P. Kuipers. 2008. 'Bistability, epigenetics, and bet-hedging in bacteria', Annu Rev Microbiol, 62: 193-210.

Veening, Jan-Willem, Eric J. Stewart, Thomas W. Berngruber, François Taddei, Oscar P. Kuipers, and Leendert W. Hamoen. 2008. 'Bet-hedging and epigenetic inheritance in bacterial cell development', Proceedings of the National Academy of Sciences, 105: 4393-98.

Wilhelm, Thomas, and Reinhart Heinrich. 1995. 'Smallest chemical reaction system with Hopf bifurcation', Journal of Mathematical Chemistry, 17: 1-14.

Xavier, Joao B., and Kevin R. Foster. 2007. 'Cooperation and conflict in microbial biofilms', Proceedings of the National Academy of Sciences, 104: 876.

Zimmer, J, I Issoufou, G Schmiedeknecht, and H Bochow. 1998. 'Population dynamics of *Bacillus subtilis* as biocontrol agent under controlled conditions', Mededelingen-Faculteit Landbouwkundige en Toegepaste Biologische Wetenschappen Universiteit Gent (Belgium).

V. General Discussion

Biofilms are communities of bacterial cells that usually form under environmental stress, for example, nutrient scarcity. This enables the community as a whole to tackle the insults of nature. For example, a biofilm can form a pellicle on the surface of a liquid so that the bacteria get access to oxygen. Due to a common goal of species survival, even the competing subpopulations in the biofilm can coexist in harmony in the biofilm of *Bacillus subtilis* as demonstrated by Liu *et. al*(Liu et al. 2015). The interior of the biofilm produces valuable ammonia and in return receives protection from the environment by the periphery. The periphery enjoys a relatively higher supply of nutrients and consequently a higher growth rate, in exchange of being at the mercy of the ammonia supply from the interior and the challenges of the environment. With the reins of the growth rate secured by the interior, a steady supply of nutrients to the interior is ensured. Liu *et al* report periodic halting in the growth of the biofilm, which arises due to the co-dependence of the interior and peripheral cells(Liu et al. 2015)

This thesis is inspired by the findings of Liu *et al* with the aim to model their findings using a minimal model. We then also make different modifications to the model in order to make it biologically accurate. Furthermore, we employ the same minimal model to describe the population dynamics of a community of a social organism, taking inspiration from the interacting populations of the interior and peripheral cells.

In order to better examine both interior and peripheral cells, the experimental setup of Liu *et. al*(Liu et al. 2015) was designed in such a way that the biofilm can only spread in one plane. The microfluidics chamber, where the cells grow, measures $3mm^2$ in area and only 6µm in thickness. This imparts a pancake-like structure to the biofilm and so the interior as well as the periphery of the biofilm can be observed simultaneously. They report that under nutrient limitation, oscillations can be observed in biofilm expansion. Furthermore, they also present an ODE based model and its bifurcation analysis and sensitivity analysis with respect to different parameters.

In order to identify the cause of oscillations, Liu *et. al.* did several operon manipulation studies. One may suspect that the feedback loop driving the oscillations involves quorum sensing. However, the deletion of the operons *opp* and *comX* (making the mutant deficient in quorum sensing), does not eliminate the oscillations. Similarly, deletion or overexpression of operon *tapA* (extracellular matrix component, TasA) also does not affect oscillations indicating that the oscillations are not related to the biofilm matrix production. One may suspect that the periodic halting of expansion of the biofilm could be due to 'lunch breaks' of the motile cells; i.e. once the cells have moved to the surrounding nutrient rich region, they stop to assimilate the nutrients and then continue to move further, causing the

periodic halting. However, a mutant with a deletion of the operon *hag* (making the strain deficient in swimming and swarming) also shows oscillations. Further they also test a mutant without the *rocG* gene which makes the strain deficient in one of the two glutamate dehydrogenase (GDH) enzymes. The *rocG* GDH production is sensitive to carbon catabolite repression. Liu *et.al.*observed oscillatory growth even after the deletion of *rocG* indicating that carbon source based regulation of GDH production plays no role in biofilm oscillations.

They further find that when the oscillating biofilm is supplemented with 1 mM glutamine, the oscillations are quenched, indicating glutamine limitation to be the driver of oscillations. Further, they supplement the medium with ammonia and glutamate, both of which are required for glutamine production, to find that oscillations are quenched in the case of 1mM ammonia supplementation whereas they persist even after supplementation of 30mM glutamate. This indicates that ammonia is the reason for glutamine limitation and thus the driver of oscillations. One may argue that ammonia can be produced by every cell in the biofilm, but when the peripheral cells produce it, it leads to a futile cycle since it is lost to the environment, due to rapid diffusion.

In the experimental setup of Liu *et.al,* glutamate is the only source of nitrogen. A steady supply of glutamate ensures a steady production of ammonia by the interior cells. This causes the periphery to produce biomass and expand, which in turn causes the interior to starve. The result is a diminished supply of ammonia which halts the expansion or the periphery. Thus, a negative feedback loop due to ammonia limitation drives the oscillations.

Such oscillations in the growth rate have never been observed earlier in any biofilm. It is difficult to say whether such oscillations can be observed in nature where there are many diverse substances in the environment and thus the nutrients that the biofilm feeds on are a dynamic cocktail. However, the significance of this observation is that it highlights a hitherto unknown mechanism of mitigating nutrient limitation. Further, the study also demonstrates how the distinct interior and peripheral phenotypes, especially their different metabolic rates help in tackling chemical attacks. It is known that metabolically inactive cells are not or rarely killed by antimicrobials(Tuomanen et al. 1986). The reason is that most antimicrobials are inhibitors of metabolic enzymes (e.g. penicillins, which inhibit cell wall synthesis). This effect is known as phenotypic tolerance, which means the tolerance is only physiological and does not have a genetic basis as observed in antibiotic resistance(Wiuff et al. 2005). A similar oscillating strategy has also been reported in two biofilms that share the common nutrient source. Biofilms that share the nutrients out of phase, i.e., take turns feeding; have a better growth rate than those that do not(Liu et al. 2017).

This system has been modelled in article 1 using the smallest chemical oscillator with Hopf bifurcation(Wilhelm and Heinrich 1995). This minimal model was first proposed without a concrete application. Later it was used to study p53 oscillations (Geva-Zatorsky et al. 2006). The protein p53 plays a vital role in tumor suppression in multicellular organisms. When in a complex with Mdm2, it is inactive. Stress responses such as DNA damage increase the dissociation of this complex, resulting in an increased concentration of active p53. After its activation, p53 activates several genes involved in apoptosis, aging, DNA repair and growth arrest. Additionally, p53 also acts as a transcriptional activator of *mdm2*, thus completing a negative feedback loop. This loop consists of entities that vary on different timescales – a fast protein-protein interaction timescale and a slow transcriptional timescale. Such interactions suggest an oscillatory regime in the concentrations of the interacting components. Sustained undamped oscillations were observed in in fluorescent tagged p53-CFP and mdm-YFP in individual living breast cancer (MCF7) cells following gamma irradiation(Geva-Zatorsky et al. 2006). This system was modelled using several families of models which also included the minimal model by Wilhelm and Heinrich(Wilhelm and Heinrich 1995).

In article 1 we see the application of the minimal oscillator by Wilhelm and Heinrich to describe the observations of Liu *et. al.* The parameters have been adapted to best describe the experimental observations and also tuned in a way that is biologically plausible. For example, the diffusion rates of glutamate and ammonia, namely k_4 and k_3, are chosen such that $k_3 = 2k_4$ since the diffusion coefficient for ammonia(Cussler 2009) is about 1.6E-05 cm^2s^{-1} while that for glutamate(Kullmann et al. 1999; Ribeiro et al. 2014) is about 8E-06 cm^2s^{-1}. This makes the model more realistic. A major result is that limi-cycle oscillations in biofilms can be described by simpler models than used by Liu *et al*(Liu et al. 2017) and Bocci *et al* (Bocci et al. 2018).

Further, we can also see the sensitivity analysis of various parameters. This is done in two ways. Firstly, we present bifurcation diagrams which involve scanning of a parameter value plotted against any one variables of the model. This allows us to see how the change in the parameter value affects the variable and the oscillations as a whole. Secondly, we differentiate all the steady state values of the variables with respect to each parameter. The major strengths of this model include the minimal nature and the precision. Being minimal, it can easily be analysed both analytically as well as numerically.

Although the model successfully describes the metabolic oscillations in the growth of the biofilm, being a minimal model, it runs the risk of being an oversimplified version of the observation. For example, the model is based on ODEs which usually involve time as the only independent variable. This ignores any spatial effect that the variables may exhibit. In other words, the gradients of the

different substances in the biofilm are assumed to play no part in the oscillations. This is one of the limitations of ODE based models and can be overcome by using PDEs (Bocci et al. 2018). Further, the model uses irreversible mass action kinetics for every single reaction. This is not necessarily a drawback but in the biological scenario, reversible diffusion seems to be a more realistic assumption.

In order to tackle these shortcomings, we make several modifications of the model in chapter III. First, we test if an ODE model is an oversimplification of the problem. In order to do so, we simply represent the gradient of substances using an additional layer (described by additional ODEs). Note that, in doing so, we increase the number of variables in the model thus making it no longer minimal.We find that although the model shows slight displacement in the bifurcation points, there is no qualitative difference in the model. We thus conclude that adding additional variables representing additional layers of the biofilm is unnecessary.This reinforces the robustness of the minimal model and how accurately it describes the biofilm oscillations. This also shows that the oscillations are temporal in nature and spatial effects hardly seem to play a role. Thus a smooth gradient of concentrations is not required and a distinction of the biofilm into interior and peripheral regions is sufficient.

The uptake of nutrients, especially glutamate is an active process mediated by the proton glutamate symport protein(Tolner et al. 1995). Thus Michaelis-Menten kinetics is more suited to model this as compared to mass action kinetics. This has been considered as a separate modification and analysed further. This modification of the model predicts that oscillations are a means to mitigate the nutrient limitation and not a default in the *B. subtilis* biofilm system. This implies that oscillations will not be observed in the absence of nutrient limitation. Further, in the natural environment, where there are several alternative sources of nitrogen, it will be difficult to observe such a negative feedback loop driven by the nitrogen source (for example, ammonia in this study). This prediction is attributed to the bubble-like Hopf bifurcation which is likely caused by the saturation type kinetics.

Another important drawback of the model in article 1 is the unidirectional nature of diffusion, which is justified if the concentration on one side is much higher than on the other. Normally, however, diffusion is a bidirectional process. This can be easily addressed by using reversible reactions. The reaction for the uptake of glutamate from the environment and the diffusion of ammonia into the surroundings remain irreversible to mimic the experimental observations. There exists a reversible version of the mathematical model my Wilhelm and Heinrich in which all the reactions are considered to be reversible and the rate of backward reactions is 10% of that of forward reactions(Wilhelm, Schuster, and Heinrich 1997). In the biofilm scenario, all reactions need not be reversible. In model R in chapter III, we show that it is possible to have the rates of forward reactions equal to that of the backward reactions and still model the oscillations with precision. Further we also investigate a special

case (see Chapter III section S) where we obtain the Hopf-bubble when the only irreversible reaction is the diffusion of ammonia. Such a bifurcation was not anticipated by Wilhelm *et. al*. This peculiar bifurcation could be the result of reversibility of the bilinear term. Model R in chapter III models the oscillations considering the reversibility of diffusion. In doing so, the number of ODEs used is unchanged and thus the model is minimal with respect to number of variables used.

Model MMR combines the reversibility and Michaelis Menten kinetics resulting in a more precise depiction of the scenario. This modification also uses just three variables and maintains its minimality. The Hopf bubble is the most notable observation of this modification.

The four modifications show how simple models can be fortified with suitable modifications. It also shows the strength of minimal models to describe biological observations and their plasticity to various modifications. This has also been realized successfully in models of calcium oscillations (for review, see Schuster *et al*., 2002(Schuster, Marhl, and Hofer 2002)). Furthermore, each individual modification unravels new knowledge about the system. In a nutshell, oscillations in biofilms are observed under nutrient limitation and are mainly brought about by ammonia limitation, and a monopoly over ammonia production enables the interior population to control the growth of the periphery. When an influx of enough nutrients is experienced, oscillations will no longer persist. Concentration gradients may not be directly involved in oscillations.

In chapter IV, we apply the same mathematical model in the context of population dynamics. This also highlights the strength of minimal models – versatility. Just by making new assumptions and reassigning the variables, the model can be completely changed without changing mathematically. Note that the original model had been proposed by Wilhelm and Heinrich(Wilhelm and Heinrich 1995) to describe chemical reactions rather than biofilms. Variables that were used earlier to describe reactants(Wilhelm and Heinrich 1995) and metabolites(Garde et al. 2020; Garde, Ibrahim, and Schuster 2020), now represent subpopulations.

In chapter I and II, we had a worm's eye look at the oscillatory behaviour in the biofilm. In chapter IV, we have a bird's eye look at the oscillatory regime occurring within a community. To further broaden the scope of the model, we make our variable assignments and model assumptions based on well-studied phenomena in microbiology with no particular organism in mind, instead of focusing on *Bacillus subtilis*. Processes like chemotaxis(Hansen, Endres, and Wingreen 2008; Tso and Adler 1974), antibiotic resistance(Ventola 2015), production of public goods(Levin 2014; Özkaya et al. 2017) such as siderophores(Lee, van Baalen, and Jansen 2016) or the biofilm matrix(Brockhurst et al. 2008) are covered by the approach.In order to have a broad range of applicability of the model, we consider a hypothetical unicellular social organism that is faced with several choices during its life cycle. We

tackle this decision making problem through evolutionary game theory (see below). In the new scenario, the variables *R*, *M*, and *P* signify the population of resistant cells, motile cells and producer cells respectively.The model relies on the assumption that *R* cells show resistance to the antibiotic, whereas *P* cells are susceptible to it and the motile cells, although susceptible, can move away from the antibiotic due to chemotaxis. The producer cells produce public goods..

The antibiotic threat is reflected through the costs of producing public goods. In the absence of the antibiotic, producing resistance is a costly choice, whereas if the antibiotic is present, then producing public goods is costlier. This is adequate in a minimal sense, but one could also define a term for the concentration of the antibiotic and connect it to each of the cell types through a death function. In our system, we distinguish three different levels of antibiotic stress from no antibiotic to very high concentration of the antibiotic.

Interestingly, resistance is observed even in the absence of the antibiotic (Chapter IV figure 2a). One can see a periodic rise in the proportion of resistant cells in relation to that of the producer cells. This phenomenon is called bet hedging and it ensures that some cells will survive if the environment suddenly becomes hostile. Bet hedging is routinely observed not just in bacteria (Beaumont et al. 2009; Veening, Smits, and Kuipers 2008) but several organisms with social dynamics (Weinkauf et al. 2014). It is also reported that bet hedging is better when the environment fluctuates spatially more than temporally and unpredictably rather than frequently (Villa Martín, Muñoz, and Pigolotti 2019). Another study reports that sporulation occurs as a bet hedging strategy in B. *subtilis* even before glucose has been depleted(Siebring et al. 2014). Thus in some aspects the resistant cells can be thought of as sporulating cells: the most resilient to harsh conditions and the speres they produce are the progenitor of all the subpopulations of the community. Their major role is to disperse to a favourable substrate and germinate.

One may apply the minimal model to the biofilm community of *B. subtilis*. The three subpopulations would then be the sporulating type cells, the motile cells and the biofilm producers given by the variables *S*, *M*, and *B* respectively. The model would be described as follows:

- $\frac{dS}{dt} = k_1 NS - k_4 S - k_2 SB$ (D1)
- $\frac{dB}{dt} = -k_3 B + k_5 M$ (D2)
- $\frac{dM}{dt} = k_4 S - k_5 M$ (D3)

Here, k_2SB represents the costs for propagating the spores. Since the spores are liberated, the term is negative. It also follows that the higher the number of biofilm producing cells is, the more active

sporulation will be. *B. subtilis* biofilms are known to exhibit fruiting bodies(Claessen et al. 2014b; Branda et al. 2001). These structures help disperse the spores and are made of the same matrix as the biofilm. Hence it is justified to model the liberation of spores as a product of not just *S* but also *B*. The model only focuses on the switching of phenotypes and does not consider the growth and death rates of each individual subpopulation. This implies that the oscillations signify the generations of the life cycle of the community. Thus, according to this model, the spores grow into subpopulation *S*, which produces more spores (and is therefore self-amplifying). Subpopulation *M* arises from *S* which helps the cells spread over the substratum. Finally, subpopulation *B* arises when the *M* cells lose their motility and a biofilm matrix is created over the substratum. Then in order to ensure species survival, the biofilm forms fruiting bodies which enclose the *S* type cells within the matrix. The spores are liberated such that they land on new substratum with favourable growth conditions.

Translating the results from the model in chapter III, one can expect that sporulation cycles or life cycles in general are a natural outcome of basic principles. In particular, the sporulation cycles or 'spikes' will be seen even under no stress.On the other hand, under extreme stress, sporulation would be the only dominant strategy. Under regular conditions, one can expect a regular life cycle of the biofilm community.

We have seen the application and modification of a minimal model to two different scenarios. Such models however, cannot easily make use of high throughput data. With the explosion of data through the high throughput methods, there is a requirement for large scale models that can make use of such data. However, such large scale models are dependent on the availability of data and are affected by the quality of the data. Minimal models however, are based on the knowledge within the field of study and are targeted to describe a specific phenomenon with precision. Further, as seen in chapters II and III, minimal models are highly adaptable and can be modified and analysed quite easily.

One interesting adaptation to consider is to test the behaviour of the system when two or more models are coupled through one of the variables, as has been done earlier for other systems (Wolf and Heinrich…, Strogatz book). Biologically, this represents sharing of one of the metabolites, for example, glutamate, being shared between two biofilms.

One may also consider an interaction between overproducer biofilm and an auxotrophic biofilm. The auxotroph biofilm system would lack one of the three reactions required to produce one of the three metabolites. Ideally, this could be the metabolite with the self-amplification term (G_p). This metabolite is produced in excess by the overproducer biofilm system and released into the environment. The auxotroph uses this for growth. Cross feeding can also be modelled using a similar approach where the

two biofilms lack two different reactions and overproduce the corresponding reaction the other system lacks.

Bacteria themselves are quite similar to minimal models in the sense that they lack cellular organisation into membrane bound organelles and only contain the very minimal constituents required to sustain their generations. Yet, they exhibit fascinating processes as an individual and as a community, interact with their surroundings and other organisms. Bacterial communities have even been thought to be an origin to multicellularity. They have been around for longer than most of the higher, multicellular organisms and still continue to exist even today. Their application in industry and medicine is irreplaceable but on the other hand they also pose some of the greatest challenges in the agricultural and clinical fields. They are an excellent example to show that even the most minimal organisms can exhibit complex behaviours that are strikingly similar to those observed in the complex organisms.

References

Altay, F., F. Karbancioglu-Guler, C. Daskaya-Dikmen, and D. Heperkan. 2013. 'A review on traditional Turkish fermented non-alcoholic beverages: microbiota, fermentation process and quality characteristics', Int J Food Microbiol, 167: 44-56.

Amanatidou, Elli, Andrew C. Matthews, Ute Kuhlicke, Thomas R. Neu, James P. McEvoy, and Ben Raymond. 2019. 'Biofilms facilitate cheating and social exploitation of β-lactam resistance in Escherichia coli', npj Biofilms and Microbiomes, 5: 36.

Anderl, J. N., M. J. Franklin, and P. S. Stewart. 2000. 'Role of antibiotic penetration limitation in Klebsiella pneumoniae biofilm resistance to ampicillin and ciprofloxacin', Antimicrob Agents Chemother, 44: 1818-24.

Aristides Yayanos, A. 2001. 'Deep-sea piezophilic bacteria.' in, Methods in Microbiology (Academic Press).

B. Knoke, C. Bodenstein, M. Marhl, M. Perc, S. Schuster. 2010. 'Jensen's inequality as a tool for explaining the effect of oscillations on the average cytosolic calcium concentration', Theory Biosci.

Bais, H. P., R. Fall, and J. M. Vivanco. 2004. 'Biocontrol of *Bacillus subtilis* against infection of Arabidopsis roots by Pseudomonas syringae is facilitated by biofilm formation and surfactin production', Plant Physiol, 134: 307-19.

Beaumont, H. J., J. Gallie, C. Kost, G. C. Ferguson, and P. B. Rainey. 2009. 'Experimental evolution of bet hedging', Nature, 462: 90-3.

Becskei, A., and L. Serrano. 2000. 'Engineering stability in gene networks by autoregulation', Nature, 405: 590-3.

Bocci, F., Y. Suzuki, M. Lu, and J. N. Onuchic. 2018. 'Role of metabolic spatiotemporal dynamics in regulating biofilm colony expansion', Proc Natl Acad Sci U S A, 115: 4288-93.

Bodenstein, C., B. Knoke, M. Marhl, M. Perc, and S. Schuster. 2010. 'Using Jensen's inequality to explain the role of regular calcium oscillations in protein activation', Phys Biol, 7: 036009.

Boyle, K. E., S. Heilmann, D. van Ditmarsch, and J. B. Xavier. 2013. 'Exploiting social evolution in biofilms', Curr Opin Microbiol, 16: 207-12.

Branda, S. S., J. E. Gonzalez-Pastor, S. Ben-Yehuda, R. Losick, and R. Kolter. 2001. 'Fruiting body formation by *Bacillus subtilis*', Proc Natl Acad Sci U S A, 98: 11621-6.

Branda, Steven S., Frances Chu, Daniel B. Kearns, Richard Losick, and Roberto Kolter. 2006. 'A major protein component of the *Bacillus subtilis* biofilm matrix', Molecular Microbiology, 59: 1229-38.

Bratsun, D., D. Volfson, L. S. Tsimring, and J. Hasty. 2005. 'Delay-induced stochastic oscillations in gene regulation', Proc Natl Acad Sci U S A, 102: 14593-8.

Brockhurst, Michael, Angus Buckling, Dan Racey, and Andy Gardner. 2008. 'Resource supply and the evolution of public-goods cooperation in bacteria', BMC biology, 6: 20.

Burdett, I. D., T. B. Kirkwood, and J. B. Whalley. 1986. 'Growth kinetics of individual *Bacillus subtilis* cells and correlation with nucleoid extension', J Bacteriol, 167: 219-30.

Castorph, H., and D. Kleiner. 1984. 'Some properties of a Klebsiella pneumoniae ammonium transport negative mutant (Amt-)', Arch Microbiol, 139: 245-7.

Checinska Sielaff, Aleksandra, Camilla Urbaniak, Ganesh Babu Malli Mohan, Victor G. Stepanov, Quyen Tran, Jason M. Wood, Jeremiah Minich, Daniel McDonald, Teresa Mayer, Rob Knight, Fathi Karouia, George E. Fox, and Kasthuri Venkateswaran. 2019. 'Characterization of the total and viable bacterial and fungal communities associated with the International Space Station surfaces', Microbiome, 7: 50.

Cheema, M. S., J. E. Rassing, and C. Marriott. 1986. 'The Diffusion Characteristics of Antibiotics in Mucus Glycoprotein Gels', Journal of Pharmacy and Pharmacology, 38: 53P-53P.

'Cholera vaccines: WHO position paper'. 2010. Wkly Epidemiol Rec, 85: 117-28.

Chu, F., D. B. Kearns, S. S. Branda, R. Kolter, and R. Losick. 2006. 'Targets of the master regulator of biofilm formation in *Bacillus subtilis*', Mol Microbiol, 59: 1216-28.

Claessen, Dennis, Daniel E. Rozen, Oscar P. Kuipers, Lotte Søgaard-Andersen, and Gilles P. van Wezel. 2014a. 'Bacterial solutions to multicellularity: a tale of biofilms, filaments and fruiting bodies', Nature Reviews Microbiology, 12: 115-24.

———. 2014b. 'Bacterial solutions to multicellularity: a tale of biofilms, filaments and fruiting bodies', Nature Reviews Microbiology, 12: 115.

Cohn, Ferdinand. 1875. 'Beiträge zur Biologie der Pflanzen', Beiträge zur Biologie der Pflanzen.

Collins, Douglas P., Barry J. Jacobsen, and Bruce Maxwell. 2003. 'Spatial and temporal population dynamics of a phyllosphere colonizing *Bacillus subtilis* biological control agent of sugar beet cercospora leaf spot', Biological Control, 26: 224-32.

Coyte, Katharine Z., Hervé Tabuteau, Eamonn A. Gaffney, Kevin R. Foster, and William M. Durham. 2017. 'Microbial competition in porous environments can select against rapid biofilm growth', Proceedings of the National Academy of Sciences, 114: E161.

Cussler, E. L. 2009. Diffusion (Cambridge University Press: New York).

Czárán, Tamás L., Rolf F. Hoekstra, and Ludo Pagie. 2002. 'Chemical warfare between microbes promotes biodiversity', Proceedings of the National Academy of Sciences, 99: 786-90.

Darouiche, R. O., A. Dhir, A. J. Miller, G. C. Landon, Raad, II, and D. M. Musher. 1994. 'Vancomycin penetration into biofilm covering infected prostheses and effect on bacteria', J Infect Dis, 170: 720-3.

Davey, M. E., and G. A. O'Toole. 2000. 'Microbial biofilms: from ecology to molecular genetics', Microbiology and molecular biology reviews : MMBR, 64: 847-67.

Davies, D. 2003. 'Understanding biofilm resistance to antibacterial agents', Nat Rev Drug Discov, 2: 114-22.

de Beer, Dirk, Paul Stoodley, Frank Roe, and Zbigniew Lewandowski. 1994. 'Effects of biofilm structures on oxygen distribution and mass transport', Biotechnology and Bioengineering, 43: 1131-38.

Diggle, S. P., A. S. Griffin, G. S. Campbell, and S. A. West. 2007. 'Cooperation and conflict in quorum-sensing bacterial populations', Nature, 450: 411-4.

Donlan, R. M., and J. W. Costerton. 2002. 'Biofilms: survival mechanisms of clinically relevant microorganisms', Clin Microbiol Rev, 15: 167-93.

Donlan, Rodney M. 2000. 'Role of Biofilms in Antimicrobial Resistance', ASAIO Journal, 46: S47-S52.

Dragos, A., H. Kiesewalter, M. Martin, C. Y. Hsu, R. Hartmann, T. Wechsler, C. Eriksen, S. Brix, K. Drescher, N. Stanley-Wall, R. Kummerli, and A. T. Kovacs. 2018. 'Division of labor during biofilm matrix production', Curr Biol, 28: 1903-13 e5.

Dragoš, Anna, and Ákos T. Kovács. 2017. 'The peculiar functions of the bacterial extracellular matrix', Trends in Microbiology, 25: 257-66.

Drescher, K., C. D. Nadell, H. A. Stone, N. S. Wingreen, and B. L. Bassler. 2014. 'Solutions to the public goods dilemma in bacterial biofilms', Curr Biol, 24: 50-55.

du Preez, F. B., D. D. van Niekerk, B. Kooi, J. M. Rohwer, and J. L. Snoep. 2012. 'From steady-state to synchronized yeast glycolytic oscillations I: model construction', FEBS J, 279: 2810-22.

du Preez, F. B., D. D. van Niekerk, and J. L. Snoep. 2012. 'From steady-state to synchronized yeast glycolytic oscillations II: model validation', FEBS J, 279: 2823-36.

Dunne, W. M., Jr., E. O. Mason, Jr., and S. L. Kaplan. 1993. 'Diffusion of rifampin and vancomycin through a Staphylococcus epidermidis biofilm', Antimicrob Agents Chemother, 37: 2522-6.

Dupont, G. 1993. 'Modélisation des oscillations et des ondes de calcium intracellulaire.', Université Libre de Bruxelles.

Edgar, R. S., E. W. Green, Y. Zhao, G. van Ooijen, M. Olmedo, X. Qin, Y. Xu, M. Pan, U. K. Valekunja, K. A. Feeney, E. S. Maywood, M. H. Hastings, N. S. Baliga, M. Merrow, A. J. Millar, C. H. Johnson, C. P. Kyriacou, J. S. O'Neill, and A. B. Reddy. 2012. 'Peroxiredoxins are conserved markers of circadian rhythms', Nature, 485: 459-64.

Ewald, J., P. Sieber, R. Garde, S. N. Lang, S. Schuster, and B. Ibrahim. 2019. 'Trends in mathematical modeling of host-pathogen interactions', Cell Mol Life Sci.

Ferrell, J. E., Jr., T. Y. Tsai, and Q. Yang. 2011. 'Modeling the cell cycle: why do certain circuits oscillate?', Cell, 144: 874-85.

Flemming, H. C., J. Wingender, U. Szewzyk, P. Steinberg, S. A. Rice, and S. Kjelleberg. 2016. 'Biofilms: an emergent form of bacterial life', Nat Rev Microbiol, 14: 563-75.

Fredrickson, James K., John M. Zachara, David L. Balkwill, David Kennedy, Shu-mei W. Li, Heather M. Kostandarithes, Michael J. Daly, Margaret F. Romine, and Fred J. Brockman. 2004. 'Geomicrobiology of high-level nuclear waste-contaminated vadose sediments at the hanford site, washington state', Applied and environmental microbiology, 70: 4230-41.

Garde, R., B. Ibrahim, and S. Schuster. 2020. 'Extending the minimal model of metabolic oscillations in *Bacillus subtilis* biofilms', Sci Rep, 10: 5579.

Garde, Ravindra, Bashar Ibrahim, Ákos T. Kovács, and Stefan Schuster. 2020. 'Differential equation-based minimal model describing metabolic oscillations in *Bacillus subtilis* biofilms', Royal Society Open Science, 7.

Garrett, A. J. M. 1991. 'Ockham’s Razor.' in, Maximum Entropy and Bayesian Methods.

Geva-Zatorsky, N., N. Rosenfeld, S. Itzkovitz, R. Milo, A. Sigal, E. Dekel, T. Yarnitzky, Y. Liron, P. Polak, G. Lahav, and U. Alon. 2006. 'Oscillations and variability in the p53 system', Mol Syst Biol, 2: 2006 0033.

Gintis, Herbert. 2000. Game theory evolving: A problem-centered introduction to modeling strategic behavior (Princeton university press: New Jersey).

Goel, Narendra S., Samaresh C. Maitra, and Elliott W. Montroll. 1971. 'On the Volterra and Other Nonlinear Models of Interacting Populations', Reviews of Modern Physics, 43: 231-76.

Goldbeter, A., G. Dupont, and M. J. Berridge. 1990. 'Minimal model for signal-induced Ca2+ oscillations and for their frequency encoding through protein phosphorylation', Proc Natl Acad Sci U S A, 87: 1461-5.

Goldbeter, Albert, and M. J. Berridge. 2010. Biochemical Oscillations and Cellular Rhythms (Cambridge).

González-Pastor, José Eduardo. 2011. 'Cannibalism: a social behavior in sporulating *Bacillus subtilis*', FEMS microbiology reviews, 35: 415-24.

Gonzalez, L. M., N. Mukhitov, and C. A. Voigt. 2019. 'Resilient living materials built by printing bacterial spores', Nat Chem Biol.

Gonze, D., and W. Abou-Jaoude. 2013. 'The Goodwin model: behind the Hill function', PLoS One, 8: e69573.

Goodwin, B. C. 1965a. 'Oscillatory behavior in enzymatic control processes', Adv Enzyme Regul, 3: 425-38.

Goodwin, Brian C. 1965b. 'Oscillatory behavior in enzymatic control processes', Advances in enzyme regulation, 3: 425-37.

Gordon, C. A., N. A. Hodges, and C. Marriott. 1988. 'Antibiotic interaction and diffusion through alginate and exopolysaccharide of cystic fibrosis-derived Pseudomonas aeruginosa', J Antimicrob Chemother, 22: 667-74.

Griffin, A. S., S. A. West, and A. Buckling. 2004. 'Cooperation and competition in pathogenic bacteria', Nature, 430: 1024-7.

Gunka, K., and F. M. Commichau. 2012. 'Control of glutamate homeostasis in *Bacillus subtilis*: a complex interplay between ammonium assimilation, glutamate biosynthesis and degradation', Mol Microbiol, 85: 213-24.

Hall-Stoodley, L., J. W. Costerton, and P. Stoodley. 2004. 'Bacterial biofilms: from the natural environment to infectious diseases', Nat Rev Microbiol, 2: 95-108.

Hall-Stoodley, L., and P. Stoodley. 2009. 'Evolving concepts in biofilm infections', Cell Microbiol, 11: 1034-43.

Hansen, Clinton H., Robert G. Endres, and Ned S. Wingreen. 2008. 'Chemotaxis in Escherichia coli: a molecular model for robust precise adaptation', PLOS Computational Biology, 4: e1-e1.

Hanusse, P. 1972. 'De l'Existence d'un Cycle Limite dans l'Evolution des Systèmes Chimiques Ouverts', C. R. Acad. Sci. Paris, C274 (1972): 1245-47.

———. 1973. 'Étude des systèmes dissipatifs chimiques à deux et trois espèces intermédiaires', C. R. Acad. Sci. Paris C 277: 263-66.

Harrison, F., and A. Buckling. 2009. 'Siderophore production and biofilm formation as linked social traits', ISME J, 3: 632-4.

Hartzell, T. 'Myxobacteria.' in, eLS.

Heiland, I., C. Bodenstein, T. Hinze, O. Weisheit, O. Ebenhoeh, M. Mittag, and S. Schuster. 2012. 'Modeling temperature entrainment of circadian clocks using the Arrhenius equation and a reconstructed model from Chlamydomonas reinhardtii', J Biol Phys, 38: 449-64.

Heinrich, Reinhart, and Stefan Schuster. 1996. The Regulation of Cellular Systems (Chapman & Hall, New York).

Higgins, Joseph. 1967. 'The Theory of Oscillating Reactions - Kinetics Symposium', Industrial & Engineering Chemistry, 59: 18-62.

Hillmann, F., G. Forbes, S. Novohradska, I. Ferling, K. Riege, M. Groth, M. Westermann, M. Marz, T. Spaller, T. Winckler, P. Schaap, and G. Glockner. 2018. 'Multiple Roots of Fruiting Body Formation in Amoebozoa', Genome Biol Evol, 10: 591-606.

Hoops, S., S. Sahle, R. Gauges, C. Lee, J. Pahle, N. Simus, M. Singhal, L. Xu, P. Mendes, and U. Kummer. 2006. 'COPASI--a COmplex PAthway SImulator', Bioinformatics, 22: 3067-74.

Hooshangi, S., S. Thiberge, and R. Weiss. 2005. 'Ultrasensitivity and noise propagation in a synthetic transcriptional cascade', Proc Natl Acad Sci U S A, 102: 3581-6.

Horn, H., and S. Lackner. 2014. 'Modeling of biofilm systems: a review', Adv Biochem Eng Biotechnol, 146: 53-76.

Hummert, Sabine, Katrin Bohl, David Basanta, Andreas Deutsch, Sarah Werner, Günter Theißen, Anja Schroeter, and Stefan Schuster. 2014. 'Evolutionary game theory: cells as players', Molecular BioSystems, 10: 3044-65.

Hutchison, E. A., D. A. Miller, and E. R. Angert. 2014. 'Sporulation in Bacteria: Beyond the Standard Model', Microbiol Spectr, 2.

J. Hofbauer, K. Sigmund. 1998. Evolutionary Games and Population Dynamics (Cambridge University Press: Cambridge).

Jiricny, N., S. P. Diggle, S. A. West, B. A. Evans, G. Ballantyne, A. Ross-Gillespie, and A. S. Griffin. 2010. 'Fitness correlates with the extent of cheating in a bacterium', J Evol Biol, 23: 738-47.

Kampf, J., J. Gerwig, K. Kruse, R. Cleverley, M. Dormeyer, A. Grunberger, D. Kohlheyer, F. M. Commichau, R. J. Lewis, and J. Stulke. 2018. 'Selective Pressure for Biofilm Formation in *Bacillus subtilis*: Differential Effect of Mutations in the Master Regulator SinR on Bistability', mBio, 9.

Kent, Edward, Stefan Neumann, Ursula Kummer, and Pedro Mendes. 2013. 'What can we learn from global sensitivity analysis of biochemical systems?', PloS one, 8: e79244-e44.

Klipp, E., R. Herwig, A. Kowald, C. Wierling, and H. Lehrach. 2005. Systems Biology in Practice.

Knoke, B., M. Marhl, M. Perc, and S. Schuster. 2008. 'Equality of average and steady-state levels in some nonlinear models of biological oscillations', Theory Biosci, 127: 1-14.

Kovacs, A. T., and A. Dragos. 2019. 'Evolved Biofilm: Review on the Experimental Evolution Studies of *Bacillus subtilis* Pellicles', J Mol Biol, 431: 4749-59.

Kreft, J. U. 2004. 'Biofilms promote altruism', Microbiology, 150: 2751-60.

Kullmann, D. M., M. Y. Min, F. Asztely, and D. A. Rusakov. 1999. 'Extracellular glutamate diffusion determines the occupancy of glutamate receptors at CA1 synapses in the hippocampus', Philos Trans R Soc Lond B Biol Sci, 354: 395-402.

Kummer, U., L. F. Olsen, C. J. Dixon, A. K. Green, E. Bornberg-Bauer, and G. Baier. 2000. 'Switching from simple to complex oscillations in calcium signaling', Biophys J, 79: 1188-95.

Kumon, H., K. Tomochika, T. Matunaga, M. Ogawa, and H. Ohmori. 1994. 'A sandwich cup method for the penetration assay of antimicrobial agents through Pseudomonas exopolysaccharides', Microbiol Immunol, 38: 615-9.

LeBlanc, J. G., C. Milani, G. S. de Giori, F. Sesma, D. van Sinderen, and M. Ventura. 2013. 'Bacteria as vitamin suppliers to their host: a gut microbiota perspective', Curr Opin Biotechnol, 24: 160-8.

Lee, W., M. van Baalen, and V. A. Jansen. 2016. 'Siderophore production and the evolution of investment in a public good: An adaptive dynamics approach to kin selection', J Theor Biol, 388: 61-71.

Levin, Simon A. 2014. 'Public goods in relation to competition, cooperation, and spite', Proceedings of the National Academy of Sciences, 111: 10838.

Li, Xiang-Yi, Cleo Pietschke, Sebastian Fraune, Philipp M. Altrock, Thomas C. G. Bosch, and Arne Traulsen. 2015. 'Which games are growing bacterial populations playing?', Journal of The Royal Society Interface, 12: 20150121.

Li, Yung-Hua, and Xiaolin Tian. 2012. 'Quorum sensing and bacterial social interactions in biofilms', Sensors (Basel, Switzerland), 12: 2519-38.

Linares, D. M., P. Ross, and C. Stanton. 2016. 'Beneficial Microbes: The pharmacy in the gut', Bioengineered, 7: 11-20.

Liu, J., R. Martinez-Corral, A. Prindle, D. D. Lee, J. Larkin, M. Gabalda-Sagarra, J. Garcia-Ojalvo, and G. M. Suel. 2017. 'Coupling between distant biofilms and emergence of nutrient time-sharing', Science, 356: 638-42.

Liu, J., A. Prindle, J. Humphries, M. Gabalda-Sagarra, M. Asally, D. Y. Lee, S. Ly, J. Garcia-Ojalvo, and G. M. Suel. 2015. 'Metabolic co-dependence gives rise to collective oscillations within biofilms', Nature, 523: 550-4.

Logan, B. E. 2009. 'Exoelectrogenic bacteria that power microbial fuel cells', Nat Rev Microbiol, 7: 375-81.

Logsdon, M. M., and B. B. Aldridge. 2018. 'Stable Regulation of Cell Cycle Events in Mycobacteria: Insights From Inherently Heterogeneous Bacterial Populations', Front Microbiol, 9: 514.

Lotka, Alfred J. 2002. 'Contribution to the Theory of Periodic Reactions', The Journal of Physical Chemistry, 14: 271-74.

Maass, S., S. Sievers, D. Zuhlke, J. Kuzinski, P. K. Sappa, J. Muntel, B. Hessling, J. Bernhardt, R. Sietmann, U. Volker, M. Hecker, and D. Becher. 2011. 'Efficient, global-scale quantification of absolute protein amounts by integration of targeted mass spectrometry and two-dimensional gel-based proteomics', Anal Chem, 83: 2677-84.

Magni*, P., M. Germani, G. D. Nicolao, G. Bianchini, M. Simeoni, I. Poggesi, and M. Rocchetti. 2008. 'A Minimal Model of Tumor Growth Inhibition', IEEE Transactions on Biomedical Engineering, 55: 2683-90.

Mahdinia, Ehsan, Ali Demirci, and Aydin Berenjian. 2019. 'Biofilm reactors as a promising method for vitamin K (menaquinone-7) production', Applied Microbiology and Biotechnology, 103: 5583-92.

Mancinelli, R. L., and W. A. Shulls. 1978. 'Airborne bacteria in an urban environment', Applied and environmental microbiology, 35: 1095-101.

Martinez-Corral, R., J. Liu, G. M. Suel, and J. Garcia-Ojalvo. 2018. 'Bistable emergence of oscillations in growing *Bacillus subtilis* biofilms', Proc Natl Acad Sci U S A, 115: E8333-E40.

May, Robert, and Warren Leonard. 1975. 'Nonlinear Aspects of Competition Between Three Species', SIAM J. Appl. Math., 29: 243.

McLoon, A. L., S. B. Guttenplan, D. B. Kearns, R. Kolter, and R. Losick. 2011. 'Tracing the domestication of a biofilm-forming bacterium', J Bacteriol, 193: 2027-34.

Miller, J. K., J. S. Brantner, C. Clemons, K. L. Kreider, A. Milsted, P. Wilber, Y. H. Yun, W. J. Youngs, G. Young, H. T. Badawy, A. Milsted, C. Clemons, K. L. Kreider, P. Wilber, G. Young, Y. H. Yun, P. O. Wagers, and W. J. Youngs. 2014. 'Mathematical modelling of Pseudomonas aeruginosa biofilm growth and treatment in the cystic fibrosis lung', Math Med Biol, 31: 179-204.

Monk, Nicholas A. M. 2003. 'Oscillatory Expression of Hes1, p53, and NF-κB Driven by Transcriptional Time Delays', Current Biology, 13: 1409-13.

Nadell, C. D., K. Drescher, and K. R. Foster. 2016a. 'Spatial structure, cooperation and competition in biofilms', Nat Rev Microbiol, 14: 589-600.

Nadell, Carey D., Knut Drescher, and Kevin R. Foster. 2016b. 'Spatial structure, cooperation and competition in biofilms', Nature Reviews Microbiology, 14: 589-600.

Neumann, Gunter, and Stefan Schuster. 2007. 'Continuous model for the rock–scissors–paper game between bacteriocin producing bacteria', Journal of Mathematical Biology, 54: 815-46.

Nickel, J. C., and J. W. Costerton. 1992. 'Bacterial biofilms and catheters: A key to understanding bacterial strategies in catheter-associated urinary tract infection', The Canadian journal of infectious diseases = Journal canadien des maladies infectieuses, 3: 261-67.

Novak, B., and J. J. Tyson. 2008. 'Design principles of biochemical oscillators', Nat Rev Mol Cell Biol, 9: 981-91.

Özkaya, Özhan, Karina B. Xavier, Francisco Dionisio, and Roberto Balbontín. 2017. 'Maintenance of Microbial Cooperation Mediated by Public Goods in Single- and Multiple-Trait Scenarios', JOURNAL OF BACTERIOLOGY, 199: e00297-17.

Pamp, Sünje Johanna, Morten Gjermansen, Helle Krogh Johansen, and Tim Tolker-Nielsen. 2008. 'Tolerance to the antimicrobial peptide colistin in Pseudomonas aeruginosa biofilms is linked to metabolically active cells, and depends on the pmr and mexAB-oprM genes', Molecular Microbiology, 68: 223-40.

Pantastico-Caldas, Marissa, Kathleen E. Duncan, Conrad A. Istock, and Julia A. Bell. 1992. 'Population Dynamics of Bacteriophage and *Bacillus Subtilis* in Soil', Ecology, 73: 1888-902.

Pollak, S., S. Omer-Bendori, E. Even-Tov, V. Lipsman, T. Bareia, I. Ben-Zion, and A. Eldar. 2016. 'Facultative cheating supports the coexistence of diverse quorum-sensing alleles', Proc Natl Acad Sci U S A, 113: 2152-7.

Pomerening, J. R., E. D. Sontag, and J. E. Ferrell, Jr. 2003. 'Building a cell cycle oscillator: hysteresis and bistability in the activation of Cdc2', Nat Cell Biol, 5: 346-51.

Pommerville, J.C. 2013. Fundamentals of Microbiology (Jones & Bartlett Learning).

Popat, R., S. A. Crusz, M. Messina, P. Williams, S. A. West, and S. P. Diggle. 2012. 'Quorum-sensing and cheating in bacterial biofilms', Proc Biol Sci, 279: 4765-71.

Prigogine, I., and R. Lefever. 1968. 'Symmetry Breaking Instabilities in Dissipative Systems. II', The Journal of Chemical Physics, 48: 1695-700.

Prigogine, Ilya. 1980. 'From being to becoming: Time and complexity in the physical sciences'.

Reichenbach, Tobias, Mauro Mobilia, and Erwin Frey. 2007. 'Mobility promotes and jeopardizes biodiversity in rock–paper–scissors games', Nature, 448: 1046-49.

Reimers, A. M., and A. C. Reimers. 2016. 'The steady-state assumption in oscillating and growing systems', J Theor Biol, 406: 176-86.

Ribeiro, Ana C. F., M. M. Rodrigo, Marisa C. F. Barros, Luis M. P. Verissimo, Carmen Romero, Artur J. M. Valente, and Miguel A. Esteso. 2014. 'Mutual diffusion coefficients of L-glutamic acid and monosodium L-glutamate in aqueous solutions at T=298.15K', The Journal of Chemical Thermodynamics, 74: 133-37.

Ritter AB, Douglas JM 1970. 'Frequency response of nonlinear systems', IEC Fundam.

Romero, D., C. Aguilar, R. Losick, and R. Kolter. 2010. 'Amyloid fibers provide structural integrity to *Bacillus subtilis* biofilms', Proc Natl Acad Sci U S A, 107: 2230-4.

Rotrattanadumrong, Rachapun, and Robert G. Endres. 2017. 'Emergence of cooperativity in a model biofilm', Journal of Physics D: Applied Physics, 50.

Roux, D., C. Cywes-Bentley, Y. F. Zhang, S. Pons, M. Konkol, D. B. Kearns, D. J. Little, P. L. Howell, D. Skurnik, and G. B. Pier. 2015. 'Identification of Poly-N-acetylglucosamine as a Major Polysaccharide Component of the *Bacillus subtilis* Biofilm Matrix', J Biol Chem, 290: 19261-72.

Ryan, Kenneth J.; Ray, C. George; Ahmad, Nafees; Drew, W. Lawrence; Lagunoff, Michael; Pottinger, Paul; Reller, L. Barth; Sterling, Charles R. 2014. 'Pathogenesis of Bacterial Infections.' in, Pathogenesis of Bacterial Infections (McGraw Hill Education: New York).

Salazar, C., A. Z. Politi, and T. Hofer. 2008. 'Decoding of calcium oscillations by phosphorylation cycles: analytic results', Biophys J, 94: 1203-15.

Schuster, S., J. U. Kreft, N. Brenner, F. Wessely, G. Theissen, E. Ruppin, and A. Schroeter. 2010. 'Cooperation and cheating in microbial exoenzyme production--theoretical analysis for biotechnological applications', Biotechnol J, 5: 751-8.

Schuster, S., and M. Marhl. 2001. 'Bifurcation analysis of calcium oscillations: Time-scale separation, canards, and frequency lowering', Journal of Biological Systems, 9: 291-314.

Schuster, S., M. Marhl, and T. Hofer. 2002. 'Modelling of simple and complex calcium oscillations. From single-cell responses to intercellular signalling', Eur J Biochem, 269: 1333-55.

Sel'kov, E. E. 1968. 'Self-oscillations in glycolysis. 1. A simple kinetic model', Eur J Biochem, 4: 79-86.

Siebring, Jeroen, Matthijs J. H. Elema, Fátima Drubi Vega, Ákos T. Kovács, Patsy Haccou, and Oscar P. Kuipers. 2014. 'Repeated triggering of sporulation in *Bacillus subtilis* selects against a protein that affects the timing of cell division', The ISME Journal, 8: 77-87.

Simakov, David S. A., and Juan Pérez-Mercader. 2013. 'Noise induced oscillations and coherence resonance in a generic model of the nonisothermal chemical oscillator', Scientific Reports, 3: 2404.

Simeoni, Monica, Paolo Magni, Cristiano Cammia, Giuseppe De Nicolao, Valter Croci, Enrico Pesenti, Massimiliano Germani, Italo Poggesi, and Maurizio Rocchetti. 2004. 'Predictive Pharmacokinetic-Pharmacodynamic Modeling of Tumor Growth Kinetics in Xenograft Models after Administration of Anticancer Agents', Cancer Research, 64: 1094-101.

Singh, R., D. Paul, and R. K. Jain. 2006. 'Biofilms: implications in bioremediation', Trends Microbiol, 14: 389-97.

Skoneczny, S. 2015. 'Cellular automata-based modelling and simulation of biofilm structure on multi-core computers', Water Sci Technol, 72: 2071-81.

Smith, Jeff, David C. Queller, and Joan E. Strassmann. 2014. 'Fruiting bodies of the social amoeba Dictyostelium discoideum increase spore transport by Drosophila', BMC Evolutionary Biology, 14: 105.

Somogyi, R., and J. W. Stucki. 1991. 'Hormone-induced calcium oscillations in liver cells can be explained by a simple one pool model', J Biol Chem, 266: 11068-77.

Sotiriou, Michael C., Barbara M. Stryjewska, and Carlotta Hill. 2016. 'Two Cases of Leprosy in Siblings Caused by Mycobacterium lepromatosis and Review of the Literature', The American Journal of Tropical Medicine and Hygiene, 95: 522-27.

Stannek, L., M. J. Thiele, T. Ischebeck, K. Gunka, E. Hammer, U. Volker, and F. M. Commichau. 2015. 'Evidence for synergistic control of glutamate biosynthesis by glutamate dehydrogenases and glutamate in *Bacillus subtilis*', Environ Microbiol, 17: 3379-90.

Stewart, P. S. 1998. 'A review of experimental measurements of effective diffusive permeabilities and effective diffusion coefficients in biofilms', Biotechnol Bioeng, 59: 261-72.

———. 2002. 'Mechanisms of antibiotic resistance in bacterial biofilms', Int J Med Microbiol, 292: 107-13.

Stover, A. G., and A. Driks. 1999a. 'Control of synthesis and secretion of the *Bacillus subtilis* protein YqxM', J Bacteriol, 181: 7065-9.

———. 1999b. 'Secretion, localization, and antibacterial activity of TasA, a *Bacillus subtilis* spore-associated protein', J Bacteriol, 181: 1664-72.

Strogatz, S.H. 2018. Nonlinear Dynamics and Chaos: With Applications to Physics, Biology, Chemistry, and Engineering (CRC Press: United States of America).

Strogatz, Steven. 2000. Nonlinear dynamics and chaos.

Tack, K. J., and L. D. Sabath. 1985. 'Increased minimum inhibitory concentrations with anaerobiasis for tobramycin, gentamicin, and amikacin, compared to latamoxef, piperacillin, chloramphenicol, and clindamycin', Chemotherapy, 31: 204-10.

Tanouchi, Yu, Anand Pai, Heungwon Park, Shuqiang Huang, Rumen Stamatov, Nicolas E. Buchler, and Lingchong You. 2015. 'A noisy linear map underlies oscillations in cell size and gene expression in bacteria', Nature, 523: 357-60.

Terra, R., N. R. Stanley-Wall, G. Cao, and B. A. Lazazzera. 2012. 'Identification of *Bacillus subtilis* SipW as a bifunctional signal peptidase that controls surface-adhered biofilm formation', J Bacteriol, 194: 2781-90.

Tice, Alexander K., Lora L. Shadwick, Anna Maria Fiore-Donno, Stefan Geisen, Seungho Kang, Gabriel A. Schuler, Frederick W. Spiegel, Katherine A. Wilkinson, Michael Bonkowski, Kenneth Dumack, Daniel J. G. Lahr, Eckhard Voelcker, Steffen Clauß, Junling Zhang, and Matthew W. Brown. 2016. 'Expansion of the molecular and morphological diversity of Acanthamoebidae (Centramoebida, Amoebozoa) and identification of a novel life cycle type within the group', Biology direct, 11: 69-69.

Tolner, B., T. Ubbink-Kok, B. Poolman, and W. N. Konings. 1995. 'Characterization of the proton/glutamate symport protein of *Bacillus subtilis* and its functional expression in Escherichia coli', J Bacteriol, 177: 2863-9.

Tso, W. W., and J. Adler. 1974. 'Negative chemotaxis in Escherichia coli', JOURNAL OF BACTERIOLOGY, 118: 560-76.

Tuomanen, E., R. Cozens, W. Tosch, O. Zak, and A. Tomasz. 1986. 'The rate of killing of Escherichia coli by beta-lactam antibiotics is strictly proportional to the rate of bacterial growth', J Gen Microbiol, 132: 1297-304.

van Gestel, J., H. Vlamakis, and R. Kolter. 2015. 'Division of Labor in Biofilms: the Ecology of Cell Differentiation', Microbiol Spectr, 3: Mb-0002-2014.

Veening, J. W., W. K. Smits, and O. P. Kuipers. 2008. 'Bistability, epigenetics, and bet-hedging in bacteria', Annu Rev Microbiol, 62: 193-210.

Veening, Jan-Willem, Eric J. Stewart, Thomas W. Berngruber, François Taddei, Oscar P. Kuipers, and Leendert W. Hamoen. 2008. 'Bet-hedging and epigenetic inheritance in bacterial cell development', Proceedings of the National Academy of Sciences, 105: 4393-98.

Ventola, C. Lee. 2015. 'The antibiotic resistance crisis: part 1: causes and threats', P & T : a peer-reviewed journal for formulary management, 40: 277-83.

Villa Martín, Paula, Miguel A. Muñoz, and Simone Pigolotti. 2019. 'Bet-hedging strategies in expanding populations', PLOS Computational Biology, 15: e1006529.

Vlamakis, H., C. Aguilar, R. Losick, and R. Kolter. 2008. 'Control of cell fate by the formation of an architecturally complex bacterial community', Genes Dev, 22: 945-53.

Wain, J., R. S. Hendriksen, M. L. Mikoleit, K. H. Keddy, and R. L. Ochiai. 2015. 'Typhoid fever', Lancet, 385: 1136-45.

Weinkauf, Manuel F. G., Tobias Moller, Mirjam C. Koch, and Michal Kučera. 2014. 'Disruptive selection and bet-hedging in planktonic Foraminifera: shell morphology as predictor of extinctions', Frontiers in Ecology and Evolution, 2.

Wilhelm, T., S. Schuster, and R. Heinrich. 1997a. 'Kinetic and thermodynamic analyses of the reversible version of the smallest chemical reaction system with Hopf bifurcation', Nonlinear World: 295-321.

———. 1997b. ' Kinetic and thermodynamic analyses of the reversible version of the smallest chemical reaction system with Hopf bifurcation', Nonlinear World: 295-321.

Wilhelm, Thomas, and Reinhart Heinrich. 1995. 'Smallest chemical reaction system with Hopf bifurcation', Journal of Mathematical Chemistry, 17: 1-14.

———. 1996. 'Mathematical analysis of the smallest chemical reaction system with Hopf bifurcation', Journal of Mathematical Chemistry, 19: 111-30.

Wiuff, C., R. M. Zappala, R. R. Regoes, K. N. Garner, F. Baquero, and B. R. Levin. 2005. 'Phenotypic Tolerance: Antibiotic Enrichment of Noninherited Resistance in Bacterial Populations', Antimicrobial Agents and Chemotherapy, 49: 1483.

Worthington, D. R. L. 1997. 'Minimal model of food absorption in the gut', Medical Informatics, 22: 35-45.

Xavier, Joao B., and Kevin R. Foster. 2007. 'Cooperation and conflict in microbial biofilms', Proceedings of the National Academy of Sciences, 104: 876.

Yan, Dazhuang, Zhihui Bai, Mike Rowan, Likun Gu, Ren Shumei, and Peiling Yang. 2009. 'Biofilm structure and its influence on clogging in drip irrigation emitters distributing reclaimed wastewater', Journal of Environmental Sciences, 21: 834-41.

Zeng, G., B. S. Vad, M. S. Dueholm, G. Christiansen, M. Nilsson, T. Tolker-Nielsen, P. H. Nielsen, R. L. Meyer, and D. E. Otzen. 2015. 'Functional bacterial amyloid increases Pseudomonas biofilm hydrophobicity and stiffness', Front Microbiol, 6: 1099.

Zhu, Bingyao, and Jörg Stülke. 2017. 'SubtiWiki in 2018: from genes and proteins to functional network annotation of the model organism *Bacillus subtilis*', Nucleic Acids Research, 46: D743-D48.

Zimmer, J, I Issoufou, G Schmiedeknecht, and H Bochow. 1998. 'Population dynamics of *Bacillus subtilis* as biocontrol agent under controlled conditions', Mededelingen-Faculteit Landbouwkundige en Toegepaste Biologische Wetenschappen Universiteit Gent (Belgium).

Zomorrodi, Ali R., and Daniel Segrè. 2017. 'Genome-driven evolutionary game theory helps understand the rise of metabolic interdependencies in microbial communities', Nature communications, 8: 1563-63.

Acknowledgements

I extend my sincere gratitude to Prof Schuster for supervising my study. You really kept me motivated and I learnt a lot about not only mathematical modeling but research in general.

Bashar Ibrahim constantly pushed me to work harder and really coaxed the best out of me. The momentum my thesis gained during your stay in Jena is unmatched. Shukraan!

Prof Kovács and Prof Heckel gave valuable inputs from the biological perspective. I felt confident whenever my theoretical work got your approval. Thank you for all your support and ideas.

Dr. Jan Ewald your questions at the Lehrstuhl seminars gave a new perspective to my work. Thank you for your curiosity.

Sebastian Gemerodt helped me get started off into the fascinating world of mathematical modeling. I could approach you with the silliest of my questions and you patiently answered them all. Vielen Dank!

The co-ordinators at the IMPRS-CE Dr Claudia Voelckel and Angela Kiesewetter helped me with the administrative affairs and the Deutsche Bürokratie. Special thanks to you!

Kathrin Schowtka sorgte am Lehrstuhl für einen reibungslosen Ablauf. Papierkram, Vertragsverlängerungen, Mails, du hast alles wie eine Fee gemacht.

My labmates Andre, Jan, Stefan, Patricia, Sybille, Peter, Phillip, Max, Anja, Suman and Wassili made it fun to be at the office. I really loved the laser tag session and the canoeing in the Saale.

My friends Tilottama, Sin, Prerna, Burak, Kohulan, Amol, Shambhavi, Anja, Vincent, Sagar and Prasad kept things interesting. It is never a quiet day with you guys around. Can’t wait to have the next game night!

Finally, I thank my parents and my family for their love and support. Thank you for believing in me.

Eigenenteil bei publikationen von mehren Autoren

No.	Title	Author list	Contributions
1	Differential equation-based minimal model describing metabolic oscillations in *Bacillus subtilis* biofilms	Garde, R., Ibrahim, B., Kovács, Á. T. & Schuster, S.	**RG 55%,** BI 20%, SS 20%, ATK 5%
I performed the simulations, wrote the manuscript and interpreted the results. Prof. Bashar Ibrahim carried out the mathematical analyses and supervised my work. Prof Stefan Schuster suggested the use of the smallest chemical oscillator by Wilhelm and Heinrich, performed the mathematical analysis, refined and structured the manuscript, supervised my work and helped in the interpretation of the results mathematically and biologically. Prof. Ákos T. Kovács helped in the interpretation of the results and edited and structured the manuscript.			
2	Extending the minimal model of metabolic oscillations in *Bacillus subtilis* biofilms.	Garde, R., Ibrahim, B. & Schuster, S.	**RG 60%**, BI 20%, SS 20%
I performed the simulations, wrote the manuscript and interpreted the results. Prof. Bashar Ibrahim carried out the mathematical analyses and supervised my work. Prof Stefan Schuster suggested the use of three variables for ammonia in the 6ODE models, performed the mathematical analysis, refined and structured the manuscript, supervised my work and helped in the interpretation of the results mathematically and biologically			
3	Modelling population dynamics in a unicellular social organism community using a minimal model and game theory	Garde, R., Ewald, J., Kovács, Á. T., & Schuster, S.	**RG 70%**, ATK 15%, SS 10%, JE 5%
I thought of the application of the model to describe the population dynamics and describe the model behaviour using game theory and wrote the manuscript. Prof. Kovács suggested making a generalized model that can be applied to not just bacteria but all communities of unicellular social organisms. Prof. Schuster and Dr. Ewald provided valuable inputs and shaped the manuscript.			

Candidate: Ravindra Garde, Jena, 25/06/2020

Supervisor: Prof. Stefan Schuster

Curriculum vitae

Ravindra Garde

Luther str. 26, 07743 Jena, Germany.
Phone: +49 1520 386 9985
ravindra.p.garde@gmail.com

Education	Year	Institution	Place
PhD	Mar 2017 – present Expected: June 2020	Friedrich-Schiller University	Jena, Germany
	PhD thesis: Minimal mathematical model describing metabolic oscillations in *Bacillus subtilis* biofilms		
Master of Science	2014-2016	University of Pune	Pune, India
	Master thesis: Deciphering the function of a hypothetical yeast protein (PDBid: 1NKQ). Group project: Classification of antimicrobial peptides using machine learning approaches Summer project: Functional annotation of a hypothetical yeast protein (PDBid: 3KZV)		
Bachelor of Science	2011-2014	Abasaheb Garware College, University of Pune	Pune, India
	Bachelor thesis: Determination of antimicrobial activity of *Tectona grandis* (teak), *Nerium oleander*, *Lantana sp.* and *Parthenium hysterophorus*		

List of Publications

Garde, R., Ibrahim, B., Kovács, Á. T. & Schuster, S. 2020 Differential equation-based minimal model describing metabolic oscillations in *Bacillus subtilis* biofilms. *Royal Society Open Science* **7**, doi:10.1098/rsos.190810.

Ewald, J., Sieber, P., Garde, R., Lang, S. N., Schuster, S., Ibrahim, B. 2019 Trends in mathematical modeling of host–pathogen interactions. *Cellular and Molecular Life Sciences*. (10.1007/s00018-019-03382-0)

Garde, R., Ibrahim, B. & Schuster, S. 2020 Extending the minimal model of metabolic oscillations in *Bacillus subtilis* biofilms. *Sci Rep* **10**, 5579, doi:10.1038/s41598-020-62526-6.

Poster presentations

Garde R., Ibrahim B., Kovács A.T., Schuster S. (**2019**). Differential equation based minimal model describing metabolic oscillations in *Bacillus subtilis* biofilms. Presented at the 14th Basel Computational Biology Conference **[BC]^2**, Basel, CH

Garde R., Ibrahim B., Kovács A.T., Schuster S. (**2019**) Kinetic Analysis of the minimal model to describe metabolic oscillations in *Bacillus subtilis* biofilms Presented at the 7th Metabolic Pathway Analysis (**MPA**)Conference, Riga, LV

Garde R., Ibrahim B., Kovács A.T., Schuster S. (**2019**). Differential equation based minimal model describing metabolic oscillations in *Bacillus subtilis* biofilms. Presented at 18th **IMPRS Symposium**, Max Planck Institute for Chemical Ecology, IMPRS, Dornburg, DE

Garde R. Ibrahim B., Kovács A.T., Schuster S. (**2018**). Minimal model describing oscillations in *B. subtilis* biofilms. Presented at 18th conference of the International Study Group for Systems Biology (**ISGSB**), Tromso, NO

Garde R., Schuster S., Kovács A.T. (**2018**). Modelling oscillations in biofilms. Presented at 17th **IMPRS Symposium**, International Max Planck Research School, Dornburg, DE

Courses and Industrial visits attended:

Excursion to Jena BioScience, speaker: Nadine Müller-Dittmann	**Feb 2019**
Guided tour Analytik Jena, speaker: CEO Ulrich Krauss, Frau Wittenburg	**Jun 2018**
The dark side of science – procrastination, perfectionism, doubt and dead ends, speaker: Dr. Anne-Christin Warskulat	**Apr 2018**
Principles of Microbial Adaptation, speaker: Brigitte Schoonderwoerd	**Mar 2018**
Finish it! How to finalize your thesis and how to focus on it right from the beginning, speaker: Dr. Matthias Schwarzkopf	**Jan 2018**
Adobe Illustrator, speaker: Dr. Nico Überschaar	**May 2017**
Good Scientific Practice in the Doctoral Training Phase, speaker: Dr. Dorit Schmidt	**May 2017**

Supervision and Mentoring experience:

Offered a practical course on Metabolic and Regulatory Networks (Summer semester)	**2019**
Supervised at IMPRS Institute for Chemical Ecology Recruitment 2018: candidate parenting	**Aug 2018**
Offered a practical course on Metabolic and Regulatory Networks (Summer semester)	**2018**
Supervised at IMPRS Institute for Chemical Ecology Recruitment 2017: candidate parenting	**Nov 2017**

Ehrenwörtliche Erklärung

Entsprechend der geltenden, mir bekannten Promotionsordnung der Fakultät für Biowissenschaften der Friedrich-Schiller-Universität Jena erkläre ich, dass ich die vorliegende Dissertation eigenständig angefertigt und alle von mir benutzten Hilfsmittel und Quellen angegeben habe. Personen, die mich bei der Auswahl und Auswertung des Materials sowie bei Fertigstellung der Manuskripte unterstützt haben, sind am Beginn eines jeden Kapitel genannt. Es wurde weder die Hilfe einer kommerziellen Promotionsvermittlung in Anspruch genommen, noch haben Dritte für Arbeiten, welche im Zusammenhang mit dem Inhalt der vorliegenden Dissertation stehen, geldwerte Leistungen erhalten. Die vorgelegte Dissertation wurde außerdem weder als Prüfungsarbeit für eine staatliche oder andere wissenschaftliche Prüfung noch als Dissertation an einer anderen Hochschule eingereicht. Weiterhin wurde keine ähnliche oder andere Abhandlung als Dissertation anderswo eingereicht.